Optical Properties and Molecular Orbital Analyses of Defects in Photo-CVD SiO_2 Thin Films

January 25, 1996

Kanashima Takeshi

Osaka University, Faculty of Engineering Science

Optical Properties and Molecular Orbital Analyses of Defects in Photo-CVD SiO_2 Thin Films

January 25, 1996

Kanashima Takeshi

Osaka University, Faculty of Engineering Science

Abstract

Comprehensive studies on the defect properties in low-temperature-grown SiO_2 thin film have been carried out experimentally and theoretically.

SiO_2 thin films were grown by photo-induced chemical vapor deposition (photo-CVD) at low temperature (RT–300 °C). Source gases are Si_2H_6 and O_2, and excitation light source is deuterium (D_2) lamp which emits vacuum ultraviolet light. These films show very good electrical properties in SiO_2/Si structure. Photoluminescence and absorption properties of photo-CVD produced SiO_2 thin films have been studied to identify the defects more precisely. Two kinds of distinct absorption peaks have been found, which are at 6.3 eV for low temperature deposition (around 30 °C), and at 7.6 eV for high temperature deposition (around 300 °C). It is considered from the O_2 and N_2 atmosphere treatment effects that the absorption peak at 7.6 eV is attributable to oxygen-vacancy, but the absorption peak at 6.3 eV relates to oxygen-excess defects. The photoluminescence have been studied by using excitation of D_2 lamp, ArF excimer laser, F_2 excimer lasers or N_2 laser. Photoluminescence peaks at 2.4, 3.4–3.5 eV and 4.3–4.4 eV are found in the SiO_2 film. Intensity changes of the photoluminescence and absorption peaks have been obtained in various films which were deposited at different gas-flow-rate-ratios of Si_2H_6/O_2 and were annealed in O_2 and N_2 atmosphere. These peaks are classified to oxygen-deficient defect (4.4 eV) and oxygen-excess defect (2.4 and 3.5 eV). Moreover, the intensity of the photoluminescence peak at around 2.4 eV initially increases with increase of shot number of ArF excimer laser irradiation but decreases after about 2000 shots. On the other hand, it decreases monotonously with F_2 excimer laser irradiation. The other peaks at 3.5 and 4.4 eV are decreased monotonously with exposure of ArF and F_2 excimer lasers.

Energy states of various defects in SiO_2 such as (≡Si–O–O–Si≡, ≡Si–O–O–H, ≡Si–Si≡) have been studied theoretically by using molecular orbital (MO) calculation and discussed on the basis of comparison with optical absorption and photoluminescence of SiO_2 thin films. Theoretical analyses have been carried out using both the semi-empirical and ab-initio methods. The ab-initio calculation of oxygen-excess defect of ≡Si–O–O–Si≡ shows that the transition energy from the excited singlet state to the ground state is 2.32 eV with the STO-3G basis set and 2.40 eV with the 3-21G basis set, which are very close to the 2.4 eV photoluminescence peak measured in the photo-CVD deposition SiO_2 thin film. Moreover, the ab-initio calculation of hydrogen-related defect of ≡Si–O–O–H shows that the transition energy from the excited singlet state to the ground state is 3.9 eV with the STO-3G basis set and the excitation energy from ground state to excited singlet is 6.4 eV, which are close to the 3.5 eV photoluminescence peak and 6.3 eV absorption peak measured in the photo-CVD SiO_2 thin film, respectively.

Acknowledgment

This work has been done at the Semiconductor Laboratory, Department of Electrical Engineering, Faculty of Engineering Science, Osaka University, Toyonaka, Osaka, Japan, under the direction of Professor M. Okuyama. The author sincerely acknowledges his indebtedness to Professor M. Okuyama for his kind advice, suggestion, continuous supporting and encouragement through this study.

The author would like to express his deep thanks to Professor Y. Hamakawa for his continuous guidance, useful advises and critical comments. The author would like to thank to Professor K. Gamo and Professor H. Okamoto for their kind advice and the critical reading of this thesis. The author is extremely grateful for the advice offered by Professor S. Yamamoto, Professor Ta. Kobayashi, Professor Te. Kobayashi and Professor K. Nishihara for their kind guidance in the course of this study at Osaka University.

The author wishes his thanks to Professor H. Takakura, Mr. K. Yamashita, Dr. K. Hattori, Dr. W. Ma, Mr. C. Sada for their kind advices and helpful discussions in the course of this study in the Semiconductor Laboratory. The author would like to thank to Professor K. Yamaguchi and Dr. M. Nakano for their kind advices about molecular orbital analyses. The author would like to thank to Mr. S. Koshida for his support on ESR measurement. The author would like to thank to Mr. Y. Kamada and staff of Project Team DoGA for preparation of schematic animation of atomic configuration.

The author is indebted to Dr. A. Fujimoto, Dr. M. Yoshimi, Mr. R. Nagayoshi, Mr. Y. Matsui, Mr. Y. Miyagawa, Miss J. Izumitani, Mr. M. Nishida, Mr. H. Katsumi, Mr. S. Iwasaki, Mr. K. Okumura, Mr. Y. Kurioka, Mr. H. Yamamoto, Mr. T. Imai and all members of the Semiconductor Laboratory for their kind guidance and their technical assistances in the course of the Semiconductor Laboratory.

The author would like to thank my parents for their endless and whom encouragement.

Contents

Chapter 1

Introduction

1.1 Background

Recently, integration of semiconductor devices such as dynamic random access memory (DRAM) and read only memory (ROM) is markedly high and the size of one element on a single chip is minute [1]. For example, the storage capacity in a DRAM becomes 4 times by 2–3 years [2]. Especially, rapid development of large capacity memory is required for multimedia, and many researchers are working to realize a 1 Gbit DRAM. Table 1.1 shows CMOS scaling guidelines for the next 10 years. This figure shows that a film thickness of insulator is 1/3 in 2003 [3, 4]. However, conventional technique leads to problems for making very thin insulator film, and new fabrication method must be developed to break through the problem. SiO_2 thin film is very important in large scale integrated circuit (LSI) devices.

- Insulator among elements and wiring.
- Passivation of elements and wiring.
- MOS gate insulator.
- Mask for dopant diffusion and ion implantation.

So, the quality of SiO_2 thin film affects LSI reliance, and it is necessary to prepare a high quality SiO_2 thin film for a high performance. Addition to this, SiO_2 film must be very thin to reduce an element size, and its dielectric constant must be small to operate high frequency. At present, thermally grown SiO_2 film is generally used because of its high reliability, but this oxidation process requires a high temperature (nearly 1000 °C). Here, this high temperature process has some problems.

- Deterioration of the impurity profile by thermal diffusion.
- Accumulation of stress by different thermal expansion coefficient between the layers.

Table 1.1. CMOS scaling guidelines for the next 10 years.

	Late 1980's	1992	1995	1998	2001	2004
Supply Voltage (V)						
High Performance	5	5/3.3	3.3/2.5	2.5/1.8	1.5	1.2
Low Power	—	3.3/2.5	2.5/1.5	1.5/1.2	1.0	1.0
Lithography Resolution (μm)						
General	1.25	0.8	0.5	0.35	0.25	0.18
Gate Level for Short L	—	0.6	0.35	0.25	0.18	0.13
Channel Length (μm)	0.9	0.6/0.45	0.35/0.25	0.2/0.15	0.1	0.07
Gate Insulator Thickness (nm)	23	15/12	9/7	6/5	3.5	2.5
Relative Density	1.0	2.5	6.3	12.8	25	48
Relative Speed						
High Performance	1.0	1.4/2.0	2.7/3.4	4.2/5.1	7.2	9.6
Low Power	—	1.0/1.6	2.0/2.4	3.2/3.5	4.5	7.2
Relative Power/Function						
High Performance	1.0	0.9/0.55	0.47/0.34	0.29/0.18	0.12	0.077
Low Power	—	0.27/0.25	0.20/0.09	0.08/0.056	0.036	0.041
Relative Power/Unit Area						
High Performance	1.0	2.25/1.38	3.0/2.1	3.7/2.34	3.12	3.70
Low Power	—	0.7/0.63	1.25/0.6	1.02/0.72	0.90	1.97

- Difficulties of thermal oxidation technique to prepare SiO_2 thin film on the finished layer for making three-dimension (3D) structure.

Therefore, direct photo-induced chemical vapor deposition (photo-CVD) — a new fabrication method is being studied to solve these problems. Because, photo-CVD has some advantage of deposition [5–10] in thin film fabrication methods.

- Low temperature process (room temperature to 300 °C). Thus, Al-Si metalization and changing of dopant profile do not occur.

- Possibility of deposition on not only Si substrate but also metal, glass, etc. It can be prepared on finished pattern, and it is able to create a 3D-structural LSI.

- Damage-free by high energy charged particle in plasma-CVD. It can keep both surface and interface clean and safe.

- Needless sensitization material used in indirect photo-CVD. Thus, impurity doesn't come in a film.

Photo-CVD has these merits on fabrication process. Quality of the SiO_2 thin film prepared by photo-CVD is good, but not fully enough to use LSI. We must clarify various properties of the film precisely to improve the film quality and utilize the photo-CVD SiO_2 thin film for practical use.

1.2 Purpose of This Work

In order to develop good quality SiO_2 thin film for practical use, it is very important to clarify the cause of deterioration — defect — of the quality of SiO_2 thin film and its generation mechanism. If generation mechanism of this defect is clear, we can know a deposition condition of photo-CVD and the way to suppress the defects. Fundamental properties of these films have been studied by means of various analyses such as 1) electrical property analyses : capacitance-voltage (C-V) analysis, deep-level transient spectroscopy (DLTS), photo-current-voltage (photo-IV) analysis, 2) composition analyses : secondary ion mass spectroscopy (SIMS), 3) binding (vibration) energy analyses : X-ray photoelectron spectroscopy (XPS), infrared absorption (IR) spectroscopy. Among these methods, optical properties relate directly to electron energy level, and these yield good information about peroxy linkage and other defects [11–14], many of which are related closely to electrical characteristics [15]. In addition, this method has some advantages.

- No electrode on the sample.
- Non-destructive, no-contact and highly sensitive.
- Potentiality to estimate a small area to focus a light and to measure defect's distribution.

The SiO_2 is an insulator and its band gap is about 9 eV, and then it must be studied in the optical properties in the vacuum ultraviolet (VUV), and ultraviolet (UV) region. Fused quartz (silica glass) has been characterized using optical absorption and photoluminescence in VUV and UV region by many workers. In addition to this, it is reported that the photoluminescence and optical absorption due to the oxygen-vacancy defect $O_3{\equiv}Si{-}Si{\equiv}O_3$ on the various silica glasses were analyzed theoretically [16–18]. However, photoluminescence of SiO_2 thin films have not been characterized yet, because the film thickness is too small for photoluminescence measurement. Moreover, the theoretical analyses of photoluminescence about the oxygen-excess defects such as $O_3{\equiv}Si{-}O{-}O{-}Si{\equiv}O_3$, $O_3{\equiv}Si{-}O{-}H$, $O_3{\equiv}Si{-}O{-}O\cdot$ and $O_3{\equiv}Si{-}O\cdot$ [19–22] have not been reported yet. (The symbols $\equiv$ and $\cdot$ represent three bonds and an unpaired electron.) So, I have tried to characterize the defects theoretically, too. Molecular orbital (MO) analysis is known as a powerful method to obtain not only energies of the ground and excited states but also bonding orbital and electron density. Therefore, the oxygen-excess defect structure existing in the SiO_2 thin film should be identified by comparison between calculated energy and photoluminescence peak energy.

First, I have attempted to measure photoluminescence and optical absorption of the photo-CVD SiO_2 thin film using a high-sensitivity spectroscopic measurement system including laser, monochromator and photo-multiplier tube in VUV region. This experimental result gives various kinds of properties of defects, but it may be

difficult to determine the defect structure only by optical properties. Therefore, I have analyzed theoretically defect state by MO method. In this analysis, the cluster model of defects was constructed, and he energy levels of these clusters were calculated. Finally, the photoluminescence peak energies of the photo-CVD SiO_2 thin film have been compared with the calculated energy levels and the structure of the defects, and was identified.

This thesis includes 7 chapters. Figure 1.1 shows the schematic diagram of contents of this thesis. Chapter 1 is introduction, and clarify background and motivation of this work.

In chapter 2, the sample preparation procedure and its basic properties are described. The photo-CVD have some advantage over coming conventional thermally oxidation technique. The SiO_2 thin film is prepared by photo-CVD using VUV light at room temperature (RT) to 300 °C in this thesis. Source gases are Si_2H_6 and O_2. Deposition rate, refractive index, fixed charge density and IR absorption spectrum in the film are measured, and it is found that VUV light irradiation is effective to deposit at low temperature. However, IR spectra show that the concentration of Si – H and Si – OH in photo-CVD SiO_2 thin film is larger than thermally grown oxide film. It is shown how these defects could be reduced.

In chapter 3, optical absorption of SiO_2 thin films deposited by using photo-CVD is described. Optical measurement is non-destructive, no-contact and high sensitive. SiO_2 is an insulator and its band gap is about 9 eV, then it must be measured in vacuum ultraviolet (VUV) and ultraviolet (UV) region. It is found that the photo-CVD SiO_2 thin films have two absorption peaks. Film thickness dependence, growth condition dependence and annealing effects are studied to clarify the origins of the peaks. As a result, one is caused by oxygen-excess defect, and the other is caused by oxygen-deficient defect.

In chapter 4, photoluminescence of SiO_2 thin film is described. The photoluminescence in silica glass is reported, but that in SiO_2 thin film has not yet. Thus, photoluminescence of SiO_2 thin film prepared by photo-CVD is studied. The ultraviolet light source such as deuterium lamp, ArF and F_2 excimer laser and N_2 laser are used to excite samples for photoluminescence. These excitation light energies are lower than the band gap of SiO_2, and so the photoluminescence relates to the energy levels in the band gap which are originated from defects in SiO_2 thin film. Its growth condition dependence, annealing effects, film thickness dependence and measurement temperature dependence are measured, too. As a result, defects in SiO_2 thin film are classified into oxygen-excess and oxygen-deficient type. It is shown that the oxygen-deficient defect distributes in the film uniformly.

In chapter 5, excimer laser irradiation effect is described. Irradiation effects to optical absorption, photoluminescence and electron spin resonance (ESR) are measured to find the origins and stability of the defects. Recently, the element size of LSI becomes very minute, the ultraviolet light sources such as KrF excimer laser are examined to use for photo-lithography. Thus, it needs to study the changes of

the film properties under irradiation of high energy photon. As a result, it is shown that the oxygen-excess defect is unstable and its bond is broken into dangling bond by ArF and F_2 excimer laser irradiation. On the other hand, the oxygen-deficient defect is more stable than oxygen-excess one and its bond is broken into dangling bond only by F_2 excimer laser irradiation.

In chapter 6, energy levels, charge density and binding states are analyzed by MO method. Optical properties such as photoluminescence and absorption yield the characteristics of defects, but these physical structures and microscopic information such as charge density belonging to each atom are not clarified. So, I try to construct the SiO_2 cluster and some defect clusters such as oxygen-excess defects (≡Si–O–O–Si≡, ≡Si–O–O–H, ≡Si–O–H) and oxygen-deficient defects (≡Si–Si≡), and calculate their energy levels, charge densities and IR absorption by semi-empirical and/or ab-initio MO method. In addition to this, the energy to remove hydrogen atom is obtained about O_3≡Si–O–H and O_3≡Si–H by MO method and the stability of defects is discussed.

In chapter 7, conclusion of this thesis is presented.

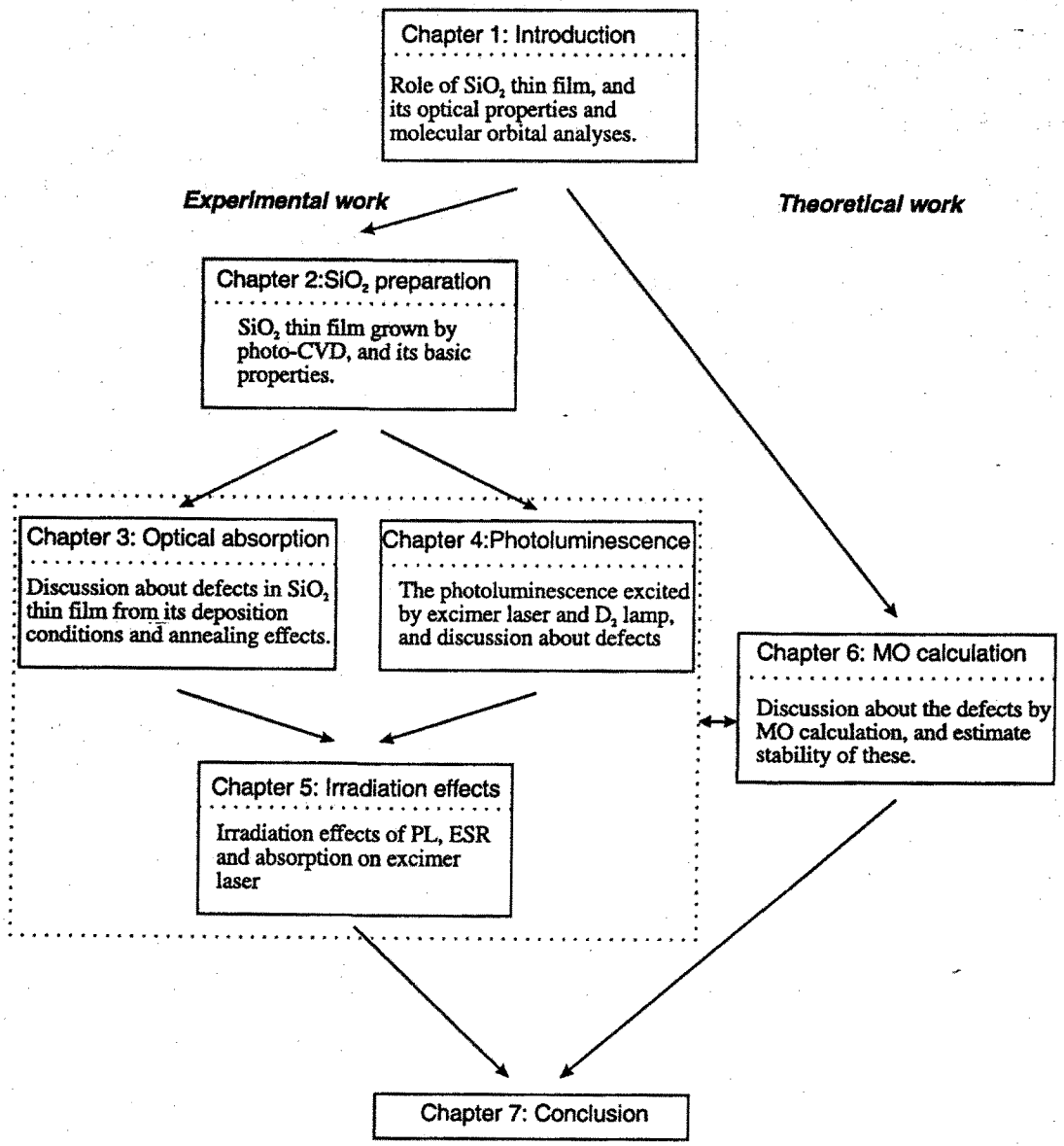

Figure 1.1. Construction of this thesis.

Reference

[1] F. Shimura: *Handoutai Silicon Kessyo Kogaku* (Technology of Semiconductor Crystalline Silicon) (Maruzen, Tokyo, 1993) Chap. 4, p. 156 [in Japanese].

[2] Y. Mochizuki and Y. Nagahiro: Nikkei Microdevices **117** (1995) 26.

[3] B. Davari, R. H. Dennard and G. G. Shahidi: Proc. of the IEEE **83** (1995) 595.

[4] B. Davari, R. H. Dennard and G. G. Shahidi: NIKKEI Electronics **646** (1995) 153 [in Japanese].

[5] Y. Toyoda, K. Inoue, M. Okuyama and Y. Hamakawa: Jpn. J. Appl. Phys. **26** (1987) 835.

[6] K. Inoue, M. Michimori, M. Okuyama and Y. Hamakawa: Jpn. J. Appl. Phys. **26** (1987) 805.

[7] M. Okuyama, N. Fujiki, K. Inoue and Y. Hamakawa: Jpn. J. Appl. Phys. **26** (1987) L908.

[8] K. Inoue, Y. Nakatani, M. Okuyama and Y. Hamakawa: J. Appl. Phys. **64** (1988) 6496.

[9] K. Inoue, M. Okuyama and Y. Hamakawa: Jpn. J. Appl. Phys. **27** (1988) L2152.

[10] M. Tsuji, N. Itoh and Y. Nishimura: Jpn. J. Appl. Phys. **30** (1991) 2868.

[11] M. Kohketsu, K. Awazu, H. Kawazoe and M. Yamane: Jpn. J. Appl. Phys. **28** (1989) 622.

[12] R. Tohmon, Y. Shimogaichi, H. Mizuno and Y. Ohki: Phys. Rev. Lett. **62** (1989) 1388.

[13] M. Kohketsu, K. Awazu, H. Kawazoe and M. Yamane: Jpn. J. Appl. Phys. **28** (1989) 615.

[14] Y. Hibino and H. Hanafusa: J. Appl. Phys. **60** (1986) 1797.

[15] D. M. Fleetwood, R. A. Reber, Jr., and P. S. Winokur: Appl. Phys. Lett. **60** (1992) 2008.

[16] O'Keeffe and G. V. Gibbs: J. Chem. Phys. **81** (1984) 876.

[17] R. Tohmon, Y. Shimogaichi, H. Mizuno, Y. Ohki, K. Nagasawa and Y. Hama: Phys. Rev. Lett. **62** (1989) 1388.

[18] R. Tohmon, H. Mizuno, Y. Ohki, K. Sasagane, K. Nagasawa and Y. Hama: Phys. Rev. B. **39** (1989) 1337.

[19] H. Nishikawa, R. Nakamura, R. Tohmon, Y. Ohki, Y. Sakurai, K. Nagasawa and Y. Hama: Phys. Rev. B **41** (1990) 7828.

[20] H. Imai, K. Arai, J. Isoya, H. Hosono, Y. Abe and H. Imagawa: Phys. Rev. B **48** (1993) 3116.

[21] J. Robertson: *The Physics and Technology of Amorphous SiO_2*, ed. Roderick A. B. Devine (Plenum Press, New York and London, 1988), p. 91

[22] David L. Griscom: *The Physics and Technology of Amorphous SiO_2*, ed. Roderick A. B. Devine (Plenum Press, New York and London, 1988), p. 125

Chapter 2

Preparation of Photo-CVD SiO_2 Thin Film

2.1 Introduction

SiO_2 thin film is very important material in LSI and is used as MOS gate insulator, insulating layer for wiring, passivation of devices and lithography mass for ion-implantation and diffusion, etc. SiO_2 thin film grown at low temperature by various methods has been studied from the demands for avoiding the process temperatures. Comparing conventional fabrication methods such as plasma-CVD and thermally oxidation, photo-CVD is low temperature process, and has some advantage. Because the source gases are decomposed by high energy photon, not by thermal, and generated radicals are neutral, not charged. Therefore, it is studied by many workers to prepare SiO_2, a-Si, Si and Si_3N_4 by using photo-CVD [1–5]. We have tried to prepare low defect and low interface state density SiO_2 thin film by photo-CVD with VUV light [6–10].

In this chapter, lowering of the SiO_2 deposition temperature and reduction of the defects by direct-excitation photo-CVD are described. It is shown that SiO_2 thin films can be deposited at RT to 300 °C from source gases of O_2 and Si_2H_6 (disilane) by using the VUV light of a deuterium (D_2) lamp and reduction of the defects by photo-excitation.

2.2 Preparation Method of SiO_2 Thin Film

In direct-excitation photo-CVD, it is very important to match the radiation spectra of excitation light to the absorption spectra of source gases for decomposition source gases effectively. The family of silane gases such as SiH_4 (monosilane) and Si_2H_6 (disilane) have been used to grow SiO_2 thin film. Figure 2.1 shows the radiation spectra of the various ultraviolet (UV) and VUV light sources such as deuterium

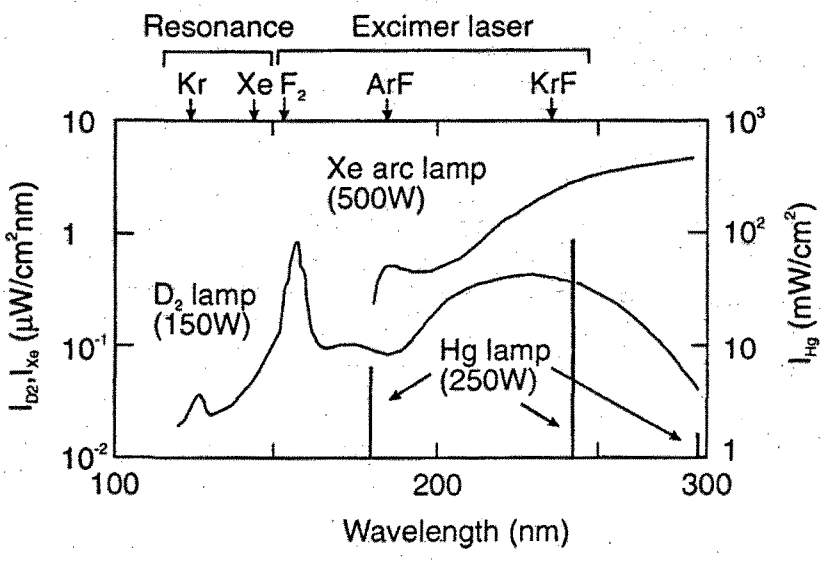

Figure 2.1. Radiation spectra of various VUV and UV light sources.

lamp, ArF excimer laser and mercury lamp. Figure 2.2 shows that the absorption spectra of source gases such as Si_2H_6, O_2 and O_3. Recently, Si_2H_6 which is more radical than SiH_4 has become commercially available, and has been used as a reactant gas for preparation of a good quality SiO_2 films [6–10]. Si_2H_6 gas has strong absorption in the wavelength region below about 180 nm. O_2 has strong absorption in the VUV region from 130 to 175 nm wavelength. Thus, these source gases can be excited and decomposed by the D_2 (broad, 110 – 200 nm), Xe (monochrome, 147 nm), Kr (monochrome, 123.6 nm) lamp, ArF (monochrome pulse, 193 nm), F_2 (monochrome pulse, 157 nm) excimer laser and synchrotron radiation (SR; very broad, spreading from soft-X-ray to IR). The D_2 lamp has strong radiation in the VUV region around 160 nm which matches as well with those of the source gases, and is a very convenient light source. F_2 excimer laser is also strong VUV light source which wavelength is 157 nm, but the cost of maintenance comes high since F_2 gas is expensive and gas life-time is short. Moreover, it is reported that a good quality SiO_2 thin film was grown by using the light from SR, because SR is very strong light source spreads from infrared to soft X-ray, and can excite core electron [11]. However, SR facility is run on a very extensive scale. Moreover, there is no window glass (material) to translate VUV to soft X-ray, then we cannot irradiate wide area on a sample. Therefore, the D_2 lamp is very suitable for excitation of source gases, and this is used to prepare SiO_2 thin film.

Figure 2.3 shows the schematic diagram of photo-CVD apparatus. Table 2.1 shows deposition conditions of SiO_2 thin film. The reaction chamber is consisting

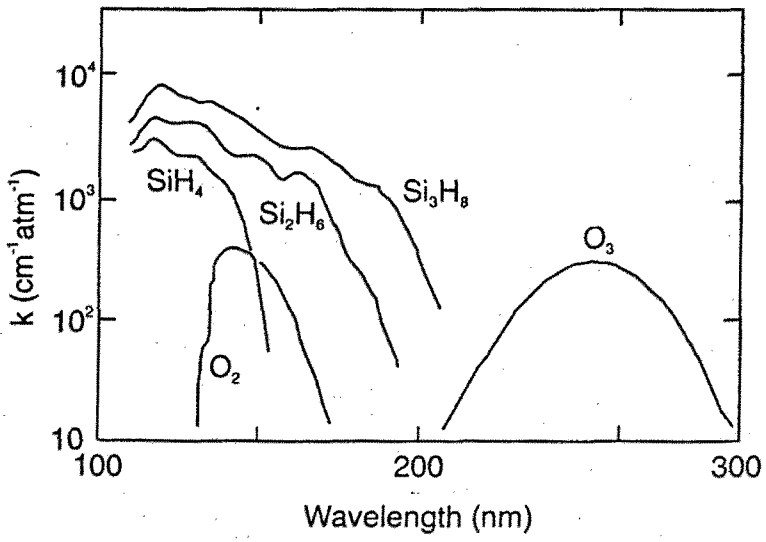

Figure 2.2. Absorption spectra of source gases such as Si_2H_6, O_2 and O_3.

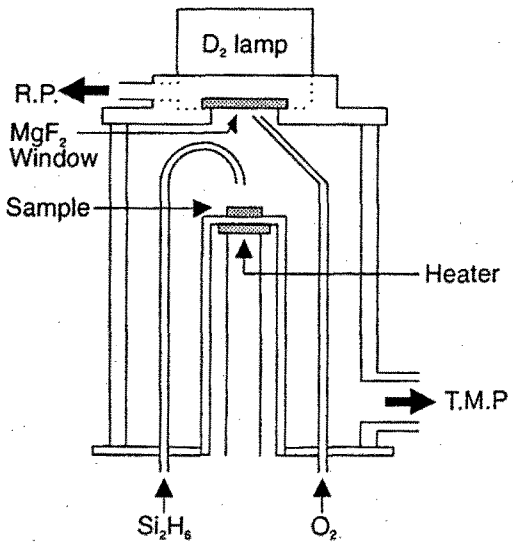

Figure 2.3. Schematic diagram of photo-CVD apparatus.

Table 2.1. Deposition conditions of SiO_2 thin films.

Light source	D_2 lamp
Working pressure	27 Pa
Back pressure	$1.0x10^{-3}$ Pa
Substrate temp.	RT – 300 °C
Si_2H_6/O_2	0.103 – 0.241
Substrate	MgF_2 or n-Si(100)

made of outside silica glass cylinder 240 mm high and 90 mm diameter, inner silica cylinder 30 mm diameter, and D_2 lamp supporter. This chamber is evacuated by turbo molecular (Shimadzu, TMP280) and rotary pumps. The light to decompose source gases is the D_2 lamp (Hamamatsu Photonics, L1835). The window between lamp and chamber is made from MgF_2 which transmits VUV light more than 115 nm wavelength, the space between window and lamp is evacuated by rotary pump. The window is blown by O_2, one of the source gases, to prevent to deposit SiO_2. Because, SiO_2 film cannot transmit less than about 160 nm wavelength light. The heater is set under the sample stage, and the sample can be heated upper to 300 °C. The substrates are used Si(100) for photoluminescence and ESR measurement, or MgF_2 for optical absorption measurement. The electronic conductivity of Si substrates is 1 Ω·cm for photoluminescence or 1000 Ω·cm for ESR.

2.3 Basic Properties of SiO_2 Thin Film

Figure 2.4 show the growth rate of SiO_2 thin films deposited from Si_2H_6 and O_2 by thermal-CVD and photo-CVD with D_2 lamp as a function of substrate temperature. This figure shows that the SiO_2 thin film can be grown even at RT by photo-CVD. Moreover, the growth rate in photo-CVD is larger than thermal-CVD at RT to 300 °C. This dependence indicates that the VUV light irradiation is effective. The growth rate in photo-CVD decreases with increasing substrate temperature. This behavior indicates that as increasing substrate temperature, more adsorbed atom and radical leave away from substrate. So, adsorption of the species decomposed by VUV light irradiation is rate-determining process, and the deposition of SiO_2 thin film is caused by high energy photon rather than heat. The refractive index and the film thickness were measured by the ellipsometer using He-Ne laser light (Mizojiri, DVA-36). The refractive index is nearly 1.45 in the samples deposited at above 50 °C, and the refractive index is independent of the substrate temperature (from 50 to 300 °C). This value almost agrees with 1.457 of thermal oxide.

Figure 2.5 shows the relative concentrations of Si–H and Si–OH bonds as a function of substrate temperature for the films deposited by thermal-CVD and photo-

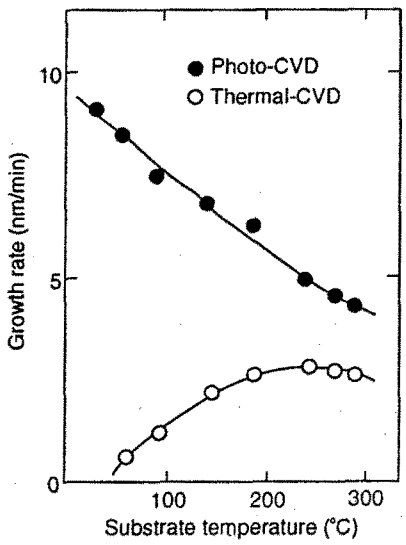

Figure 2.4. Growth rate of SiO_2 thin films deposited from Si_2H_6 and O_2 by thermal-CVD and photo-CVD as a function of substrate temperature.

CVD. This concentration is determined by IR absorption spectrum. IR measurement was done by Fourier transform infrared absorption spectrometer (FT-IR; Jasco, FT-IR3). This figure shows that the Si–H and Si–OH remains in the film. Measurement of quadruple mass spectroscopy shows that both the Si_2H_6 and O_2 may be decomposed into various radials and in this photo-CVD and the species such as Si_2H_5O and Si_2H_6O become adsorption species, it is thought. However, this figure shows that the Si–H and Si–OH concentrations in photo-CVD SiO_2 thin film are larger than ones in thermal-CVD. This indicates that the VUV light is effective to decrease the defects (Si–H, Si–OH).

Figure 2.6 shows the oxide charge density in the MOS diodes made of SiO_2 film deposited by photo-CVD as a function of substrate temperature. This figure shows that the oxide charge density is not very small, and increases with decreasing growth temperature.

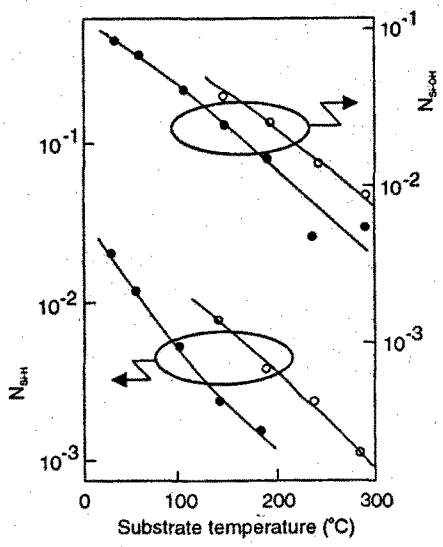

Figure 2.5. Relative concentrations of Si–H and Si–OH bonds as a function of substrate temperature for the films deposited by thermal-CVD and photo-CVD.

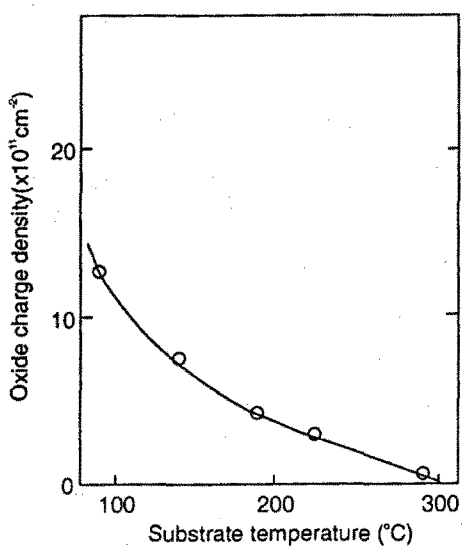

Figure 2.6. The oxide charge density in the MOS diodes made SiO_2 film deposited by photo-CVD as a function of substrate temperature.

Reference

[1] A. Yoshikawa and S. Yamada: Jpn. J. Appl. Phys. **23** (1984) L91.

[2] M. Menu, T. R. Gattuso, D. Adler and J. S. Haggerty: Appl. Phys. Lett. **43** (1983) 273.

[3] P. K. Boyer, G. A. Roche, W. H. Richie and G. J. Collins: Appl. Phys. Lett. **40** (1982) 716.

[4] Y. Mishima, M. Hirose, Y. Osaka and Y. Ashida: J. Appl. Phys. **55** (1984) 1234.

[5] C. H. Brekel and P. J. Serverin: J. Electrochem. Soc. **119** (1972) 372.

[6] Y. Toyoda, K. Inoue, M. Okuiyama and Y. Hamakawa: Jpn. J. Appl. Phys., **26** (1987) 835.

[7] K. Inoue, M. Michimori, M. Okuyama and Y. Hamakawa: Jpn. J. Appl. Phys. **26** (1987) 805.

[8] K. Inoue, M. Okuyama and Y. Hamakawa: Jpn. J. Appl. Phys. **27** (1988) L2152.

[9] M. Okuyama, N. Fujiki, K. Inoue and Y. Hamakawa: Jpn. J. Appl. Phys. **26** (1987) L908.

[10] K. Inoue, Y. Nakatani, M. Okuyama and Y. Hamakawa: J. Appl. Phys. **64** (1988) 6496.

[11] Y. Matsui, R. Nagayoshi, M. Nakamura, O. Okuyama and Y. Hamakawa: Jpn. J. Appl. Phys. **31** (1992) 1972.

Chapter 3

Optical Absorption of SiO_2 Film

3.1 Introduction

It is shown that the SiO_2 thin films can be deposited even at RT by using photo-CVD, but various defects such as Si–H and Si–OH exists in these films. Thus, these properties must be revealed to reduce these concentrations. In addition to this, the defects besides Si–H and Si–OH in the photo-CVD SiO_2 films are also characterized. As described in chapter 1, optical measurement has some merits. It needs electrode to measure electrical properties such as I-V, C-V, but no electrode to measure optical properties, and not only Si but also insulated materials can be used as a substrate. Then, optical properties were studied to estimate the defects in the SiO_2 films.

Optical properties such as absorption and photoluminescence relate to energy transfer between energy levels directly. The SiO_2 is an insulator and its band gap is very wide (about 9 eV [1,2]), and there are no levels in band gap in various quartz [3]. Thus, the photon which energy is less than the band gap is not absorbed principally. It is thought that if there are defects in the SiO_2 thin film, these defects may cause the peculiar energy levels. Especially, some of such levels may be placed into band gap. So, it is thought that defects in SiO_2 thin film can be estimated by using optical properties.

Optical properties of silica glass (bulk SiO_2), especially absorption in the VUV region and photoluminescence in UV to visible region have been studied so much [4–12]. No-electrode and non-destructive optical characterization has been adopted to SiO_2 thin films which were deposited on MgF_2 substrate by using photo-CVD at low temperature.

In this chapter, UV and VUV absorption of SiO_2 films deposited by photo-CVD using a deuterium lamp [13] is described. It is shown two kinds of optical absorption peaks exist, and these peaks are classified into oxygen-deficient and oxygen-excess

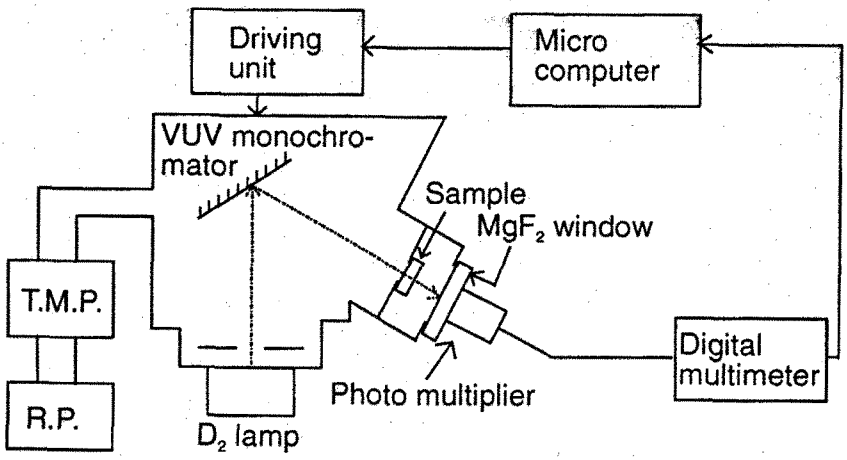

Figure 3.1. Schematic diagram of the VUV and UV absorption measurement system using D_2 lamp.

defects.

3.2 Measurement Method of Absorption Spectra

The SiO_2 films were prepared from Si_2H_6 and O_2 gases by photo-CVD using VUV light from D_2 lamp, and were deposited on MgF_2 at room temperature to 300 °C. Si substrate can not be used to measure the transmittance in VUV region, as silicon cannot transmit VUV rays. So, the crystalline MgF_2 plate of 7x7x1 mm^3 was used as a substrate and is polished both sides for optical use, since MgF_2 transmits in light from 110 nm VUV to 7.5 μm IR the wide range wavelength. Typical SiO_2 film thicknesses are in the range of 300–1000 nm. Figure 3.1 shows schematic diagram of absorption measurement system. Optical transmission spectra of the SiO_2 films deposited on MgF_2 substrates were measured by using the D_2 lamp (Hamamatsu Photonics, L1835), the VUV monochromator (Acton Research, VM502) and the photo-multiplier tube (EMI 9781BS5 with sodium-salitilate scintillator). The inside of the monochromator was evacuated by a turbo molecular pump (Shimadzu, TMP-50) and a rotary pump. The sample was set in the sample chamber that was attached directly to the monochromator in vacuum. This system is under computer control to measure automatically. The transmittance is decided to divide transmission of the SiO_2 film on MgF_2 by one of MgF_2 substrate without SiO_2 film.

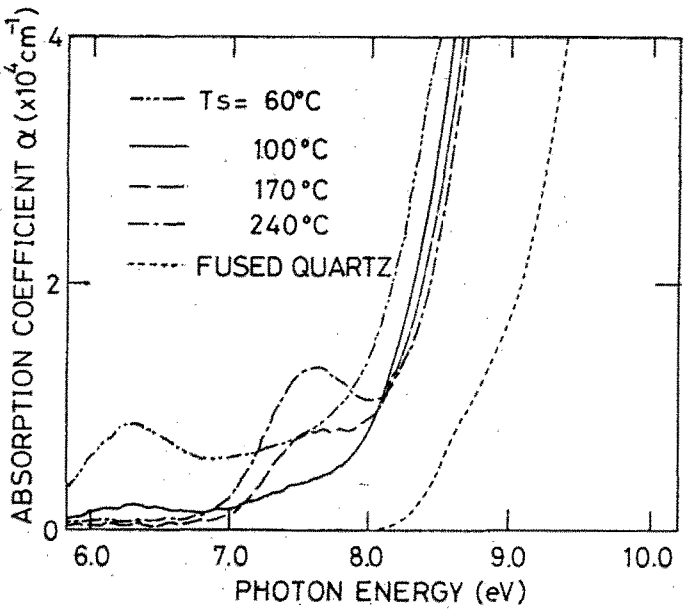

Figure 3.2. Absorption coefficient spectra of the films deposited on MgF_2 at 60–240 °C, and fused quartz.

3.3 Growth Condition Dependence

Figure 3.2 shows the absorption spectra of the photo-CVD-produced SiO_2 films deposited on MgF_2 at 60, 100, 170 and 240 °C. The absorption spectrum of fused quartz [2] is also shown for a comparison in this figure. The absorption band edge shifts to low energy with decreasing substrate temperature. As mentioned in chapter 2, the SiO_2 film deposited by photo-CVD at low temperature has considerable absorption peaks of Si–H and Si–OH, and these peaks decrease with increasing substrate temperature. So, the shifts of the absorption edge toward low energy may have relation to such impurities, incomplete Si–O network and dangling bonds. Moreover, an absorption peak at around 7.6 eV exists in the films deposited at higher temperatures (240 and 170 °C), and increases with increasing substrate temperature. On the other hand, the film deposited at low temperature (60 °C) has a peak at around 6.3 eV. These peaks are considered to arise from defects or imperfections, because there are no peaks in the spectrum of stoichometric and pure fused quartz and the energies of these peaks are smaller than the band gap of the SiO_2 (about 9 eV).

First, the absorption peak at 7.6 eV in the film deposited at high temperature is

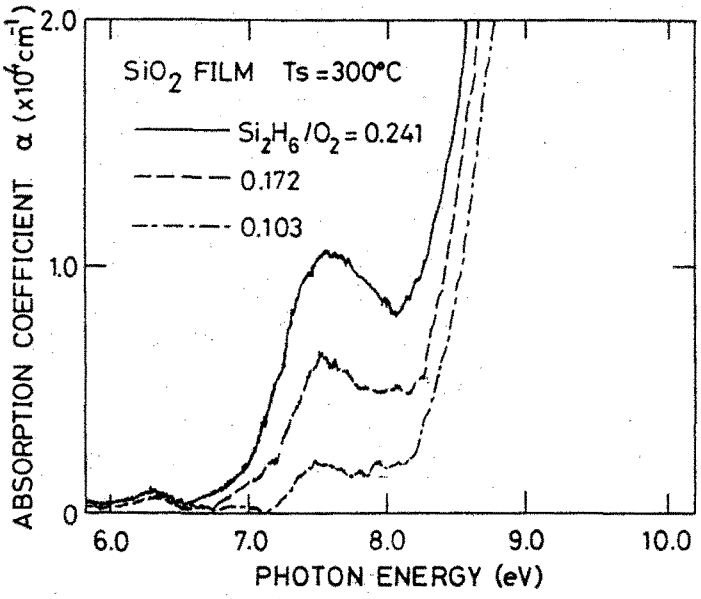

Figure 3.3. Absorption coefficient spectra of the films deposited at high temperature (300 °C) as a parameter of Si_2O_6/O_2 gas-flow-rate-ratio.

discussed. Figure 3.3 shows dependence of the absorption coefficients on Si_2H_6/O_2 gas-flow-rate-ratio. The SiO_2 films were deposited on MgF_2 at comparatively high temperature (300 °C). Si_2H_6 flow-rate and working pressure were fixed during the deposition. The absorption peak at 7.6 eV decreases with increasing O_2 flow-rate. This suggests that this peak originates from an oxygen-deficient defect. Moreover, the origin of this peak is not Si–H or Si–OH, because the peak increases with increasing growth temperature, but the concentrations of Si–OH and Si–H in the film decrease. It is reported that the silica glass has 7.6 eV absorption peak and its origin is Si–Si [12]. It has been shown in energy calculations using ab-initio MO methods that the cluster $(HO)_3Si–Si(OH)_3$ may have absorption peaks at 7.6 eV and 5.0 eV [4, 5]. Simultaneously, this calculation suggests that a photoluminescence peak at 2.7 eV can occur by excitation of 5.0 eV light. Then, the 7.6 eV peak in photo-CVD SiO_2 film is thought to result from an oxygen-vacancy such as Si–Si, and may be the same defect as in silica glass.

Next, the absorption peak at 6.3 eV in the film deposited at low temperature (around 60 °C) is discussed. Figure 3.4 shows the dependence of the absorption coefficient spectra on Si_2H_6/O_2 flow-rate-ratio. The SiO_2 films were deposited on

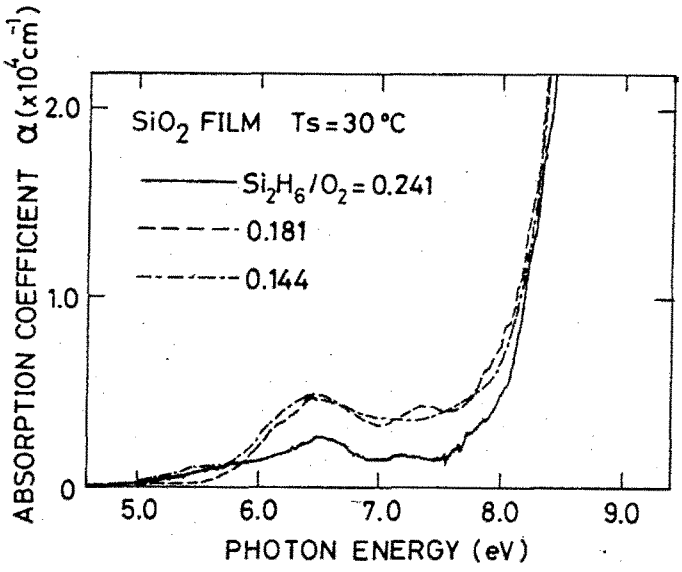

Figure 3.4. Absorption coefficients of the films deposited at low temperature (30 °C) as a parameter of Si_2O_6/O_2 gas-flow-rate-ratio.

MgF_2 at low temperature (30 °C). These films have a peak at around 6.3 eV, and this peak increases with increasing O_2 flow-rate. This suggests that this peak originates from oxygen-excess defect. This peak has not been reported in silica glass, and this is peculiar to the photo-CVD SiO_2 film.

Figure 3.5 shows film thickness dependence of absorptivity spectra of SiO_2 films. The samples were grown on MgF_2 at high temperature (280 °C) by using photo-CVD. Film thicknesses are 100, 500 and 1500 nm. A prominent absorption peak is observed at 7.6 eV, and measurements on 100, 500 and 1500 nm thick SiO_2 films indicate that the this peak increases with increasing film thickness. This shows that the origin of the 7.6 eV peak exists in bulk SiO_2, rather than near SiO_2/substrate interface (localized near interface).

Figure 3.6 shows the dependence of absorptivity spectra of SiO_2 films on the film thickness. The samples were grown on MgF_2 at high temperature (47 °C) by using photo-CVD. Film thicknesses are 100, 500 and 1500 nm. In contrast, this figure shows that the absorption magnitude of the 6.3 eV peak is independent of film thickness. This thickness independence suggests that the 6.3 eV peak is due to a defect localized near the SiO_2/MgF_2 interface, or is formed during the initial stage of the deposition. Figure 3.5 and 3.6 show that the absorption band edge shifts

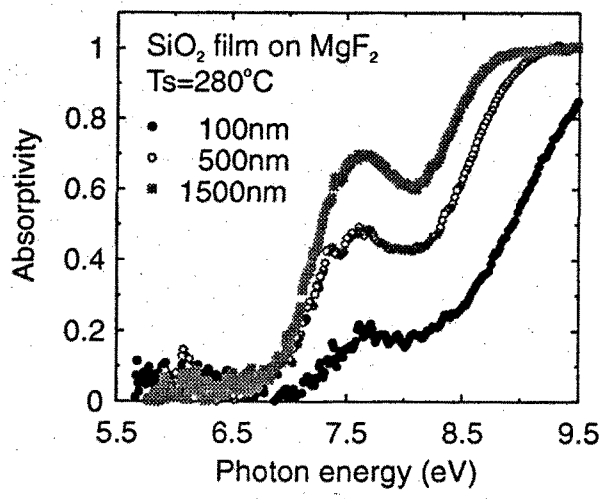

Figure 3.5. Absorptivity spectra of the photo-CVD SiO_2 films of various film thicknesses. The SiO_2 films were deposited at high temperature (280 °C).

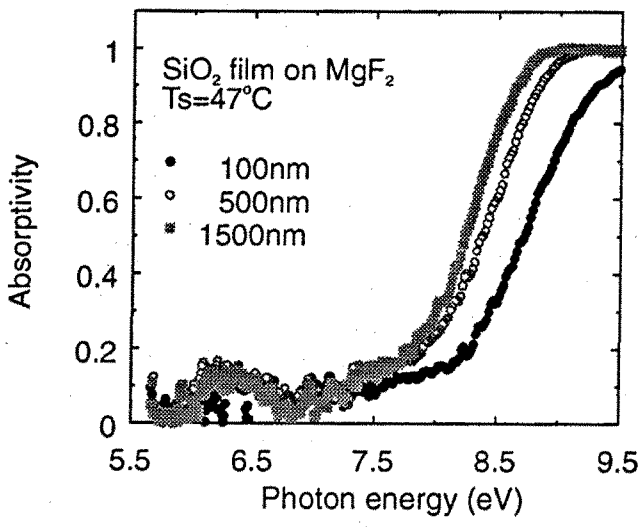

Figure 3.6. Absorptivity spectra of the photo-CVD SiO_2 films of various film thicknesses. The SiO_2 films were deposited at low temperature (47 °C).

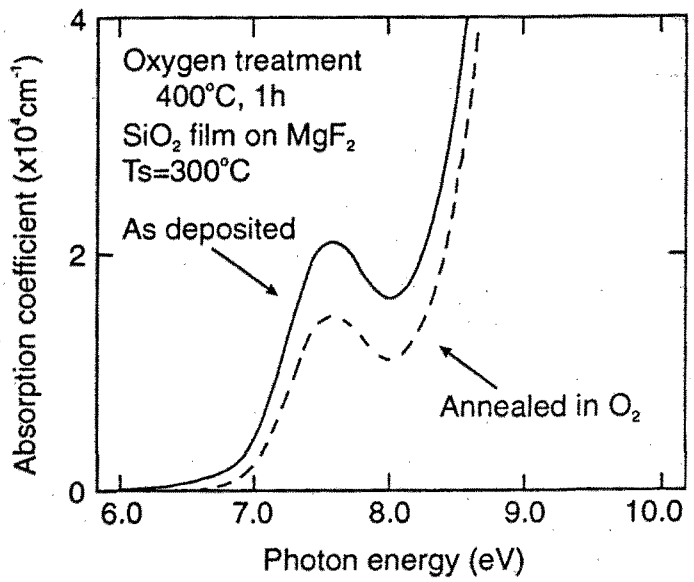

Figure 3.7. Absorption spectra of the SiO_2 film deposited at high temperature (300 °C) and the film annealed in O_2 atmosphere for one hour.

to lower energy with increasing film thickness at both low and high temperatures grown SiO_2 films. If this shift may be caused by the Si–OH and/or Si–H defect, it is considered that these defects distribute in the film.

3.4 Annealing Effect

Effects of annealing to the absorption peaks were investigated in order to confirm the origin of the absorption peaks at 7.6 and 6.3 eV. Figure 3.7 shows absorption spectra of the film before and after annealing in O_2 atmosphere at 400 °C for one hour. The film was deposited on MgF_2 at high temperature (300 °C). The peak at 7.6 eV was decreased by annealing in O_2 atmosphere at 400 °C for an hour, but does not change by annealing in N_2 atmosphere. This behavior also supports that the peak at 7.6 eV may be attributed to oxygen-vacancy. Here, diffusion coefficient of oxygen in silica glass is small at 400 °C, but that of H_2O is not so small. So, there remain a possibility that H_2O included in the film initially or formed by oxidation of Si–OH or Si–H may decrease oxygen-vacancy. Moreover, the annealing temperature is higher than the deposition, and then the species imperfectly decomposed may be react to reduce defects in the film.

Figure 3.8 shows absorption spectra of the film before and after annealing in O_2

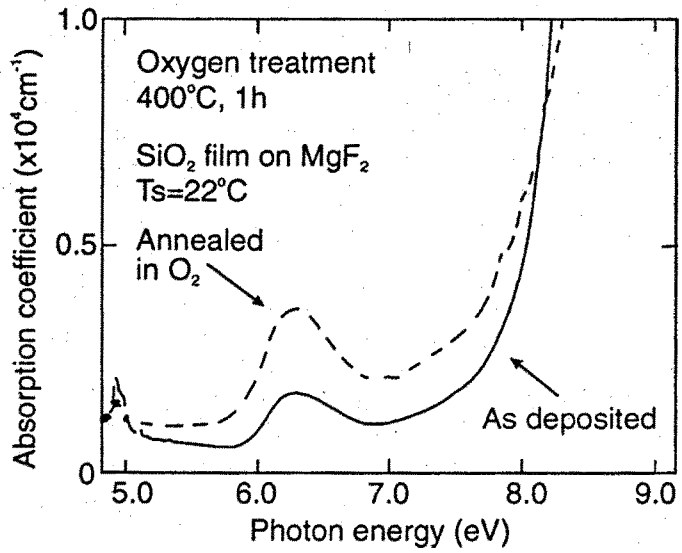

Figure 3.8. Absorption spectra of the SiO_2 film deposited at low temperature (22 °C) and the film annealed in O_2 atmosphere for one hour.

atmosphere at 400 °C for one hour. The film was deposited at low temperature (22 °C). The absorption peak at 6.3 eV was increased by the annealing in O_2 atmosphere, but decreased by the annealing in Ar atmosphere. This behavior also supports that this peak may be due to oxygen-excess defects. It is reported that oxygen-excess or oxygen-related defects such as Si–O–O–Si, Si–O–O · exists in silica glass, and it is thought that the origin of the 6.3 eV peak relates such defects or O_2 molecule. The 6.3 eV absorption may still arise from the other imperfections such as Si–O–H or Si–H, because Si_2H_6 was broken into SiH_3 and SiH_2 radicals by high energy photon, but these radicals may not break perfectly at low temperature, it is possible that Si–O–H and Si–H may remain in the film.

3.5 High Pressure Oxygen Treatment

The SiO_2 films were annealed in O_2 atmosphere at high pressure. The sample was placed in a portable reactor (Taiatsu Techno, TVS-2N). The annealing temperature is from 50 to 250 °C, annealing time is 1 hour, and the O_2 pressures are 1.52 MPa (15 atm at RT) and 10.1 MPa (100 atm at RT). The sample was grown on MgF_2 substrate by using photo-CVD at high temperature (300 °C). The film thickness is about 500 nm. It is considered oxygen atom or molecule is diffused into inside of the SiO_2 film.

Before annealing, the sample has absorption peak at 7.6 eV which is caused by oxygen-vacancy. After the annealing on this condition, this peak does not change. It is considered that the Si–Si bond in this oxygen-deficient defect is very tight, and the temperature below 250 °C which is the upper limit of our portable reactor, is not enough to break this bond. In addition to this, any other peak was produced by high pressure (10 MPa) O_2 annealing.

Reference

[1] Y. Ito, K. Tanimura and C. Ito: Kotaibuturi **22** (1987) 1000 [in Japanese].

[2] H. R. Philipp: J. Phys. Chem. Solids **32** (1971) 1935.

[3] Yong-nian Xu and W. Y. Ching: Phys. Rev. B **44** (1991) 11048.

[4] R. Tohmon, H. Mizuno, Y. Ohki, K. Nagawasa, Y. Hama: Phys. Rev. B **39** (1989) 1337.

[5] R. Tohmon, Y. Shimogaichi, H. Mizuno, Y. Ohki, K. Nagasawa and Y. Hama: Phys. Rev. Lett. **62** (1989) 1388.

[6] R. Tohmon, Y. Shimogaichi, H. Mizuno, Y. Ohki, K. Nagasawa and Y. Hama: Phys. Rev. Lett. **62** (1992) 1667.

[7] H. Imai, K. Arai, T. Saito, S. Ichimura, H. Nonaka, J. P. Vigouroux, H. Imagawa, H. Hosono and Y. Abe: *The Physics and Technology of Amorphous SiO_2*, ed. Roderick A. B. Devine (Plenum Press, New York and London, 1988) p.153.

[8] M. Kohketsu, K. Awazu, H. Kawazoe and M. Yamane: Jpn. J. Appl. Phys. **28** (1989) 615.

[9] R. Tohmon, Y. Shimogaichi, S. Munekuni, Y. Ohki, Y. Hama and K. Nagasawa: Appl. Phys. Lett. **54** (1989) 1650.

[10] S. Munekuni, T. Yamanaka, Y. Shimogaichi, R. Tohmon, Y. Ohki, K. Nagasawa and Y. Hama: J. Appl. Phys. **68** 1212.

[11] N. Dohguchi, S. Munekuni, H. Nishikawa, Y. Ohki and Y. Nagasawa: J. Appl. Phys. **70** (1991) 2788.

[12] K. Awazu: Bunko Kenkyu **41** (1992) 81 [in Japanese].

[13] T. Kanashima, R. Nagayoshi, M. Okuyama and Y. Hamakawa: J. Appl. Phys. **74** (1993) 5742.

Chapter 4

Photoluminescence of SiO_2 Thin Film

4.1 Introduction

It is reported in the photoluminescence (PL) of various silica glasses, that some defects are proposed as origines of photoluminescence peaks [1–7], but SiO_2 thin film is not yet. In optical properties, photoluminescence gives useful information about the defect energy levels that are participated in electronic transitions [8]. In addition to the same merits as the optical absorption on measurement, the photoluminescence of any materials on any substrates such as silicon and MgF_2 can be measured, and it can give much information about the energy relaxation process by studing various characteristics such as excitation-energy dependence and life-time [9, 10].

In this chapter, the photoluminescence of the SiO_2 thin film deposited by photo-CVD has been investigated. The UV light needs to be used as excitation of photoluminescence, since the band gap of SiO_2 is very wide. D_2 lamp (110–200 nm), ArF excimer laser (193 nm), F_2 excimer laser (157 nm) and N_2 laser (337.1 nm) were used as excitation UV light source of the SiO_2 thin film. As mentioned in chapter 3, the SiO_2 film has 7.6 and 6.3 eV absorption peak. Thus, the photon energies from ArF excimer laser (6.4 eV) and F_2 excimer laser (7.9 eV) match well with these absorption peaks, and these lasers are suitable for the characterization of defects. It is shown that the three peaks are found, and these peaks are strong depend on growth condition.

4.2 Measurement Method of Photoluminescence

The SiO_2 thin films were prepared from Si_2H_6 and O_2 gases by photo-CVD using VUV light of a D_2 lamp, and were deposited on Si substrate at room temperature to 300 °C. Typical film thicknesses are in the range of 300–1000 nm.

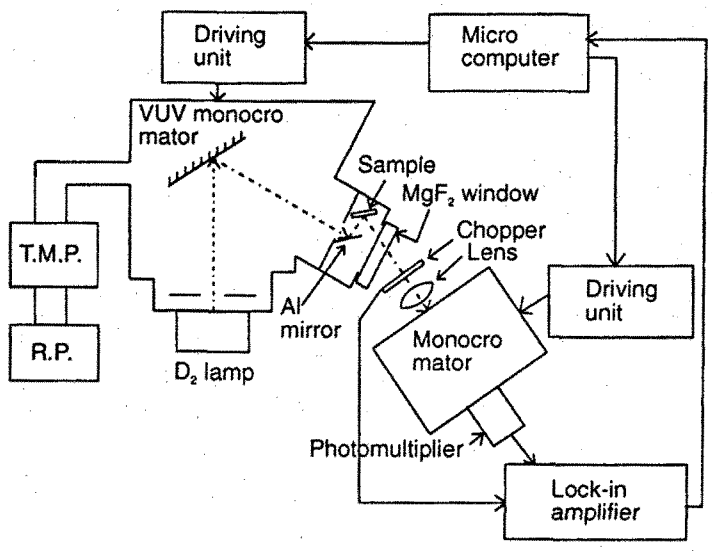

Figure 4.1. Schematic diagram of photoluminescence measurement system using D_2 lamp.

D_2 lamp, ArF and F_2 excimer lasers and N_2 laser are used as an excitation light source for photoluminescence measurement. Figure 4.1 shows schematic diagram of photoluminescence measurement system using D_2 lamp (Hamamatsu Photonics, L1835). The light of 7.7 eV dispersed by VUV monochromator (Acton Research, VM502) was applied to the sample through an Al mirror, and the photoluminescence of the sample was chopped and detected by another monochromator (Nikon, G-250) and the photomultiplier tube (Hamamatsu Photonics, R1508). The sample was set in the VUV monochromator which is kept in vacuum at pressures around 10^{-3} Pa (10^{-5} Torr) to prevent absorption of atmosphere.

Photoluminescence spectra excited by ArF and F_2 excimer laser (Lambda Physik, LPX105i) were measured as shown in the schematic diagram given in Fig. 4.2. The sample in the optical dewar was irradiated by the light from the excimer laser, and the photoluminescence was detected by monochromator (Nikon, G250) and photomultiplier (Hamamatsu Photonics, R1508). The optical dewar was evacuated by the rotary pump, and the pressure is around some Pa (some ten mTorr) in it. The MgF_2 was used as the window to transmit a VUV light. The F_2 excimer laser light was guided in a N_2-purged metal tube from the laser output to the optical dewar to prevent attenuation via the O_2 absorption. Puse width of the excimer laser pulse width was about 20 ns and the fluence was about 1 mJ/cm^2. This laser power may be small to cause multi-photon process. Figure 4.3 shows that the ArF excimer laser pulse output measured by bi-plane photo-tube (Hamamatsu Photonics, R1193U-04)

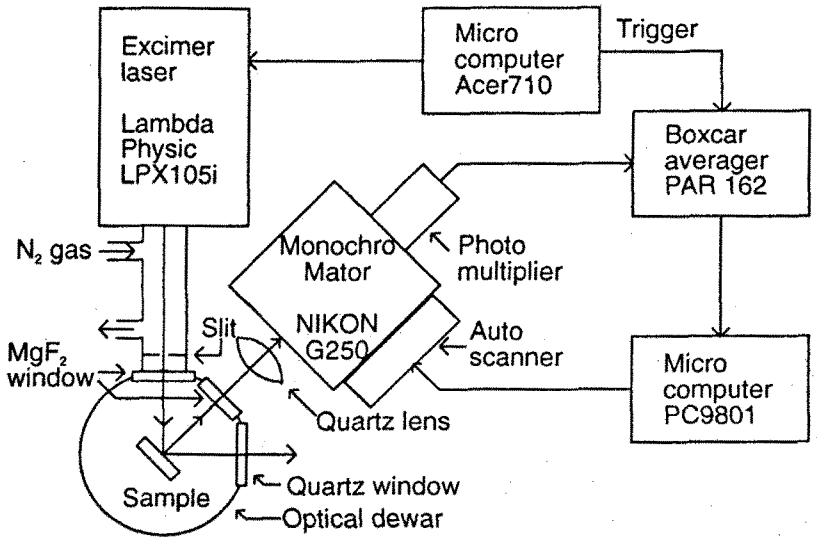

Figure 4.2. Schematic diagram of photoluminescence measurement system using excimer laser.

and storage oscilloscope (Philips, PM3302A).

4.3 Photoluminescence Excited by Deuterium Lamp

4.3.1 Growth Condition Dependence

The excitation light has a peak at around 7.7 eV, and spread from 7.47 to 8.05 eV. The emitted photon energy is smaller than the band gap of the SiO_2 (about 9 eV), and then the origin of the photoluminescence is radiative transition via defect energy levels instead of recombination through direct inter-band excitation. Moreover, the absorption peak at 6.3 eV is broad, and its full width at half maximum (FWHM) is about 1 eV. So, the defects corresponding to absorption peaks at 7.6 eV and 6.3 eV would be excited simultaneously under this excitation. Figure 4.4 shows the photoluminescence spectra of the photo-CVD SiO_2 thin films deposited on Si substrate at low (30 °C) and high (300 °C) temperatures. The photoluminescence peaks at 2.7, 3.6–3.8 and 4.4 eV were found in the SiO_2 film deposited at high temperature (300 °C), but the peak at 4.4 eV was not obtained in that deposited at low temperature (30 °C). It is reported that the photoluminescence peaks at around 2.7 and 4.3 eV exist in silica glass, and are caused by oxygen-deficient defect. However, 3.6–3.8 eV peak is not found in silica glass.

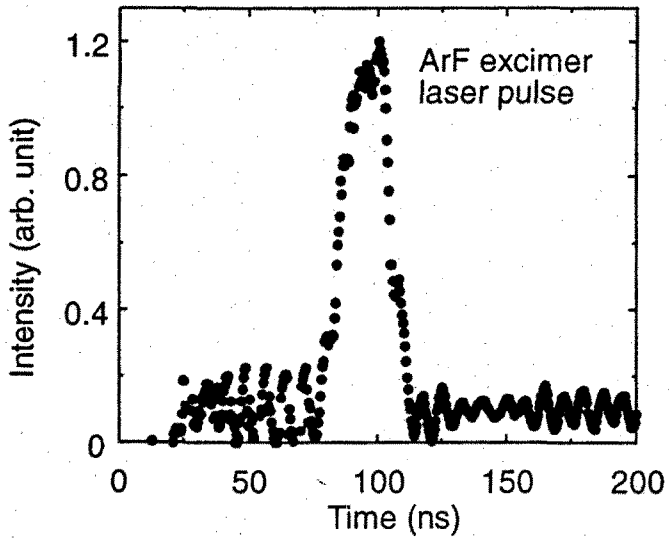

Figure 4.3. Transition intensity of ArF excimer laser output.

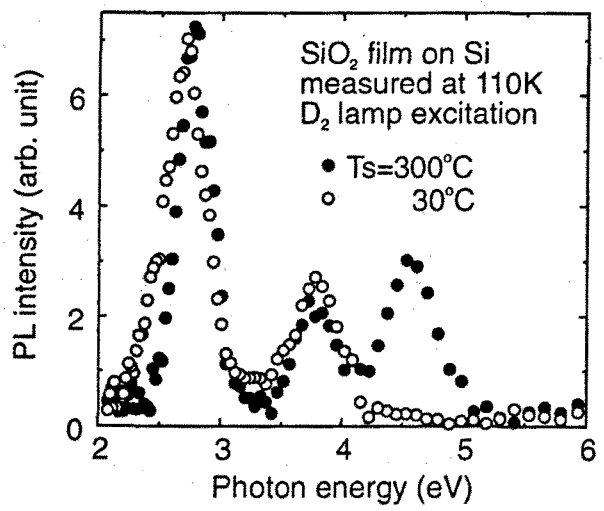

Figure 4.4. Photoluminescence spectra of the photo-CVD SiO_2 films deposited on Si substrate at low (30 °C) and high (300 °C) temperature.

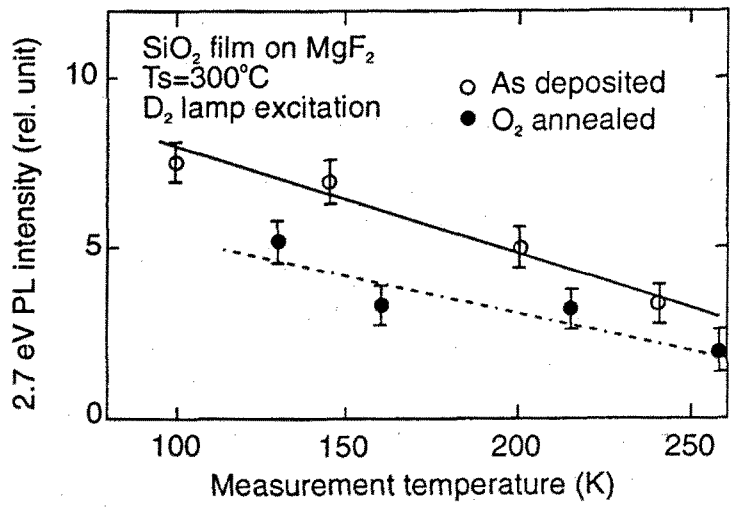

Figure 4.5. Intensity of photoluminescence peak at 2.7 eV in the film deposited at high temperature (300 °C) as a function of measurement temperature, and the film annealed in O_2 atmosphere at 400 °C for one hour.

4.3.2 Annealing Effect

The spectral change of the SiO_2 thin film deposited at high temperature is discussed to reveal the origins of a photoluminescence. Figure 4.5 shows the intensities of the photoluminescence peak at 2.7 eV as a function of the measurement temperature. The SiO_2 film was deposited at high temperature (300 °C), and this figure shows spectra before and after annealing in O_2 atmosphere for 1 hour. This figure shows that the 2.7 eV peak was decreased by the annealing in O_2 atmosphere. This suggests that this peak is closely related to oxygen-deficient defect. Another peak at 4.4 eV decreases with increasing O_2 flow-rate, but doesn't change by annealing in O_2 atmosphere. The result of the O_2 flow-rate dependence suggests that this 4.4 eV peak is closely related to oxygen-deficient defect. The reason why the intensity of this 4.4 eV peak doesn't decrease by the annealing is due to the fact that the annealing temperature is too low to activate the origin of this peak.

The spectral change of the film deposited at low temperature (30 °C) is discussed. Figure 4.6 shows the intensities of the photoluminescence peak at 2.7 eV as a function of the measurement temperature. The SiO_2 films were prepared at various gas-flow-rate-ratios (Si_2H_6/O_2 = 0.144, 0.181, and 0.241). It is shown that the intensities of all the photoluminescence peaks decrease with increasing measurement temperature, and can be interpolated by one line. This indicates that the photoluminescence peak at 2.7 eV in the film deposited at low temperature (30 °C) has little relation to

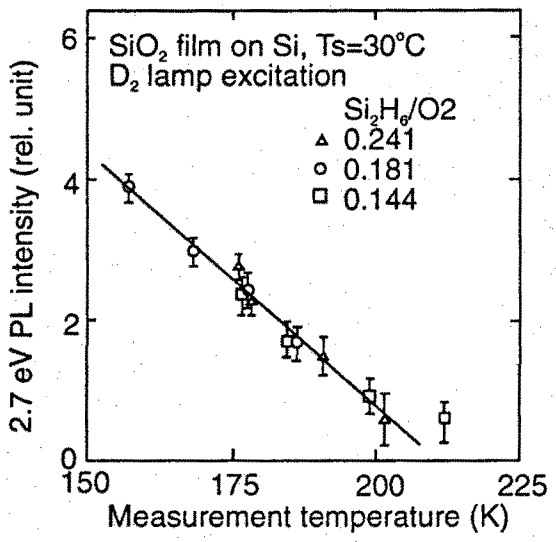

Figure 4.6. Intensities of photoluminescence peak at 2.7 eV as a function of the measurement temperature in the films deposited at various gas-flow-rate-ratio at low temperature (30 °C).

gas-flow-rate-ratio. Figure 4.7 shows the change of peak at 2.7 eV in the films deposited at low temperature (30 °C) and annealed in O_2 and N_2 atmosphere. Little change is found in the peak intensifies of the films annealed in O_2 and N_2 in comparison with that of the film deposited at high temperature (300 °C). Then this peak is thermally stable in both the O_2 and N_2 atmosphere and may be independent on oxygen amount during the deposition. This result may be attributable to a defect made from imperfectly broken species of Si_2H_6 unresolved at low growth temperature. Figure 4.8 shows the intensity changes of the photoluminescence peak at 3.6–3.8 eV as a function of measurement temperature. The film was deposited at low temperature (30 °C) and annealed in O_2 and N_2 atmosphere. In contrast to the peak at 2.7 eV shown in Fig. 4.7, the intensity of the peak at 3.6–3.8 eV was decreased by the annealing in O_2 or N_2 atmosphere, and the change is independent on the atmosphere. So, this peak is unstable thermally.

4.3.3 Summary

Table 4.1 and 4.2 summarize the substrate temperature, O_2 flow-rate dependence and annealing effects of various absorption and photoluminescence peaks excited by D_2 lamp. The changes of the absorption and photoluminescence peaks in the film deposited at high temperature (nearly 300 °C) are shown in Table 4.1. It is shown

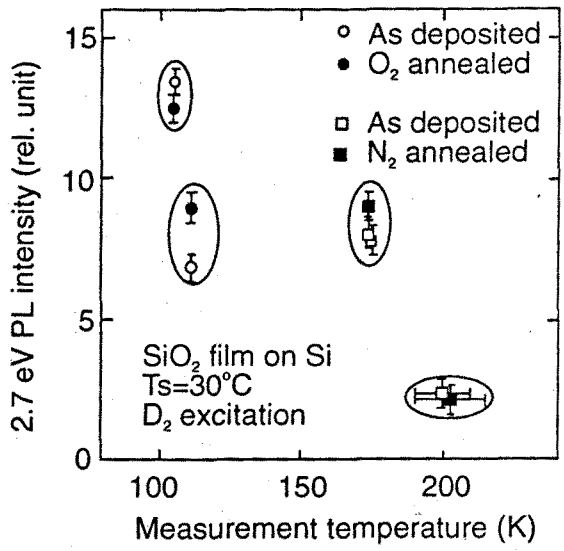

Figure 4.7. Intensity of photoluminescence peak at 2.7 eV in the films deposited at low temperature (30 °C) as a function of measurement temperature, and the films annealed in O_2 and N_2 atmosphere at 400 °C for 2 hours.

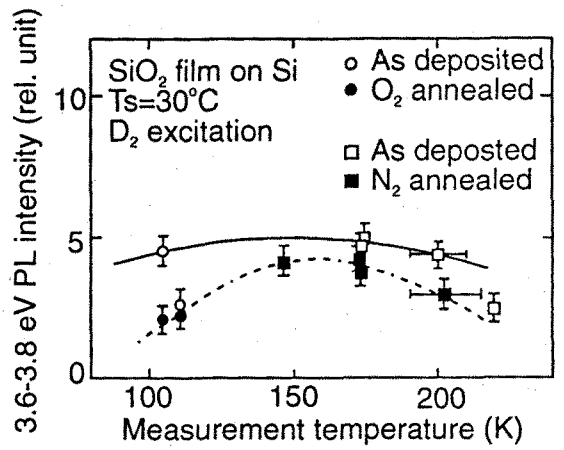

Figure 4.8. Intensity of photoluminescence peak at 3.6–3.8 eV in the film deposited at low temperature (30 °C) as a function of measurement temperature, and the film annealed in O_2 and N_2 atmosphere at 400 °C for 2 hours.

Table 4.1. Intensity change of the absorption peak at 7.6 eV and photoluminescence peaks at 2.7 eV and 4.4 eV in the SiO_2 film deposited at high temperature (nearly 300 °C) as parameters of substrate temperature (Ts) and O_2 flow-rate dependence and annealing in O_2 and N_2(Ar).

	Absorption	Photoluminescence	
	7.6 eV	2.7 eV	4.4 eV
Ts	↗	↘↗	↗
O_2 flow rate	↘	↘	↘
O_2 anneal	↘	↘	→
N_2 (Ar) anneal	→		

Table 4.2. Intensity change of the absorption peak at 6.3 eV and photoluminescence peaks at 2.7 eV and 3.6–3.8 eV in the SiO_2 film deposited at low temperature (nearly 30 °C) as parameters of substrate temperature (Ts) and O_2 flow-rate dependence and annealing in O_2 and N_2(Ar).

	Absorption	Photoluminescence	
	7.6 eV	2.7 eV	3.6–3.8 eV
Ts	↘	↘↗	↘↗
O_2 flow rate	↗	→	
O_2 anneal	↗	→	↘
N_2 (Ar) anneal	↘	→	↘

in this table that the change of the absorption peak at 7.6 eV is similar to that of the photoluminescence peak at 4.4 eV except for O_2 annealing effect. The reason that the 4.4 eV photoluminescence peak is insensitive to annealing may be that the temperature (400 °C) is not high enough to react O atom and/or O_2 with the defect giving rise to this peak, and the excited electron energy cannot be transferred to the radiative recombination center in incomplete Si–O network. Then, such difference of the behavior between 7.6 eV absorption and 4.4 eV photoluminescence occurs. So, the origin of the absorption peak at 7.6 eV may relate to the photoluminescence peak at 4.4 eV in the film deposited at high temperature, and this origin is an oxygen vacancy. Moreover, the change of the photoluminescence peak at 2.7 eV in the film deposited at high temperature is also similar to the peak at 7.6 eV, and the intensities of these peaks are reduced by O_2 annealing. This suggests that these absorption and photoluminescence peaks in the film deposited at high temperature are caused by the same oxygen-vacancy.

The changes of the absorption and photoluminescence peaks in the film deposited at low temperature (nearly 30 °C) are shown in Table 4.2. The changes of the photoluminescence peaks at 2.7 eV and 3.6-3.8 eV are different for annealing in O_2 and N_2. This suggests that these peaks originate from different defects. Furthermore, the change of the absorption peak at 6.3 eV is different from that of the photoluminescence peaks at 2.7 eV and 3.6–3.8 eV in the film deposited at low temperature. It seems that these photoluminescence peaks and this absorption peak originate in different defects. That is, the absorption peak at 6.3 eV relates to oxygen-excess defect, and the photoluminescence peak at 2.7 eV is independent on oxygen and is stable thermally.

Next, comparing Table 4.1 and 4.2, the photoluminescence peak at 2.7 eV in the film deposited at high temperature does not show the same behavior as that of the film deposited at low temperature. This suggests that the origin and/or thermal stability of the peak at 2.7 eV in the film deposited at high temperature (nearly 300 °C) is different from that in the film deposited at low temperature (nearly 30 °C), or electron energy transfers are different in both the films, although the peak energies are agree with each other.

It has been shown that the behaviors of the absorption and photoluminescence are different in the films deposited at low and high temperature. This may be because that the reaction processes between Si_2H_6 and O_2 are quite different at low and high temperature during the deposition. Si_2H_6 is broken thermally and photochemically at high temperature, but at low temperature this is broken only by high energy photon. So, the amounts of Si–O–H and Si–H may increase with decreasing growth temperature, and imperfectly broken silicon hydrides such as H_x–Si–Si–H_y may remain in films made at low growth temperature. Moreover, insufficient reaction on the surface of substrate causes defects or deteriorates film quality. On the other hand, oxygen may adsorb on the surface of substrate during the deposition, but these may leave the substrate easily at high substrate temperature. Then the oxygen

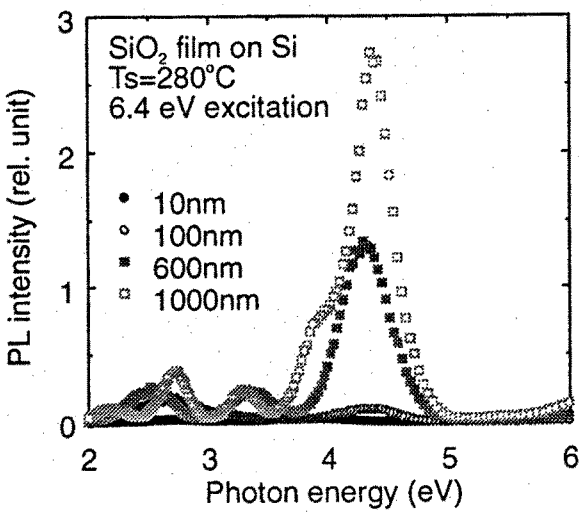

Figure 4.9. Photoluminescence spectra under 6.4 eV excitation. SiO_2 films of various thicknesses were deposited at high temperature (280 °C) by photo-CVD.

vacancy may be formed in the film deposited at high temperature.

4.4 Photoluminescence Excited by ArF Excimer Laser

4.4.1 Growth Condition Dependence

In this section, photoluminescence excited by excimer lasers were discussed. An excimer laser is a strong UV light source, for example the maximum output power of LPX105i is 200 mJ/cm^2 / 20 ns = 10 MW. Moreover, as used lasers emit a short pulse, photoluminescence life-time can be studied by inspecting energy transfer mechanism. Figure 4.9 shows the photoluminescence spectra under 6.4 eV excitation on photo-CVD SiO_2 films deposited at high temperature (280 °C). The film thicknesses are 10, 100, 600, and 1000 nm. Photoluminescence peaks are observed at around 2.4, 3.5 and 4.4 eV. The magnitude of the 4.4 eV peak increases with increasing film thickness, but the 2.4 eV peak is nearly independent of film thickness. The thickness independence suggests that the photoluminescence peak at 2.4 eV results from a defect localized near the interface. The strong thickness dependence of the 4.4 eV peak suggests that its origin distributes in a bulk. Figure 4.10 shows the photoluminescence spectra from SiO_2 thin films. The SiO_2 thin films were deposited at low temperature (47 °C). This figure shows that the peaks appear at around 2.7, 3.4 and 4.3 eV in all films. The peaks at 2.7 and 4.3 eV increase with increasing film thickness. This incrase indicates that the photoluminescence peaks

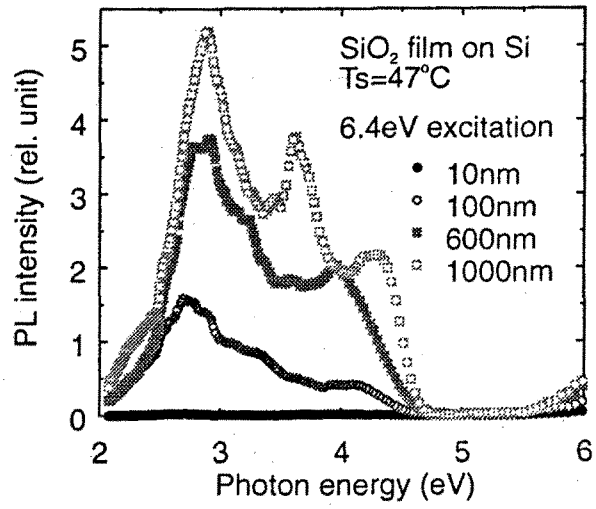

Figure 4.10. Photoluminescence spectra under 6.4 eV excitation. SiO_2 films of various thicknesses were deposited at low temperature (47 °C) by photo-CVD.

at 2.7 eV and 4.4 eV in the photo-CVD SiO_2 thin film deposited at low temperature (47 °C) result from a defect distributed wholly in the bulk. Although the peak energies are not very different between high (280 °C) and low (47 °C) temperature, the thickness dependence of the 2.4–2.7 eV and 3.4–3.5 eV peaks are quite different, and hence their origins may be different or generation mechanism of these defects may be different.

The 4.4 eV peak was not found on photoluminescence using D_2 lamp for excitation in the SiO_2 thin film deposited at low temperature (around 30 °C), but found on ArF excimer laser excitation. The light intensity of the excimer laser is much larger than D_2 lamp. Therefore, energy transfer mechanisms may by different each other, or the absorption cross section may be small. The light intensity of D_2 lamp may be insufficient to measure with this system.

The gas-flow-rate-ratio dependence was also measured. The gas-flow-rate-ratio is changed from 0.18 to 0.36 (Si_2H_6/O_2). Photoluminescence peak at 2.4 eV increased with increasing O_2 flow-rate rate in the sample deposited at high temperature (280 °C).

4.4.2 Measurement Temperature Dependence

Figure 4.11 shows the intensities at 2.4 and 4.4 eV of the photoluminescence peaks as a function of measurement temperature. The SiO_2 thin film was deposited at high temperature (280 °C). Figure 4.12 shows the intensities at 2.7, 3.4 and 4.4

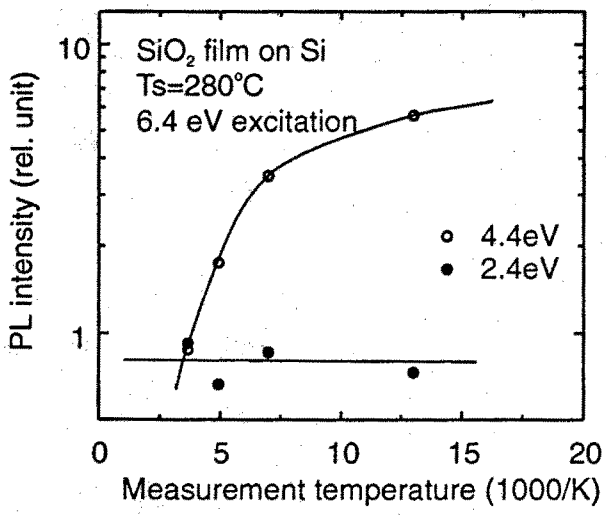

Figure 4.11. Photoluminescence peak intensities excited by ArF excimer laser as a function of measurement temperature. The SiO_2 thin film was deposited on silicon at high temperature (280 °C) by photo-CVD.

eV of the photoluminescence peaks as a function of measurement temperature. The SiO_2 thin film was deposited at low temperature (47 °C). The 4.4 eV peak intensity increases with decreasing measurement temperature in the samples grown at both high and low substrate temperatures, but the dependence of the peak intensity at about 2.4 (2.7) eV is different: the high-growth-temperature film is almost constant in the whole temperature, but low-growth-temperature film is decreased with increasing measurement temperature. These dependence suggests that 4.4 eV peak in the photo-CVD SiO_2 thin films deposited at both low and high substrate temperatures is cased by same defect, but about 2.4 eV is not. These results agree with the dependence of photoluminescence peak intensity on film thickness.

4.4.3 Decay

Transient intensity of he photoluminescence was measured, as the excimer laser emits a short pulse light of about 20 ns. The transient of photoluminescence, that is decay, is related to the mechanism of absorption, electron energy transfer and radiative recombination. Figure 4.13 shows the transient signal of the photoluminescence peak intensity at 4.4 eV measured at room temperature. This spectrum was taken with the digital storage oscilloscope (Philips PM3320A) and photo-multiplier tube (Hamamatsu Photonics, R1508). The measured transient is very fast and is comparable with the response of the laser or measurement system. In addition, the other

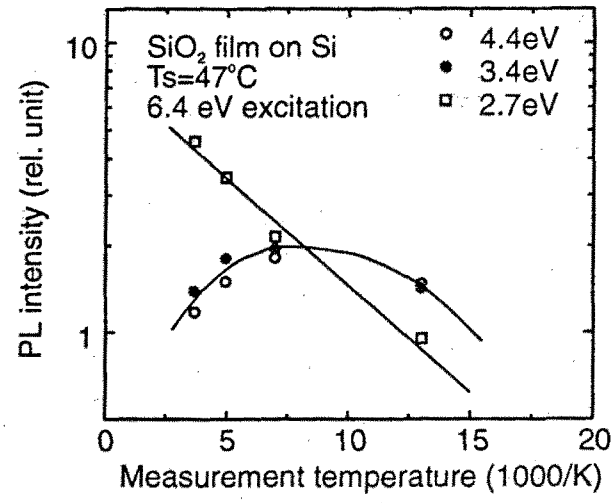

Figure 4.12. Photoluminescence peak intensities excited by ArF excimer laser as a function of measurement temperature. The SiO_2 thin film was deposited on silicon at low temperature (47 °C).

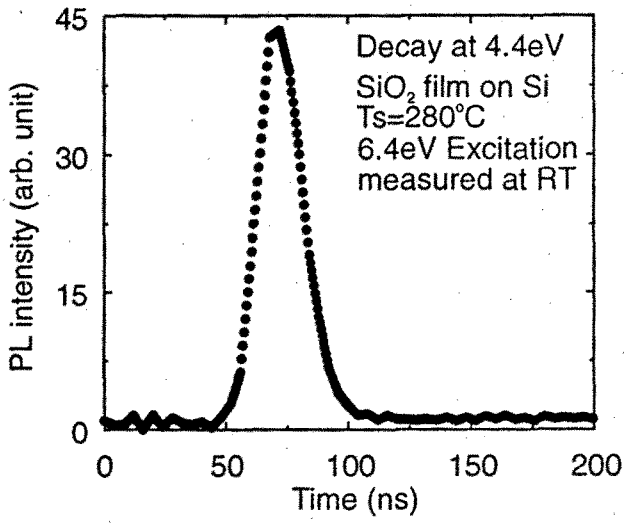

Figure 4.13. Transient signal of the peak intensity at 4.4 eV under 6.4 eV excitation. The sample was deposited on silicon at high temperature (280 °C).

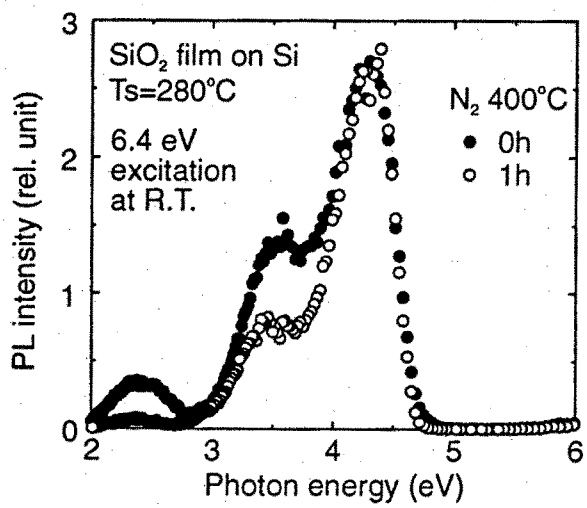

Figure 4.14. Photoluminescence spectra before and after annealing in N_2 atmosphere at 400 °C for 1 hour. The SiO_2 thin films were deposited at high temperature (280 °C) by photo-CVD.

peaks are similar to this transient, and the transient does not change even at 77 K. This indicates that the emission relates little to slow decay corresponding to a forbidden transition such as a triplet-singlet transition [1, 2] or fast non-radiative recombinations.

4.4.4 Annealing Effect

The effects of annealing in O_2 and N_2 gas atmosphere are measured to clarify the origin of the photoluminescence peaks. The annealing was done in N_2 or O_2 gas at 1 atm at 400 °C for 1 hour. Figure 4.14 shows the annealing effect of photoluminescence of SiO_2 thin film deposited at high temperature (280 °C) in N_2 atmosphere. Figure 4.15 shows the annealing effect of photoluminescence spectra of SiO_2 thin films deposited at high temperature (280 °C) in O_2 atmosphere. The photoluminescence peak at 4.4 eV decreases by annealing in O_2, but shows little change after annealing in N_2 for 1 hour. This suggests that the 4.4 eV peak results from an oxygen-deficient defect. Since the 4.4 eV photoluminescence peak and the 7.6 eV absorption peak show similar thickness dependence as well as the annealing dependence, these peaks may originate from the same defect. On the other hand, The peaks at 2.4 and 3.5 eV decreased by N_2 annealing, but increased by O_2 annealing. These suggest that the 2.4 and 3.5 eV peaks relates oxygen-excess defects, and these defects are unstable.

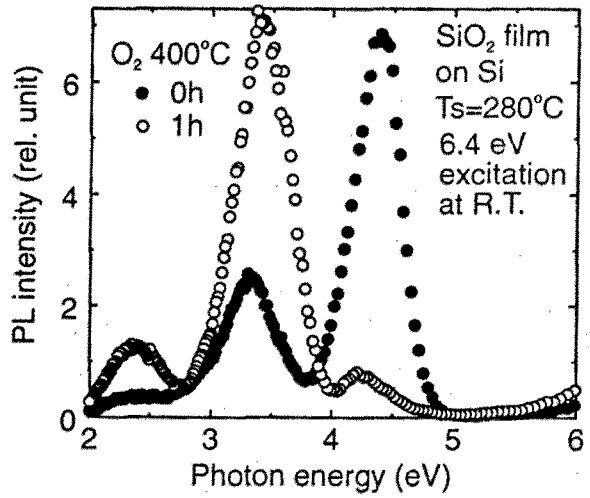

Figure 4.15. Photoluminescence spectra before and after annealing in O_2 atmosphere at 400 °C for 1 hour. The SiO_2 thin films are deposited at high temperature (280 °C) by photo-CVD.

Figure 4.16 shows the annealing effect of photoluminescence spectra of SiO_2 films deposited at low temperature (47 °C) in N_2 atmosphere. Figure 4.17 shows the annealing effect of photoluminescence spectra of SiO_2 films deposited at low temperature (47 °C) in O_2 atmosphere. These figures show that the photoluminescence peak at 4.4 eV in the film deposited at low temperature (47 °C) increases by annealing in N_2 for 1 hour, and decreases with annealing time in N_2 over 1 hour. It is considered from these results, this peak is oxygen-deficient defect rather than oxygen-excess defect, because the SiO_2 thin film of low temperature growth includes unstable defects (it plays as precursor). It may be dominant that the precursor changes into oxygen-deficient defect in early stage, and the produced oxygen-deficient defect is reduced gradually by annealing in N_2 atmosphere. The other peaks at 2.7 and 3.5 eV are decreased by annealing in N_2. This suggests that the origins of these peaks are oxygen-excess defect. This is similar to high growth temperature SiO_2 thin film.

4.5 Photoluminescence Excited by F_2 Excimer Laser

4.5.1 Film Thickness Dependence

The photoluminescence excited by high energy photon than 6.4 eV is studied. The excitation light source is F_2 excimer laser and this emits 7.9 eV photon. This photon is absorbed by 7.6 eV absorption peak and absorption edge in the photo-

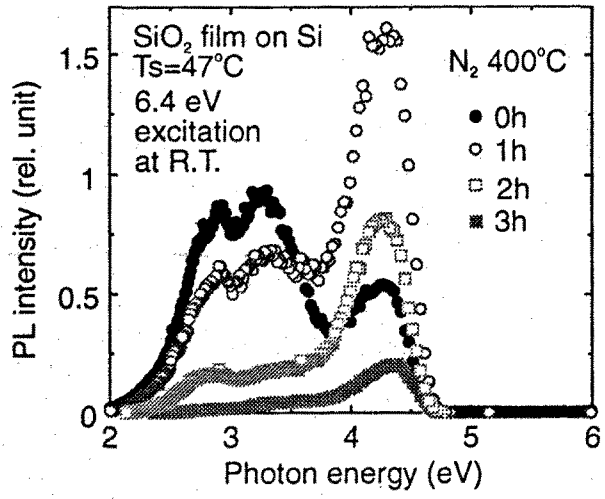

Figure 4.16. Photoluminescence spectra before and after annealing in N_2 atmosphere at 400 °C for 1 hour. The SiO_2 thin films were deposited at low temperature (47 °C) by photo-CVD.

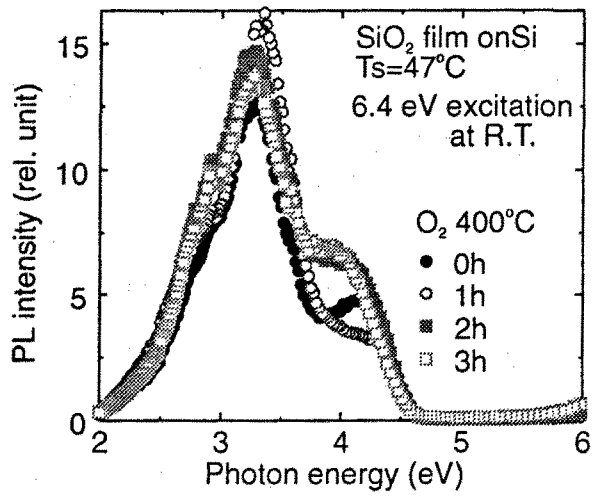

Figure 4.17. Photoluminescence spectra before and after annealing in O_2 atmosphere at 400 °C for 1 hour. The SiO_2 thin films were deposited at low temperature (47 °C) by photo-CVD.

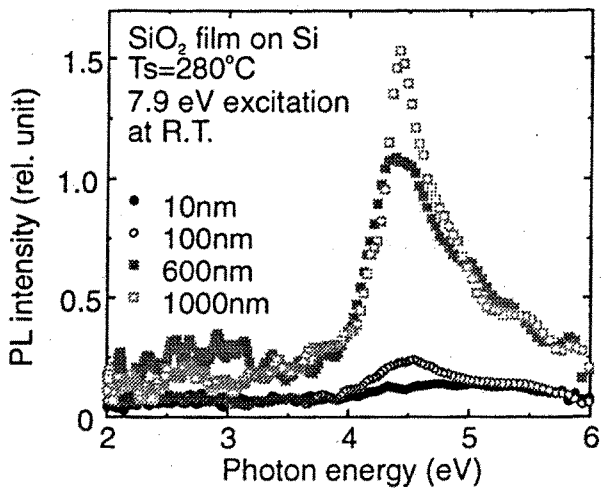

Figure 4.18. Photoluminescence spectra under 7.9 eV excitation. SiO_2 thin films of various thicknesses were deposited at high temperature (280 °C) by photo-CVD.

CVD SiO_2 thin film. Figure 4.18 shows the photoluminescence spectra measured using 7.9 eV excitation. The SiO_2 films were deposited at high temperature (280 °C), and the thicknesses are 10, 100, 600, and 1000 nm. A peak is observed at 4.4 eV whose magnitude increases with increasing film thickness. The thickness dependence of this peak agrees with that measured using 6.4 eV excitation shown in Fig. 4.9. The 4.4 eV photoluminescence peaks excited by both F_2 (7.9 eV) and ArF (6.4 eV) excimer lasers are probably caused by the same defect. On the other hand, the peaks at 2.4 eV and 3.5 eV found under 6.4 eV excitation are not measured in the spectra excited by the 7.9 eV excimer laser. This may result from a changing energy transfer system with different excitation energy, or the origins of the 2.4 and 3.5 eV peaks have no absorption and cannot be excited by 7.9 eV.

Figure 4.19 shows the photoluminescence spectra of SiO_2 thin films deposited at low temperature (47 °C), whose thicknesses are 10, 100, 600, and 1000 nm. The peaks at 2.7, 3.5 and 4.4 eV exist in the photoluminescence spectra excited by the F_2 (7.9 eV) excimer laser. The line shapes and the thickness dependence of these spectra are similar to that under 6.4 eV excitation. These results suggest the photoluminescence spectrum of the 280 °C photo-CVD SiO_2 film is sensitive to the excitation photon energy, but the 47 °C photo-CVD SiO_2 film is not sensitive to the excitation energy.

Now, behaviours of the photoluminescence excited by D_2 lamp and F_2 excimer laser are different each other in spite of nearly equal excitation energy (7.7 eV and 7.9 eV). The photon number of D_2 lamp is 5.66×10^{17} photons/s (It is assumed that D_2

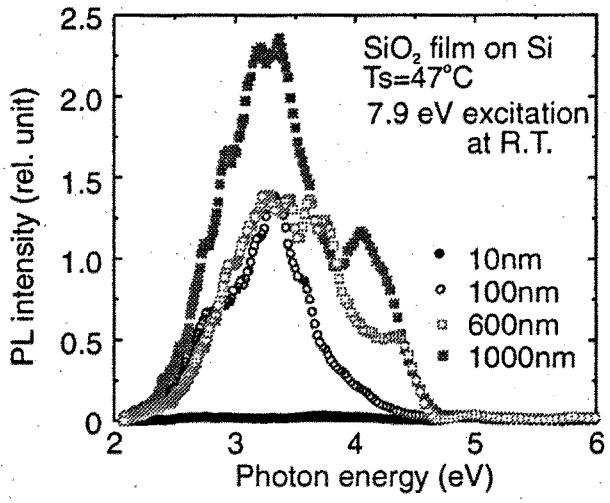

Figure 4.19. Photoluminescence spectra under 7.9 eV excitation. SiO_2 films of various thicknesses were deposited at low temperature (47 °C) by photo-CVD.

lamp output power is 150 W, the light output in the region of 160 nm±3 nm is 30 %, irradiation solid angle is 5.639 cm^2 (spread for 30 degree, the distance from the light to an object is 5 cm), transmittance of MgF_2 window is 80 %, diffraction efficiency of VUV monochromator is 11 %), one of F_2 excimer laser is 4.03×10^{22} photons/s (It is assumed: The output is 1 mJ/cm^2, Pulse width is 20 ns). To compare these, the photons from F_2 excimer laser is much larger than D_2 lamp. In addition to this, the excimer laser emits a short pulsed light. So, the mechanism of energy-transfer may be much different, and so the photoluminescence behaviours are different between D_2 lamp and F_2 excimer laesr excitatoins.

4.5.2 Measurement Temperature Dependence

Figure 4.20 shows the dependence of the photoluminescence peak intensity on measurement temperature in the SiO_2 thin film deposited at high temperature (280 °C). Figure 4.21 shows the dependence of the photoluminescence peak intensity on measurement temperature in the SiO_2 thin film deposited at low temperature (47 °C). The 4.4 eV peak intensity increased with decreasing measurement temperature in the sample grown at both high and low substrate temperatures, and this agrees with the photoluminescence excited by ArF excimer laser.

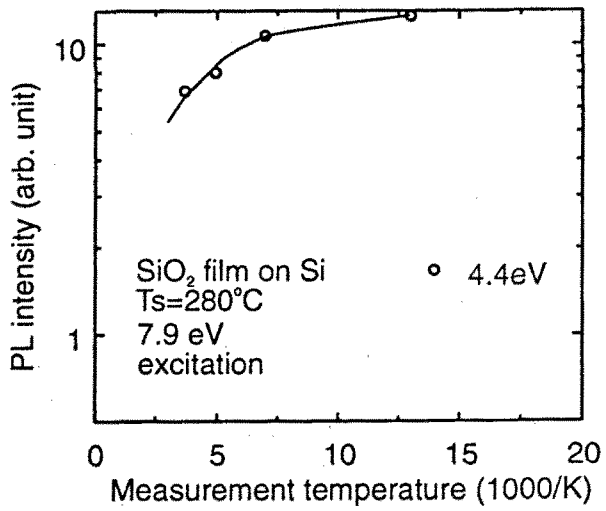

Figure 4.20. Intensities of photoluminescence peak at 4.4 eV excited by F_2 excimer laser as a function of measurement temperature. The SiO_2 thin film was deposited on silicon at high temperature (280 °C) by photo-CVD.

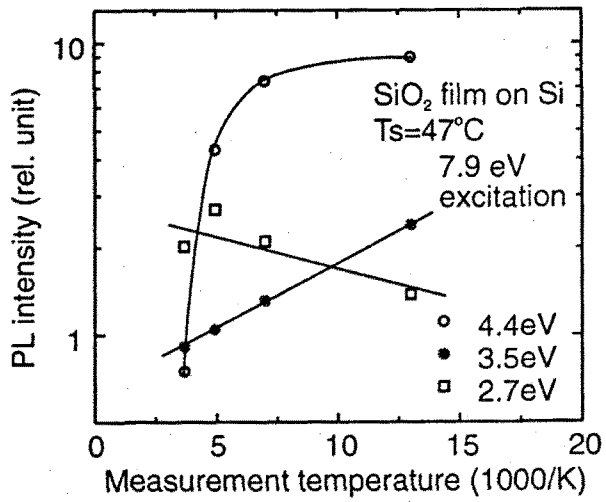

Figure 4.21. Intensities of photoluminescence peaks at 2.7, 3.5 and 4.4 eV excited by F_2 excimer laser as a function of measurement temperature. The SiO_2 thin film was deposited on silicon at low temperature (47 °C) by photo-CVD.

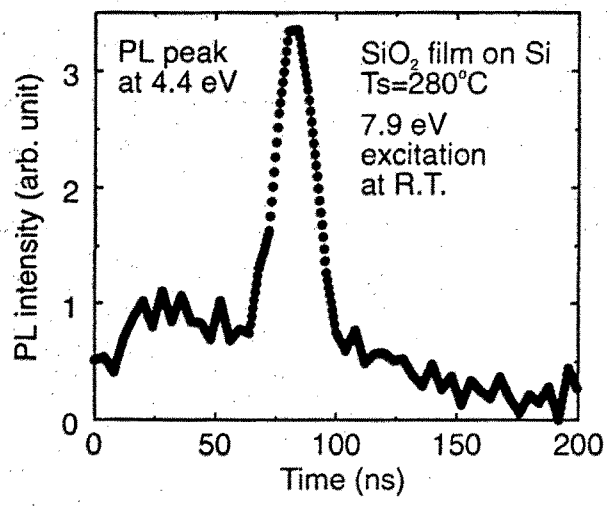

Figure 4.22. Transient signal of the peak intensity at 4.4 eV under 7.9 eV excitation. The SiO_2 thin film was deposited on silicon at high temperature (280 °C) by photo-CVD.

4.5.3 Decay

Figure 4.22 shows the transient signal of the photoluminescence peak intensity at 4.4 eV measured at room temperature. The measured transient is very fast and is comparable with the response of the laser or measurement system similarily to that excited by ArF excimer laser. In addition, the transient does not change, even at 77K. This indicates that the emission relates little to slow decay corresponding to a forbidden transition such as a triplet-singlet transition, or there are fast and main energy path relating to non-recombination. Moreover, the photoluminescence transient of the SiO_2 thin film deposited at low temperature (47 °C) is also very short. These are the same results as ArF excimer laser.

4.5.4 Annealing Effect

The annealing effect of photoluminescence spectra of the photo-CVD SiO_2 film in N_2 or O_2 atmosphere at 400 °C for 1 hour is studied using 7.9 eV excitation. The photoluminescence peak at 4.4 eV in the film deposited at 280 °C decreases by annealing in O_2, but hardly changes by annealing in N_2 for 1 hour. Similarly, to the ArF photoluminescence results, these behaviours suggest that the 4.4 eV peak results from the oxygen-deficient defect.

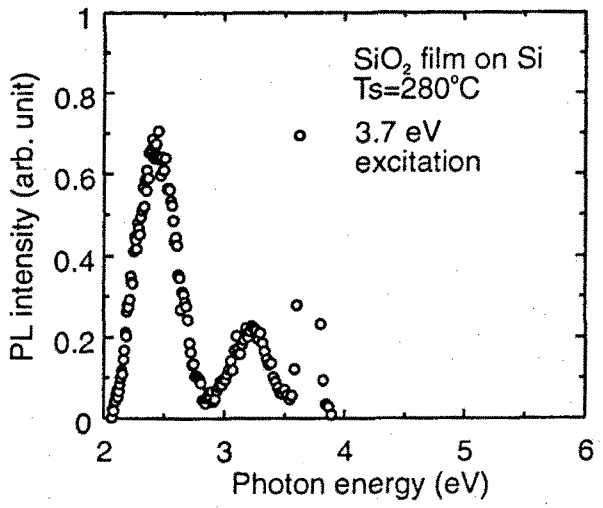

Figure 4.23. Photoluminescence spectra under 3.7 eV excitation. SiO_2 films of various thicknesses were deposited at high temperature (280 °C) by photo-CVD.

4.6 Photoluminescence Excited by N_2 Laser

The photoluminescence excited by another energy photon was also measured. The light source is N_2 laser (PAR Laser, LN120C). Wavelength is 337.1 nm (3.678 eV), pulse width is 300 ps, output power is about 50 $\mu J/cm^2$. N_2 laser is very shorter pulse width and weaker output power than excimer laser. Figure 4.23 shows the photoluminescence spectrum of SiO_2 thin film deposited by photo-CVD at high temperature (280 °C). The photoluminescence peaks at 2.4 and 3.2 eV appear. The 4.4 eV which is larger than the excitation light energy is not found, and then multi-photon process does not happen. These peak energies are similar to the case excited by ArF excimer laser, but peak shifts to low energy. The optical absorption bands of these peaks may be spread from very low (3.7 eV of N_2 laser) to high energy (6.4 eV of ArF excimer laser or 7.7 eV of D_2 lamp). Figure 4.24 shows the photoluminescence spectrum of SiO_2 thin film deposited at low temperature (47 °C). The photoluminescence peak at 2.9 eV appears, and this spectrum is different from one excited by excimer laser.

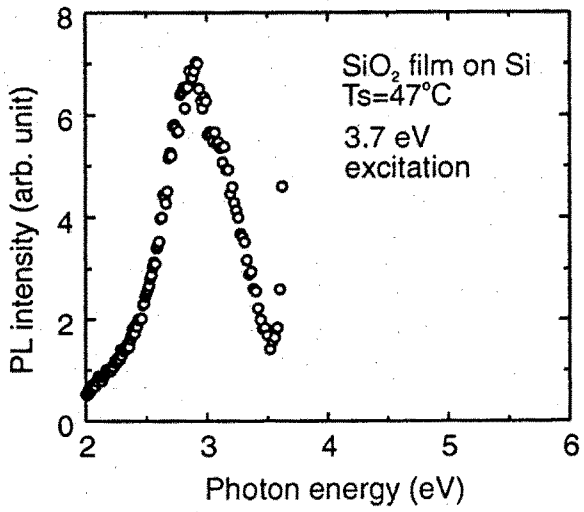

Figure 4.24. Photoluminescence spectra under 3.7 eV excitation. SiO_2 films of various thicknesses were deposited at low temperature (47 °C) by photo-CVD.

Reference

[1] J. H. Stathis and M. A. Kastner: Phys. Rev. B **35** (1987) 2972.

[2] H. Nishikawa, E. Watanabe, D. Ito, Y. Ohki: Phys. Rev. B **72** (1994) 2101.

[3] M. Kohketsu, K. Awazu, H. Kawazoe and M. Yamane: Jpn. J. Appl. Phys. **28** (1989) 615.

[4] R. Tohmon, Y. Shimogaichi, S. Munekuni, Y. Ohki, Y. Hama and K. Nagasawa: Appl. Phys. Lett. **54** (1989) 1650.

[5] P. J. Alonso, L. E. Halliburton, E. E. Kohnke, and R. B. Bossoli: J. Appl. Phys. **54** (1983) 5369.

[6] H. Nishikawa, T. Shiroyama, R. Nakamura, Y. ohki, K. Nagasawa and Y. Hama: Phys. Rev. B **45** (1992) 586.

[7] K. Awazu, K. Watanabe and H. Kawazoe: Jpn. J. Appl. Phys. **32** (1993) 2746.

[8] T. Kanashima, R. Nagayoshi, M. Okuyama and Y. Hamakawa: J. Appl. Phys. **74** (1993) 5742.

[9] T. Kanashima, M. Okuyama and Y. Hamakawa: Jpn. J. Appl. Phys. **32** (1993) 3113.

[10] T. Kanashima, M. Okuyama and Y. Hamakawa: Appl. Surf. Sci. *79/80* (1994) 321.

Chapter 5

Excimer Laser Irradiation Effect

5.1 Introduction

It is reported in photoluminescence and absorption measurements that various defect structures in silica glass (fused quartz) are changed by irradiation of an ArF excimer laser [1–5]. Therefore, it is thought that the irradiation induces production and reduction of the defects in the photo-CVD SiO_2 thin films as well, and these changes yield some information about defect characteristics. Addition all, KrF and ArF excimer lasers are used for photo-lithography, and so irradiation effects is expected to be characterized from a viewpoint of application to the lithography. In this section, the irradiation effect has been studied by means of photoluminescence, optical absorption and electron spin resonance (ESR). The result shows that ArF excimer laser irradiation is quite different from F_2 excimer laser.

5.2 Measurement Method of Irradiation Effect

The SiO_2 thin films were deposited by photo-CVD on MgF_2 for optical absorption or Si for photoluminescence and ESR measurements. The samples were set in optical dewar in vacuum, and were irradiated by ArF and F_2 excimer lasers at RT. The ArF excimer laser output power is 30 mJ/cm^2, and F_2 excimer laser output power is about 5 mJ/cm^2. Optical absorption and photoluminescence were measured by the same system as described in chapters 3 and 4. ESR spectra were measured by X-band ESR spectrometer (Jeol, JES-ME-2X). The sample was cut 15x3x0.5 mm, and set in quartz tube. Microwave power is 6 mW, and the spectra were measured at RT. or liq. N_2 temperature. The SiO_2 thin film was deposited on a high-resistivity (900–1200 Ω·cm) Si substrate.

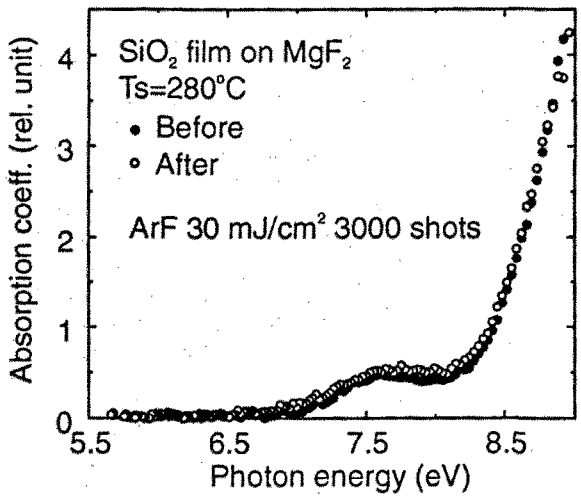

Figure 5.1. Absorption spectra before and after irradiation of ArF excimer laser. The SiO_2 film was deposited at high temperature (280 °C) on MgF_2 by photo-CVD.

5.3 Optical Absorption

The absorption peak at 7.6 eV or 6.3 eV is found in the photo-CVD SiO_2 films on the MgF_2 substrate, and its intensity greatly depends on growth temperature [6–8]. The SiO_2 film deposited at high temperature (about 300 °C) has the absorption peak at 7.6 eV which is caused by an oxygen-vacancy (Si–Si) [9, 10]. By contrast, the SiO_2 film deposited at low temperature (about 50 °C) has the peak at 6.3 eV which is related to an oxygen-excess defect. Figure 5.1 shows the absorption spectra before and after the irradiation of the ArF excimer laser. The SiO_2 film was deposited on MgF_2 plate at high temperature (280 °C). The absorption peak at 7.6 eV exists in the as-grown film, and little change is observed after the irradiation. The 6.4 eV photon may not break oxygen-vacancy such as Si–Si, or this defect may have no absorption band around 6.4 eV. Figure 5.2 shows the absorption spectra before and after ArF excimer laser irradiation in the film deposited at low temperature (47 °C). The absorption peak at 6.3 eV exists in the as-grown film. This peak is caused by a defect relating to excess oxygen, for example Si–O–H, Si–O–O ·. This peak decreased after irradiation.

Figure 5.3 shows the absorption spectra before and after the F_2 excimer laser irradiation. The SiO_2 film was deposited on MgF_2 at high temperature (280 °C). In contrast to those of the irradiation of ArF excimer laser (Fig. 5.1), the absorption peak at 7.6 eV was decreased by irradiation with the F_2 excimer laser. It is suggested

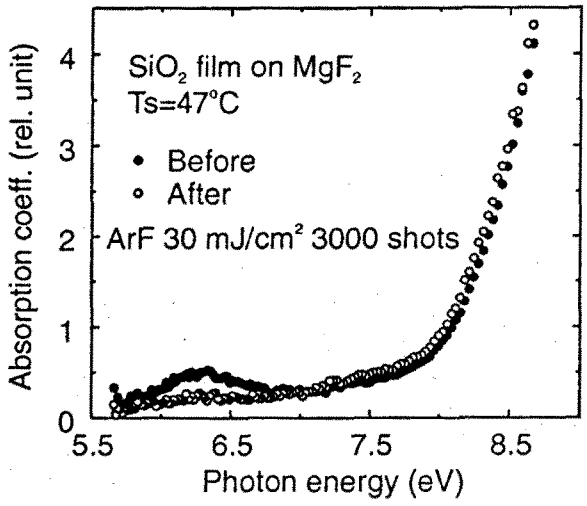

Figure 5.2. Absorption spectra before and after irradiation of ArF excimer laser. The SiO_2 film was deposited at low temperature (47 °C) on MgF_2 by photo-CVD.

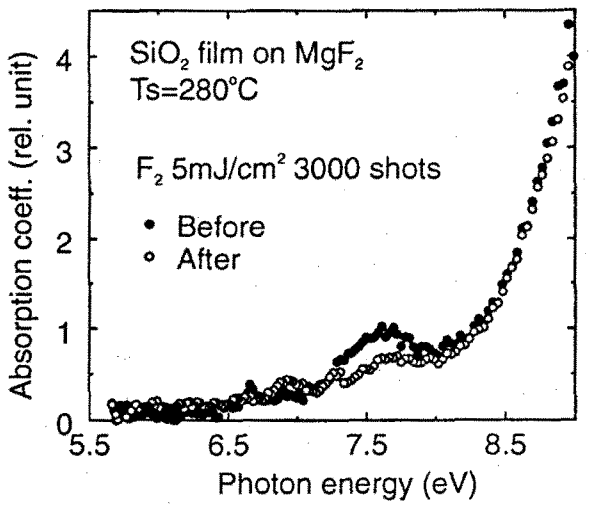

Figure 5.3. Absorption spectra before and after irradiation of F_2 excimer laser in the film deposited at high temperature (280 °C) on MgF_2 by photo-CVD.

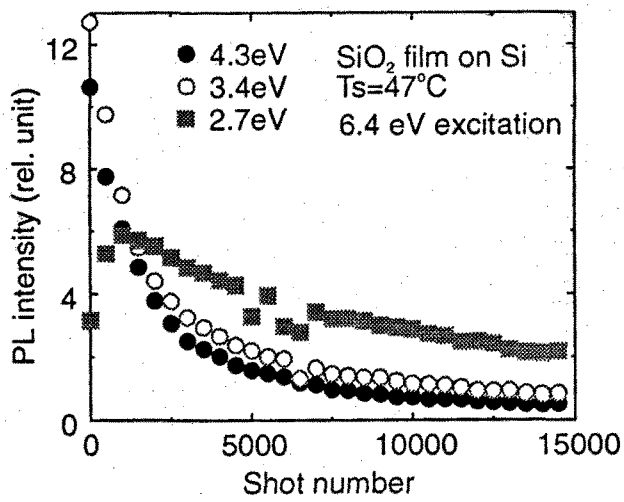

Figure 5.4. Changes of the peak intensity upon irradiation with ArF excimer laser.

that a defect such as Si–Si was broken by F_2 excimer laser irradiation. On the other hand, the peak at 6.3 eV in the film deposited at low temperature (47 °C) was decreased upon irradiation. It is thought that the defect of the absorption peak at 7.6 eV is tight and is broken only by a high energy photon, but the defect of the peak at 6.3 eV is unstable and easily broken.

5.4 Photoluminescence

Figure 5.4 shows the changes in intensity of photoluminescence peaks as a function of shot number of the ArF excimer laser. The peak intensities at 4.3 eV and 3.4 eV decrease monotonously with the shot number of ArF excimer laser irradiation, but the peak at 2.7 eV increases below 2000 laser shots and decreases above 2000 laser shots. Such behavior was observed in films deposited at both high (280 °C) and at low (47 °C) temperatures. Figure 5.5 shows the photoluminescence peak intensity at 2.7 eV before and after O_2 annealing as a function of shot number. The same behavior was also observed in the sample which was annealed in O_2 at 400 °C for 1 hour after laser irradiation. On the other hand, figure 5.6 shows that the peak intensity in the sample annealed in N_2 decreased monotonously with increasing shot number. These suggest that the increase of intensity below 2000 shots is related to oxygen. It is likely that impure structures in the thin film such as Si–H and Si–O–H, are promoted to react with oxygen by ArF excimer laser irradiation, and then form another defect having 2.7 eV luminescence which increases at the initial stage. More irradiation collapses the defect corresponding to 2.7 eV emission.

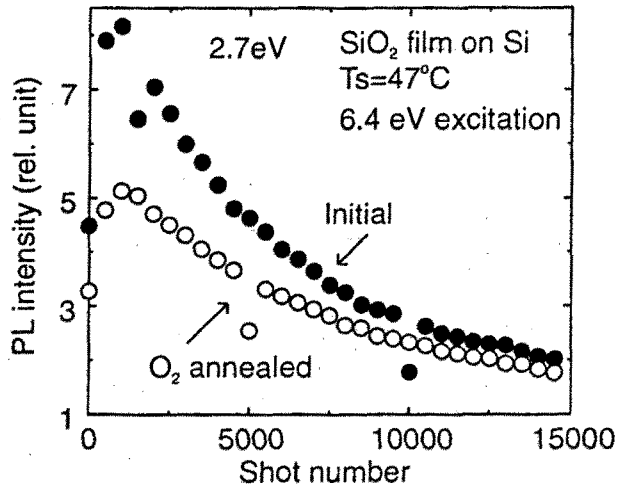

Figure 5.5. Change of the photoluminescence peak intensity at 2.7 eV upon irradiation with ArF excimer laser and the effect of annealing in O_2.

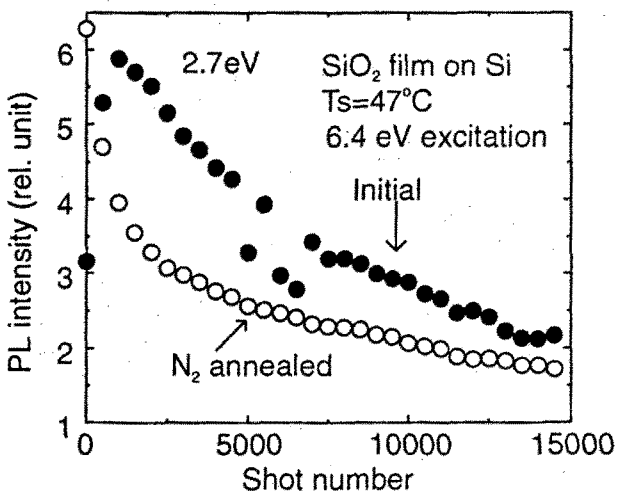

Figure 5.6. Change of the photoluminescence peak intensity at 2.7 eV upon irradiation with ArF excimer laser and the effect of annealing in N_2.

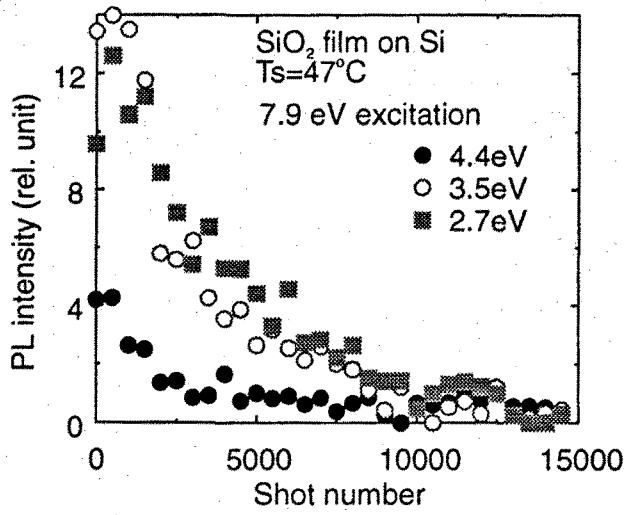

Figure 5.7. Changes of the photoluminescence peak intensities upon irradiation with F_2 excimer laser.

Figure 5.7 shows the changes in intensity of photoluminescence peaks as a function of shot number of the F_2 excimer laser. The intensity of photoluminescence peaks was measured as a function of shot number of F_2 excimer laser irradiation. The intensities in the SiO_2 thin films deposited at both high (280 °C) and low (47 °C) temperatures decreased monotonously with the shot number. Moreover, the intensity did not increase in the film after annealing in O_2, and no marked changes occurred after annealing in O_2 or N_2. This indicates that the 7.9 eV photon changes the defects, and the changed defects cannot be recovered by N_2 or O_2 annealing. This suggests that the 7.9 eV photon (F_2 excimer laser) changes the defect to a rather different one, but the 6.4 eV photon (ArF excimer laser) does not.

As a result, a 6.4 eV photon cannot break Si–Si, but can create other types of defects to which the photoluminescence peak at 2.4 eV is attributed, and so, the bond of Si–Si may be tighter than the oxygen excess defect.

5.5 Electron Spin Resonance

Figure 5.8 shows the ESR spectra of the SiO_2 thin films deposited at various temperatures by photo-CVD. There are two ESR signals in all samples. The higher g-value signal (~2.005) is substrate-related one, for example Si dangling bond, because this is found in the silicon substrate only (or native-oxide may be exist) [11, 12]. The lower g-value signal (~2.0016) relates SiO_2 thin film [13–15]. Because, this sig-

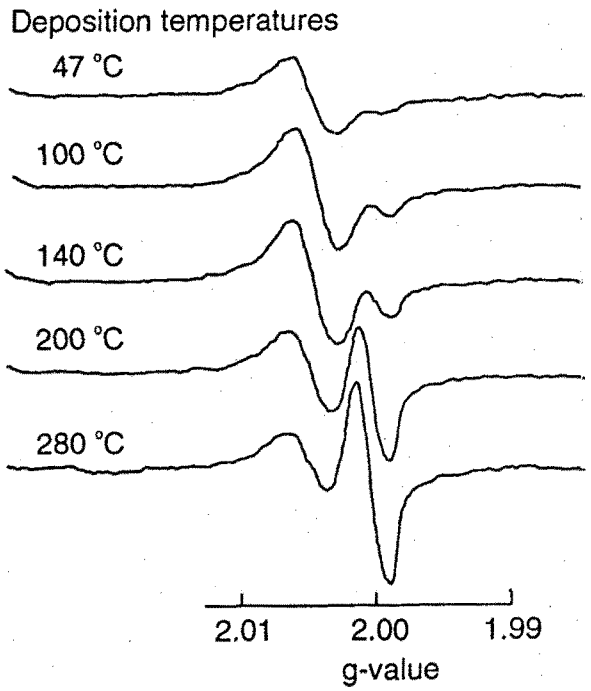

Figure 5.8. The ESR spectra of the SiO_2 thin films deposited at various temperature by photo-CVD.

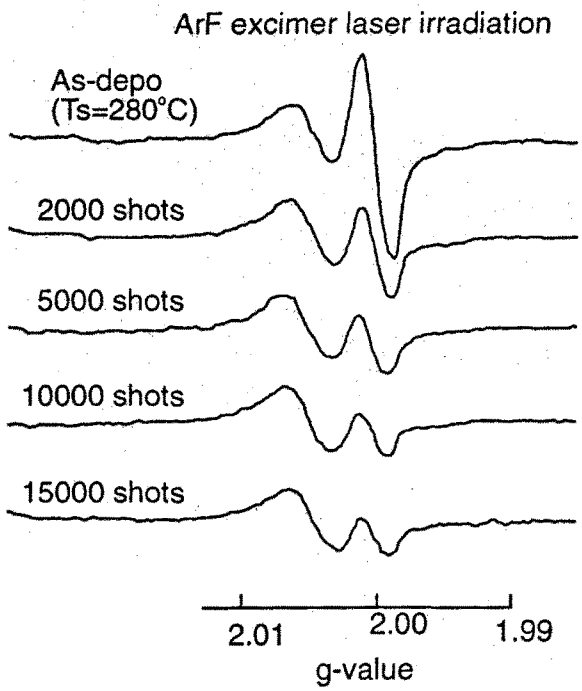

Figure 5.9. Changes of ESR spectra by irradiation of ArF excimer laser. The SiO_2 thin film was deposited at high temperature (280 °C) by photo-CVD.

nal increases with increasing grown temperature, and this is not found in the silicon substrate only. Moreover, the latter signal is independent of rotation of the Si substrate. It seems that the origin of the signal of the g-value ~2.0016 may be the E'-center. This is because oxygen tends to escape from SiO_2 thin film at a high deposition temperature. Then oxygen-deficient defects (Si–Si) remain in the thin film.

Figure 5.9 shows the change in X-band ESR spectra after irradiation of the ArF excimer laser. The SiO_2 thin film was deposited at high temperature (280 °C). The SiO_2 thin film was irradiated with 2000, 5000, 10000 and 15000 shots of ArF excimer laser light of 30 mJ/cm^2. Two kinds of ESR signals are seen in the no-irradiated sample. The signal of the g-value ~2.005 is substrate related signal, and one of the g-value ~2.0016 is caused by SiO_2 thin film. This figure shows that the resonance at g~2.0016 decreases with shot number. These suggest that dangling bonds such as E'-center exist in the as-grown film deposited at high temperature (280 °C), and since the 6.4 eV photon of the ArF excimer laser may not be sufficient to break Si–Si, the ESR signal intensity does not increase. Rather it is thought that the dangling bonds existing in the as-grown sample may react with the other

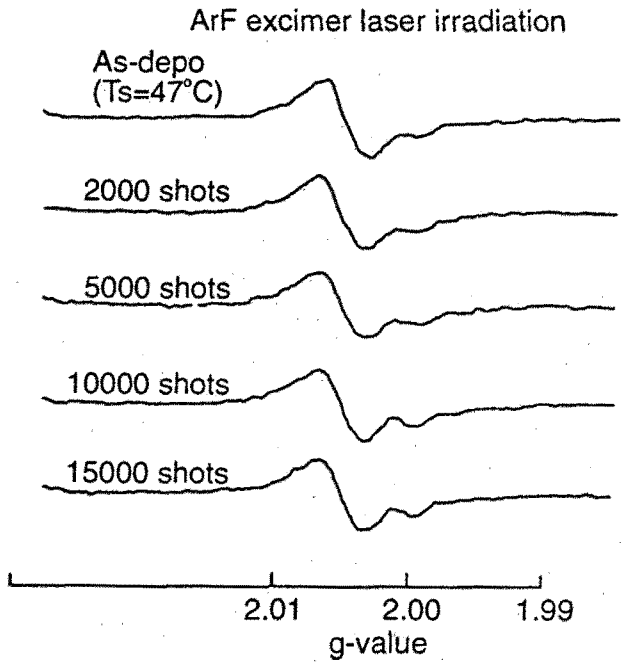

Figure 5.10. Changes of ESR spectra by irradiation of ArF excimer laser. The SiO_2 thin film was deposited at low temperature (47 °C) by photo-CVD.

dangling bond or the interstitial oxygen due to irradiation, thus decreasing the ESR signal. By contrast, Fig. 5.10 shows that the signal at g~2.0016 was not found before irradiation in the sample deposited at low temperature (47 °C). This figure shows that the signal at g~2.0016 appeared after irradiation and increased with shot number. It may be concluded from IR measurement results that the defect Si_2H_x exists in the photo-CVD SiO_2 thin film deposited at low growth temperature (47 °C), and from the photoluminescence results that an unstable defect exists in the low growth temperature film. Hence the increase of the ESR signal (creation of dangling bonds) may be caused by these unstable defects broken by ArF excimer laser irradiation.

Figure 5.11 shows the change in the ESR signal upon F_2 excimer laser irradiation. The SiO_2 thin film was deposited by photo-CVD at high temperature (280 °C). In contrast to the change with the ArF excimer laser in Fig. 5.9, the resonance signal of the g-value ~2.0016 increased with shot number. It was shown from the change of the absorption spectra in Fig. 5.3 that Si–Si may exist in the as-grown sample and may be broken upon irradiation with the F_2 excimer laser. On the basis of this, Si–Si may be broken into –Si · by F_2 excimer laser irradiation, and then the

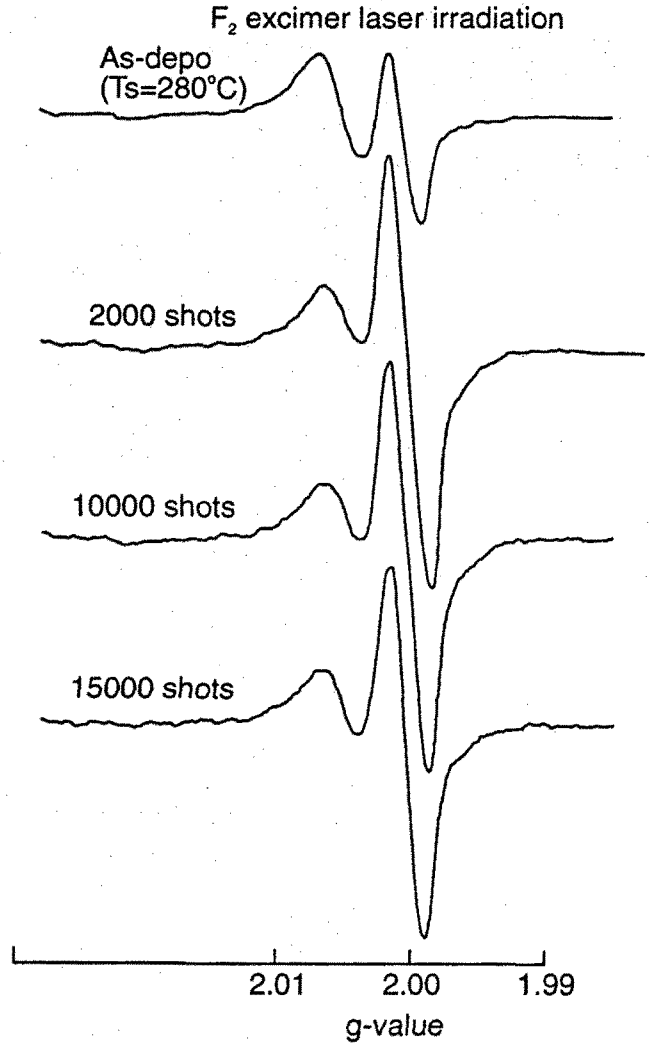

Figure 5.11. Changes of ESR spectra by irradiation of F_2 excimer laser. The SiO_2 thin film was deposited at high temperature (280 °C) by photo-CVD.

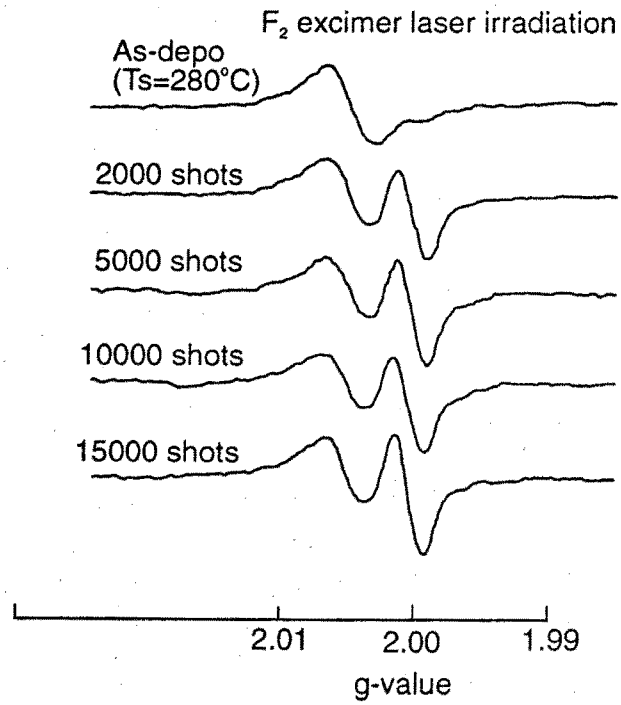

Figure 5.12. Changes of ESR spectra by irradiation of F_2 excimer laser. The SiO_2 thin film was deposited at low temperature (47 °C) by photo-CVD.

ESR signal will increase with shot number. Figure 5.12 shows the change in the ESR signal upon F_2 excimer laser irradiation. The SiO_2 thin film was deposited at low temperature (47 °C). This is similar to an ArF excimer laser irradiation. This irradiation effects may correspond to reduction of 6.3 eV absorption peak with ArF and F_2 excimer laser irradiation.

Reference

[1] K. Awazu and H. Kawazoe: J. Appl. Phys. **68** (1990) 3584.

[2] T. E. Tsai, D. L. Griscom and E. J. Friebele: Phys. Rev. Lett. **61** (1988) 444.

[3] R. Tohmon, A. Ikeda, Y. Simogaichi, S. Munekuni, Y. Ohki, K. Nagasawa and Y. Hama: J. Appl. Phys. **67** (1990) 1302.

[4] R. A. B. Devine, J-L. Leray and J. Margail: Appl. Phys. Lett. **59** (1991) 2275.

[5] D. H. Levy and K. K. Gleason, M. Rothschild, J. H. C. Sedlacek and R. Takke: Appl. Phys. Lett. **60** (1992) 1667.

[6] R. Nagayoshi, M. Nakamura, M. Okuyama and Y. Hamakawa: Inst. Electron. Inf. and Commun. Eng. Tech. Rep. SDM89-138 p. 41 (1989) [in Japanese].

[7] T. Kanashima, R. Nagayoshi, M. Okuyama and Y. Hamakawa: J. Appl. Phys. **74** (1993) 5742.

[8] T. Kanashima, M. Okuyama and Y. Hamakawa: Appl. Surf. Sci. **79/80** (1994) 321.

[9] R. Tohmon, Y. Shimogaichi, H. Mizuno, Y. Ohki, K. Nagasawa and Y. Hama: Phys. Rev. Lett. **62** (1989) 1388.

[10] H. Imai, K. Arai, T. Saito, S. Ichimura, H. Nonaka, J. P. Vigouroux, H. Imagawa, H. Hosono and Y. Abe: *The Physics and Technology of Amorphous* SiO_2, ed. Roderick A. B. Devine (Plenum Press, New York and London, 1988) p153.

[11] Y. Nishi: Jpn. J. Appl. Phys. **10** (1971) 52.

[12] E. H. Poindexter, P. J. Caplan, B. E. Deal, R. R. Razouk: J. Appl. Phys. **52** (1981) 879.

[13] J. H. Stathis and M. A. Kastner: Phys. Rev. B **29** (1984) 7079.

[14] P. M. Lenahan and P. V. Dressendorfer: J. Appl. Phys. **55** (1984) 3495.

[15] P. J. Caplan, E. H. Poindexter, B. E. Deal and R. R. Razouk: J. Appl. Phys. **50** (1979) 5847.

Chapter 6

Defect Energy Analyses by Molecular Orbital Method

6.1 Introduction

It is important that the defects in the SiO_2 thin film are identified precisely for device application to improve film quality. Optical characterization such as photoluminescence and optical absorption enable the determination of transition energies precisely and non-destructively. Moreover, photoluminescence is directly relating to electron transition between energy levels, and is one of the most sensitive methods for characterizing a defect. These studies provide pertinent information about oxygen-vacancy, peroxy linkage and other defects [1–4]. The photoluminescence and optical absorption due to the oxygen-vacancy (≡Si–Si≡) were already analyzed theoretically, and the defect structure was proposed [5–7]. We have observed some photoluminescence and absorption peaks for the SiO_2 thin film prepared by photo-CVD, and the origins of these peaks were identified as both oxygen-excess and oxygen-deficient defects [8–10]. However, theoretical analyses of photoluminescence due to oxygen-excess and hydrogen-related defects such as (≡Si–H), (≡Si–O–H), (≡Si–O–O–H), (≡Si–O–O–Si≡), (Si–O–O ·) and (Si–O ·) [11, 12] have not been reported yet. (The symbols ≡ and · represent three bonds and an unpaired electron.) Thus, a theoretical study on the oxygen-excess and hydrogen-related defects is desired. Molecular orbital (MO) analysis is known to be a powerful method for obtaining not only energies of the ground and excited states but also bonding energies, and electron density. Therefore, the oxygen-excess and hydrogen-related defect structures existing in the SiO_2 thin film should be identified by comparison of the calculated energy and the experimental photoluminescence peak energy.

In this chapter, I have constructed cluster models of the defects, and calculated the energy levels of these clusters using the MO method. Moreover, the photoluminescence peak energies of the photo-CVD SiO_2 thin film have been compared with

Table 6.1. MO calculation programs and parameters.

Semi-empirical method	
Programs	MOPAC93
Parameters	PM3, C.I.
Ab-initio method	
Programs	Gaussian92
Parameters	STO-3G(3-21G)
	Single-excitation-C.I.

the calculated energy levels, and the structure of the defect model has been discussed. It is presented that the energies of Si–O–O–Si cluster and Si–O–O–H cluster agrees well with experimental results, but Si–Si is not.

6.2 Calculation Method

MO analysis of the clusters of oxygen-excess defects has been carried out using a semi-empirical method (MOPAC93 [13]) and an ab-initio method (Gaussian92 [14]) to clarify these defect structures. Molecular orbital analysis is explained in Appendix A. These methods are summarized in appendix A. Table 6.1 shows the calculation programs and parameters. Configuration interaction (C.I.) is included in both methods to estimate the excited energy state and to provide exact energy. In general, semi-empirical calculations are relatively inexpensive and provide reasonable qualitative structural descriptions of the molecular systems and fairly accurate quantitative predictions of the energy levels for these systems. In contrast, ab-initio computations provide precise quantitative predictions for a broad range of systems, but the computational cost of these calculations is large. Thus, semi-empirical calculations were used for determining the geometry of the cluster model, and ab-initio calculations were used for the estimation of the precise energy levels and the electron density.

6.3 SiO_2 Cluster

The cluster size affects time and computational cost for calculation energy and electron density, and is important to obtain reasonable solution. The real SiO_2 has many atoms ($2x10^{22}$ atoms exist in 1 cm^3, as a density of silica glass is about 2 g/cm^3 [17]), but it cannot deal with such large number of atoms. Naturally, the cluster including many atoms provides good descriptions, and as atom number increases, calculated data gives good agreement with experimental ones. However,

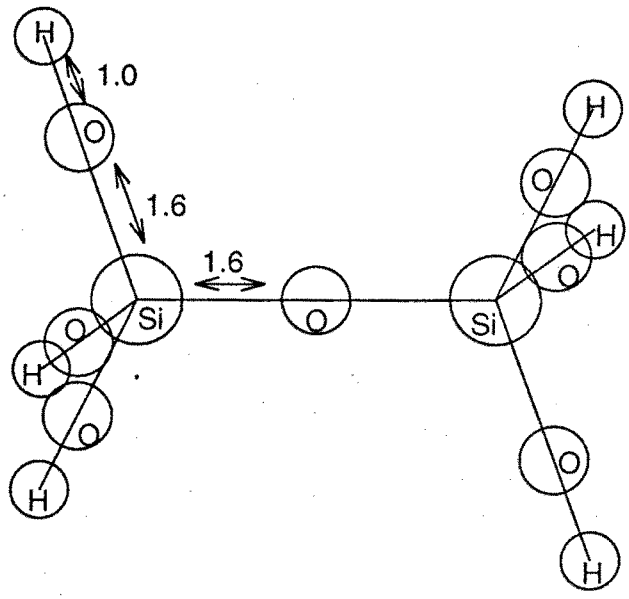

Figure 6.1. SiO_2 cluster model. This is the initial geometry before optimization using MO analysis.

as atom number in the cluster is great, the calculation time, storage size and other computational cost become big. For example, if the atom number in the cluster is twice, then computational cost is 2^n times (n≃2.5–4) [18]. The atom number in the cluster should be cut off in real situation, so I have tried to limit the atom number to explain an experimental data well.

The structure of crystalline SiO_2 (quartz) was studied a typical example. So, the SiO_2 clusters including various silicon atoms were calculated, and calculated bond length and angles were compared with reported (empirical) ones [19]. Figure 6.1 shows the initial structure (before optimization) of the SiO_2 cluster including two silicon atoms. This structure of this cluster was optimized by ab-initio MO calculation with Hartree-Fock level and STO-3G basis set. Figure 6.2 shows the dependence of Si–O bond length on number of Si atoms in cluster. These calculations were carried out by small computer (workstation; Hewlett Packard, HP712/60), and total calculation time is about 1 month. The calculated Si–O length is 0.165 nm, and is independent on the number of Si atoms. This figure shows that the calculated length almost agrees with empirical data. So, this result suggests that the cluster including small silicon atoms explain well experimental data.

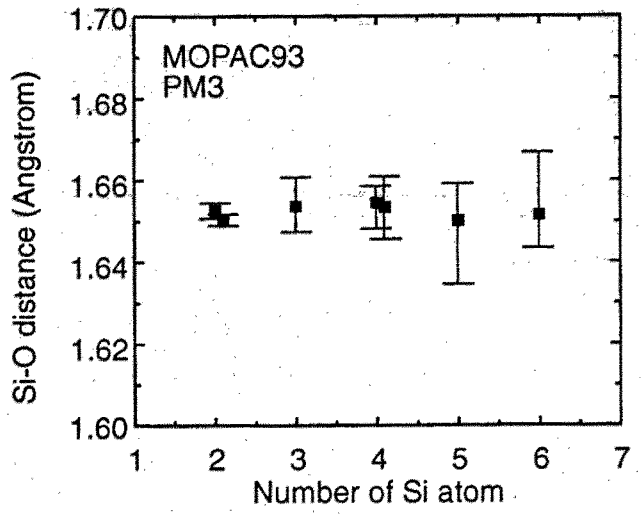

Figure 6.2. Dependence of Si–O bond length on number of Si atoms in the SiO_2 cluster model. The optimizations were carried out by ab-initio MO method.

6.4 Oxygen-Excess Defect

6.4.1 Determination of Defect Structure by Semi-Empirical Method

In this section, oxygen-excess defect, especially Si–O–O–Si was discussed. Three kinds of cluster models were discussed using the semi-empirical MO method, taking account of the influence of the Si–O network surrounding the cluster.

6.4.1.1 Model (1): Only two movable excess-oxygen atoms on Si–X axis

The cluster model (1) is shown in Fig. 6.3. The point X indicates a position of oxygen in a perfect SiO_2 network. The position of O atom adjacent to X were optimized along the O–X axis by changing the distance between Si and X and the Si–X–Si angle as parameters. The motion of the two excess oxygen atoms is similar to that of silicon atoms in the oxygen-vacancy model reported in refs [5–7]. The initial geometry of this cluster in the computational process is similar to that of the defect-free SiO_2 in which an O atom is added between two Si atoms; the Si–O bond length is 0.16 nm, and O–H bond length is 0.1 nm. The Si–O–Si bond angle is 144 °, and dangling bonds belonging to end oxygen atoms are terminated by hydrogen atoms. The dependence of the energy of the ground state on the Si–X distance and Si–X–Si angle is shown in Fig. 6.4. This cluster has no stable geometry. The excited state is calculated and shown in Fig. 6.5, but no minimum point is obtained. This means that an O–Si$\equiv$$O_3$ group tends to separate from the other O–Si$\equiv$$O_3$ group.

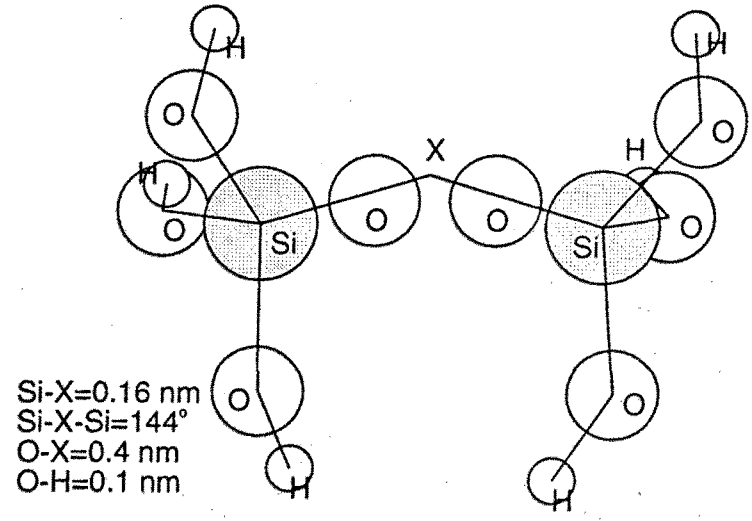

Figure 6.3. Cluster model of oxygen-excess defect (1): Only two excess oxygen atoms move along Si–X axis.

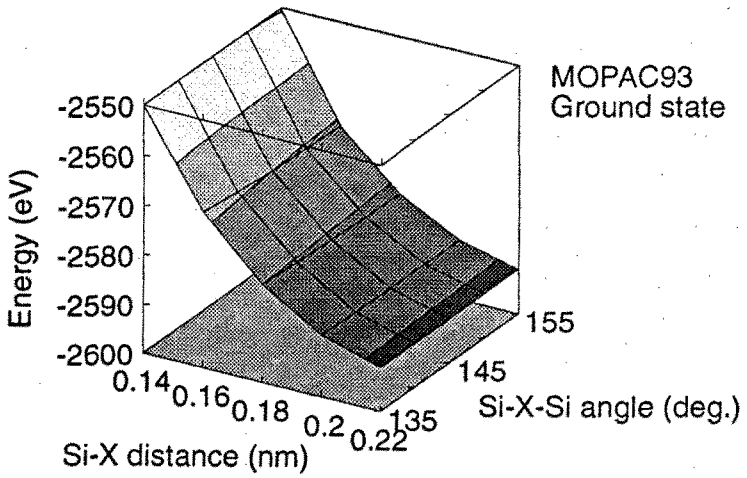

Figure 6.4. The ground state energy as functions of Si–X distance and Si–X–Si angle, calculated by semi-empirical MO method for the cluster of oxygen-excess defect (1).

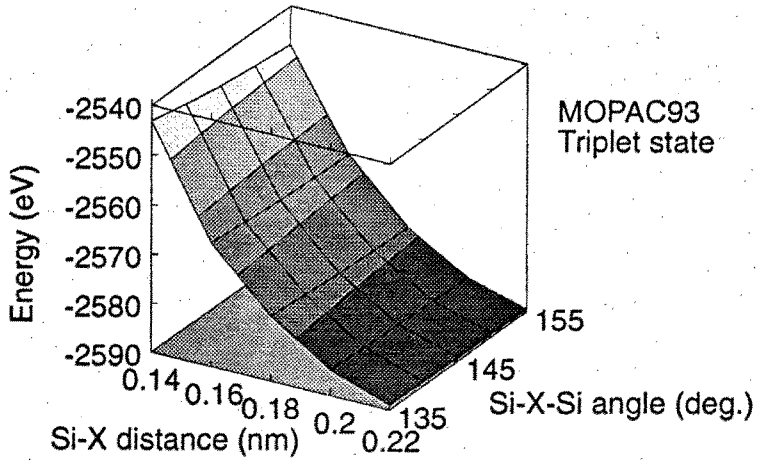

Figure 6.5. The triplet state energy as functions of Si–X distance and Si–X–Si angle, calculated by semi-empirical MO method for the cluster of oxygen-excess defect (1).

6.4.1.2 Model (2): All bond lengths and angles are fully optimized

The cluster model (2) is shown in Fig. 6.6. All bond lengths and angles were fully optimized by the semi-empirical MO method. The initial geometry in the computational process is the same as that in cluster model (1). This optimization process corresponds to a sufficiently relaxed structure of the oxygen-excess defect, and neglects surrounding atom effects. This means that the cluster is isolated, and all atomic positions are optimized by changing the Si–X distance as parameter. This optimization implies that the bonding of two excess oxygen atoms is weaker than that in the defect-free SiO_2 cluster. The dependence of the energies of the ground, excited triplet and excited singlet states on the Si–X distance calculated by the semi-empirical MO method are shown in Fig. 6.7. This cluster is quasi-stable at the point Si–X = 0.12 nm in the excited triplet state. The transition energy from the excited state to the ground state is 1.8 eV, but this value does not agree with the experimental one (2.4 or 3.5 eV).

6.4.1.3 Model (3): Only the positions of two excess oxygen atoms are optimized

The cluster model (3) is shown in Fig. 6.8. The initial geometry in the computational process is the same as the models (1) and (2), but only the positions of the two excess oxygen atoms between the two Si atoms are optimized, while Si, H and other O atoms are fixed at the positions of the defect-free SiO_2 network. This

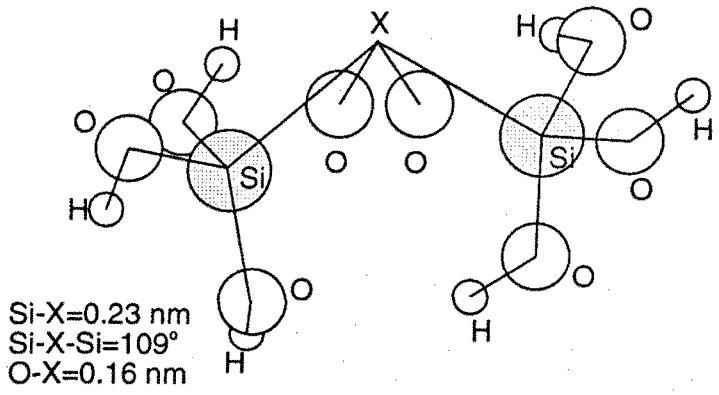

Figure 6.6. Cluster model of oxygen-excess defect (2): All bond lengths and angles are fully optimized.

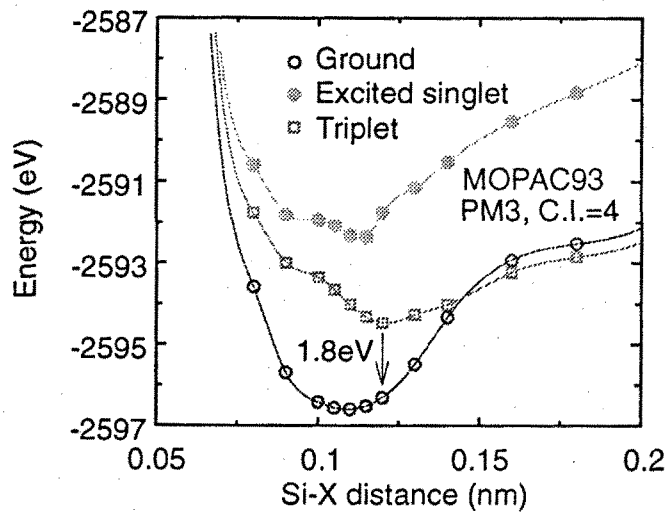

Figure 6.7. The total energy as a function of Si–X distance, calculated by semi-empirical MO method for the cluster of oxygen-excess defect (2).

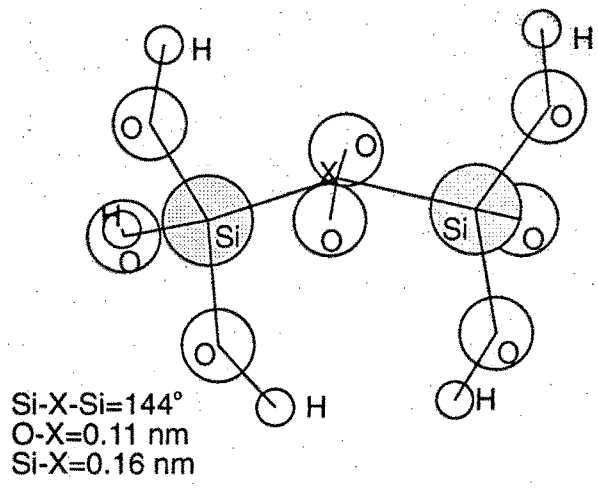

Figure 6.8. Cluster model of oxygen-excess defect (3): Only the positions of two oxygen atoms between Si atoms are optimized, and the other atoms are fixed.

optimization process assumes that the positions of the Si atoms are fixed by the other atoms surrounding them, but the excess oxygen atoms are not. Dependence of the energy of the ground state on the Si–X distance and Si–X–Si angle are shown in Fig. 6.9. The energy is little affected by the small change in the Si–X–Si angle. The excited state was calculated, and shown in Fig. 6.10. This cluster is quasi-stable near Si–X = 0.16 nm, and the transition energy from the excited state to the ground state is about 2.3 eV. Moreover, its geometry shows Si–Si coupling with O–O perpendicularly to it. This transition energy roughly agrees with the 2.4 eV photoluminescence peak measured for the photo-CVD SiO_2 thin film.

6.4.2 Energy Calculation by Ab-Initio Method

It is thought that ab-initio computations provide better quantitative predictions than the semi-empirical method, because the semi-empirical method has many parameters that must be derived from experimental data. Therefore, the transition energy of cluster model (3) is analyzed by the ab-initio MO method to study the energy status precisely, because this cluster model best explains the experimental results. Figure 6.11 shows the dependence of the energy of the excited triplet and the excited singlet states on the Si–X distance. This cluster is quasi-stable at Si–X = 0.17 nm. The transition energy from the excited singlet state to the ground state is 2.65 eV at this point, and this value agrees roughly with the experimental one. These theoretical results suggest that the defect which causes the 2.4 eV photoluminescence has an atomic structure very similar to that shown in Fig. 6.8 (model (3)).

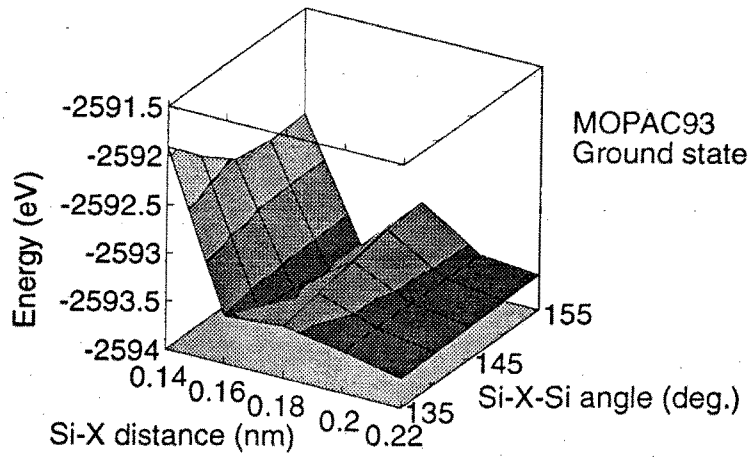

Figure 6.9. The ground state energy as functions of Si–X distance and Si–X–Si angle, calculated by semi-empirical MO method for the cluster of oxygen-excess defect (3).

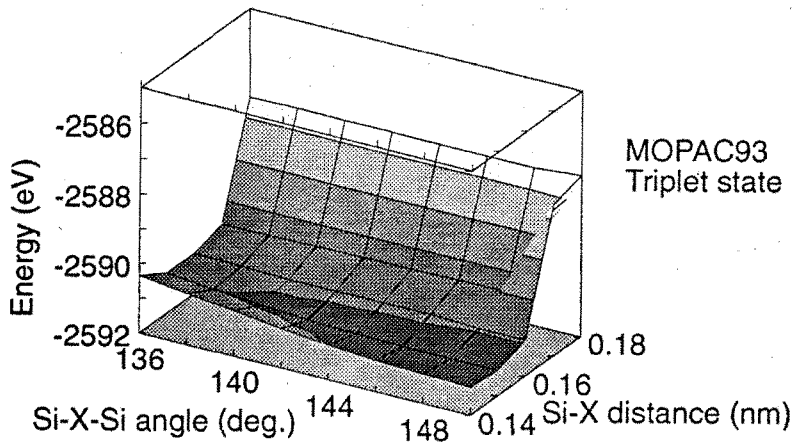

Figure 6.10. The triplet state energy as functions of Si–X distance and Si–X–Si angle, calculated by semi-empirical MO method for the cluster of oxygen-excess defect (3).

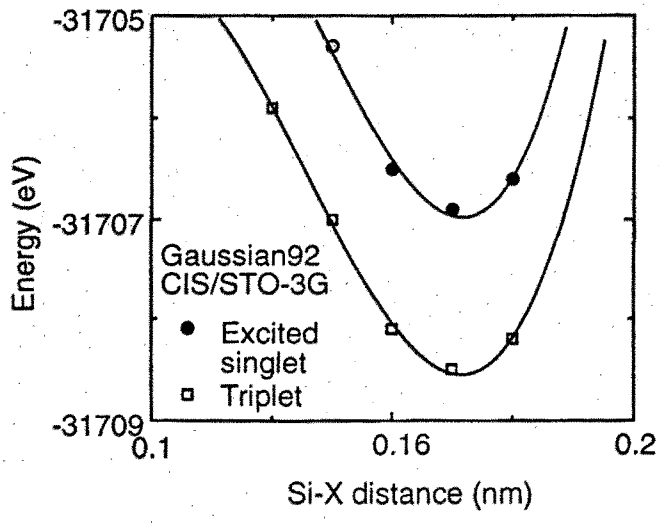

Figure 6.11. The total energy as function of Si–X distance, calculated by ab-initio MO method for the cluster of oxygen-excess defect (3).

The total atomic charge (Mulliken charge) belonging to an excess oxygen atom is -0.46 at Si–X = 0.17 nm, and that belonging a Si atom is 1.6. However, the total atomic charge (Mulliken charge) belonging to an O atom in the defect-free SiO_2 cluster is -0.74, and that belonging to a Si atom is 1.5. Therefore, the charge of a Si atom in an oxygen-excess defect is nearly equivalent to a Si atom in the defect-free cluster, but the electron density of an O atom in the oxygen-excess defect is smaller than that of an O atom in the defect-free cluster. This means that an electron is distributed the two excess oxygen atoms, and this bond energy may be smaller than that of defect-free SiO_2; thus the Si–O bonds in the cluster model may be more unstable than that in defect-free cluster. IR absorption was calculated too, but the result does not agree with experimental data.

Ab-initio MO calculations using another cluster including more Si atoms and another basis set (3-21G) were performed. Because the availability of the cluster size is desired to be confirmed, and a more precise transition energy should be obtained since the 3-21G basis set is bigger than the STO-3G basis set. Figure 6.12 shows an oxygen-excess cluster model that includes three silicon atoms. The positions of only the two oxygen atoms between the two Si atoms are optimized, and the other atoms are fixed in a similar way to that of model (3). As a result of semi-empirical calculation, the cluster including three silicon atoms is found to have quasi-stable geometry. The transition energy from the excited singlet state to the ground state calculated by ab-initio method with STO-3G basis set is 2.32 eV. In addition, MO calculation with 3-21G basis set gives a more precise result that

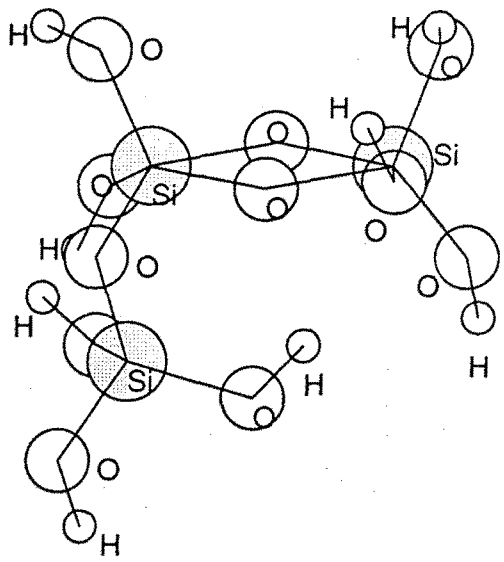

Figure 6.12. Cluster model of oxygen-excess defect that includes three silicon atoms. Only the positions of two oxygen atoms between two silicon atoms are optimized, and the other atoms are fixed.

the transition energy is 2.40 eV in cluster model (3), and this agrees well with the photoluminescence peak at 2.4 eV. Therefore, these results strongly support the fact that the oxygen-excess defect is related to the 2.4 eV photoluminescence peak. The calculation for an oxygen-excess cluster that includes more than 4 silicon atoms was not carried out because of limited of calculation time and of the ab-initio calculation result that the Si–O bond length is hardly changed in the optimization of the defect-free SiO_2 cluster structures which include 2–5 silicon atoms and are optimized by ab-initio MO method.

On the other hand, the excitation energy of the cluster model (2) was calculated using the ab-initio MO method, as the excitation energy evaluated using the ab-initio MO method was different from the energy obtained using the semi-empirical MO method in cluster model (3). This ab-initio MO calculation indicates that the transition energy from the excited triplet state to the ground state is 1.74 eV, and the transition energy from the excited singlet state to the ground state is 4.06 eV. These results do not agree with experimental ones, although results obtained using the semi-empirical and the ab-initio methods are different from experimental ones.

In this section, the structure of the oxygen-excess defect is obtained and compared with our experimental data on SiO_2 thin films deposited by photo-CVD. It has been reported that the oxygen-excess defects such as (≡Si–O–O–Si≡) exist in

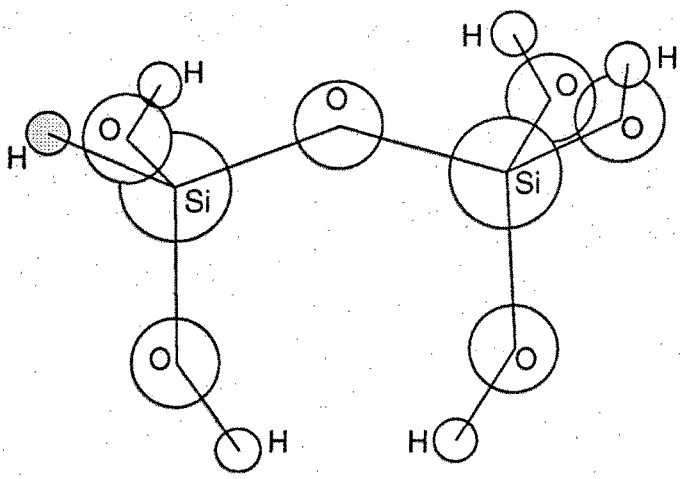

Figure 6.13. Si–H cluster model.

conventional thermally grown SiO_2 films [15, 16]. The authors consider that these results are applicable to all kinds of SiO_2 thin films, and not only to the photo-CVD films. The reduction in the photoluminescence intensity by annealing is conspicuous in photo-CVD SiO_2 thin films since the annealing temperature is higher than growth temperature of the photo-CVD SiO_2 thin films.

6.5 Hydrogen-Related Defects

6.5.1 Determination of Defect Structure by Semi-Empirical Method

In previous section, oxygen-excess defect, especially Si–O–O–Si was discussed, and the calculated energies agree well with experimental results. However, the origin of another photoluminescence peak at 3.5 eV which relates oxygen-excess defect is not clear. Thus, hydrogen-related defect clusters (Si–H, Si–O–H and Si–O–O–H) were discussed using the semi-empirical MO method.

6.5.1.1 Si–H

The Si–H cluster model is shown in Fig. 6.13. The hatched circle is defect accompanied with H atom. The initial geometry of this cluster in the computational process is similar to that of the defect-free SiO_2 in which an O atom is removed between Si and H atoms; the Si–O bond length is 0.16 nm, the O–H bond length is 0.1 nm, the Si–O–Si bond angle is 144 °, and dangling bonds belonging to end oxygen atoms are terminated by hydrogen atoms. The dependence of the energy

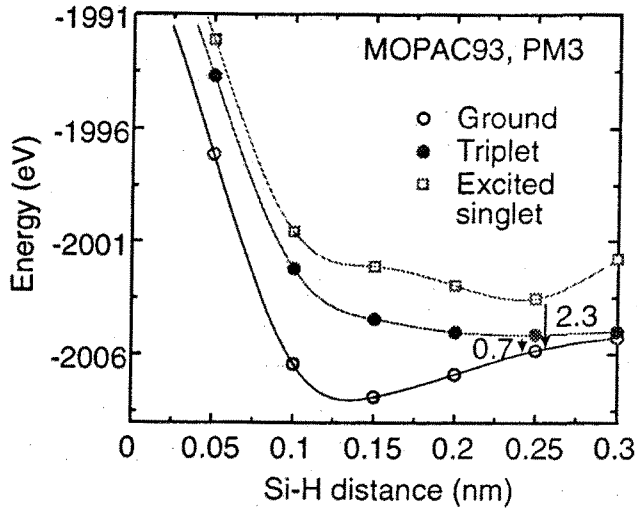

Figure 6.14. The total energy as function of O–H distance, calculated by semi-empirical MO method in the Si–H cluster.

of the ground, triplet and excited singlet states on the Si–H distance calculated by semi-empirical MO method is shown in Fig. 6.14. This cluster is quasi-stable at the point Si–H = 0.15 nm in the ground state, Si–H = 0.25 nm in the triplet and excited-singlet sates. The transition energies from the excited triplet and singlet state to ground states are 0.7 and 2.3 eV, the excitation energies from ground state to excited triplet and singlet states are 3.4 and 5.7 eV.

The energies of another cluster in which H atom is placed between two Si atoms (O_3Si–$\underline{H}$ · SiO_3) were calculated to take account of influence of neighboring atoms. This cluster has a dangling bond in one of two Si atoms, but this bond is not terminated. The H atom is fully optimized, and the other atoms are fixed during calculation. As a result, the excitation energies from ground state to 1st and 2nd exited states are 1.6 and 4.4 eV, and the energy from 2nd excited state to ground state is 2.8 eV. The 1st excited states do not have quasi-stable position. These energies agree with 4.4 eV photoluminescence which relates oxygen-deficient defect.

6.5.1.2 Si–O–H

The Si–O–H cluster model is shown in Fig. 6.15. The hatch atoms are defect O and H. The initial geometry of this cluster in the computational process is similar to the defect-free SiO_2; the Si–O bond length is 0.16 nm, the O–H bond length is 0.1 nm, the Si–O–Si angle is 144 °, and dangling bonds belonging to end oxygen atoms are terminated by hydrogen atoms similar to model 1. The atoms are fixed except

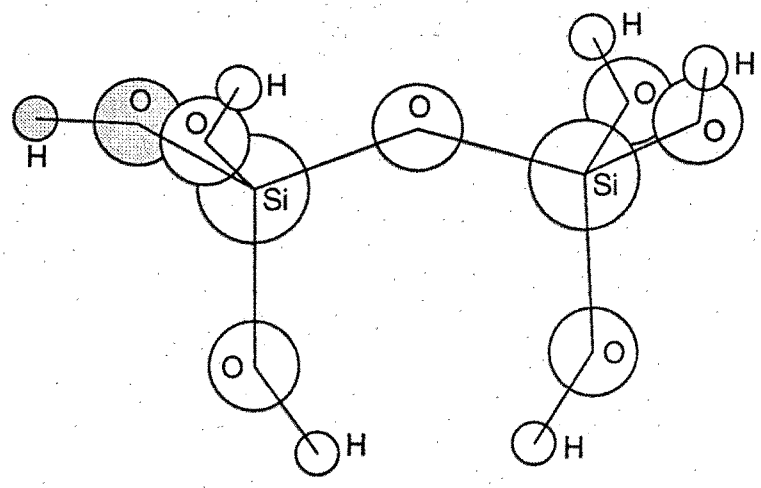

Figure 6.15. Si–O–H cluster model.

for H, and the position of only this H atom was optimized. The dependence of the energy of the ground states on the O–H distance and the Si–O–H angle calculated by the semi-empirical MO method is shown in Fig. 6.16. This cluster is quasi-stable at Si–H = 0.1 nm and Si–O–H = 120 °. Moreover, the excited state was calculated. Figure 6.17 and 6.18 show that the energies of triplet and excited singlet state. These figures show that the no minimum point is observed in the triplet state, but quasi-stable is observed at the same point as the ground state in the excited singlet state. The transition energy from the excited singlet state to the ground state is 6.2 eV.

The energies about the another cluster in which OH was inserted between two Si atoms (O_3Si–$\underline{O–H}$ · SiO_3) were calculated in the same way as Si–H. This cluster has a dangling bond in one of two Si atoms, but this bond is not terminated. The H and O atoms are fully optimized, and the other atoms are fixed during calculation. Thus, the ground state is doublet in this cluster. As a result, the energies from ground state to 1st and 2nd excited states are 5.4 and 5.1 eV, but there are no minimum point, this cluster has no quasi-stable point in the excited state. Then, this cluster has no photoluminescence.

It has been reported that silicon dioxide film of wet oxidation provides higher charge-to-breakdown and lower stressing current density (J_g^{SL}) than dry oxidation. This reason is explained by assuming that the defect Si–OH is stable than Si–H [23, 24]. So, the energy to remove the H atom has been calculated in the same way as Si–H and Si–OH. The clusters are optimized H–Si–$(OH)_3$ and HO–Si–$(OH)_3$ in which (OH)s are fixed during optimization process. Figure 6.19 and 6.20 show the Si–H and Si–O–H cluster models. The hatched H atoms are locus, then only one

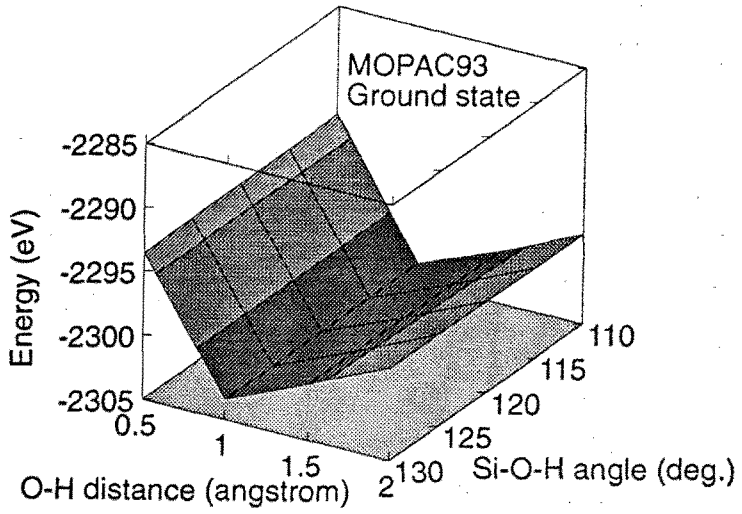

Figure 6.16. The total energy as functions of O–H distance and Si–O–H angle, calculated by semi-empirical MO method in the Si–O–H cluster.

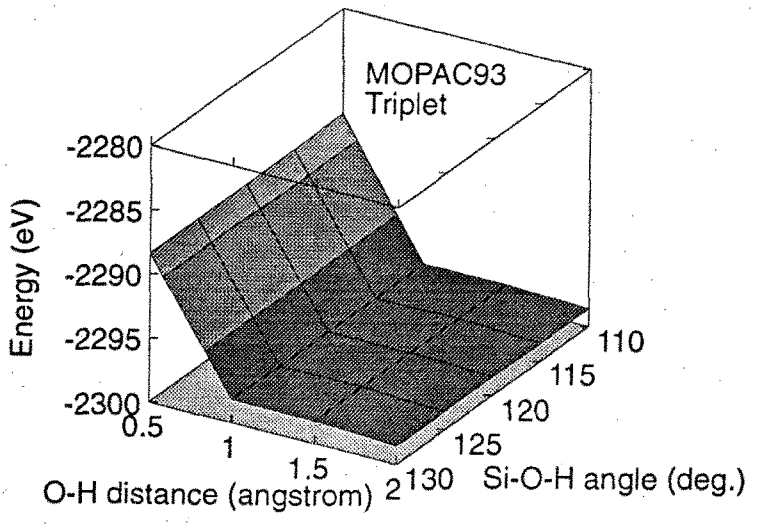

Figure 6.17. The triplet state energy as functions of O–H distance and Si–O–H angle, calculated by semi-empirical MO method in the Si–O–H cluster.

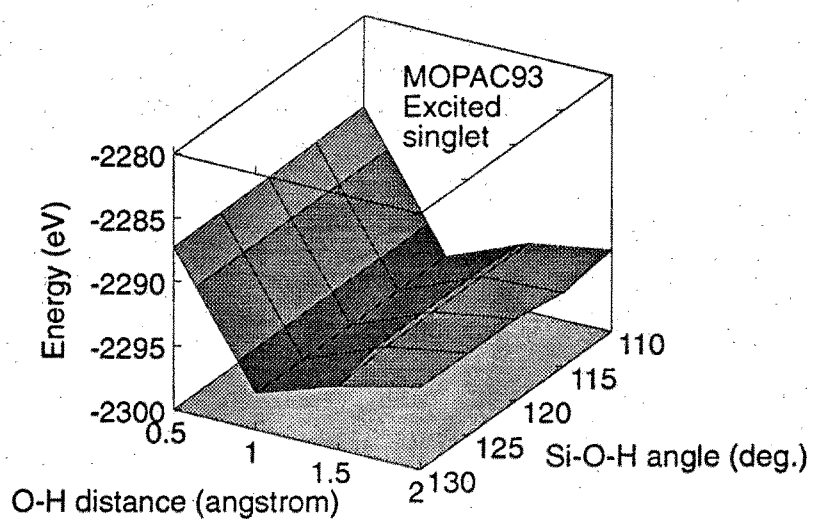

Figure 6.18. The excited singlet energy as functions of O–H distance and Si–O–H angle, calculated by semi-empirical MO method in the Si–O–H cluster.

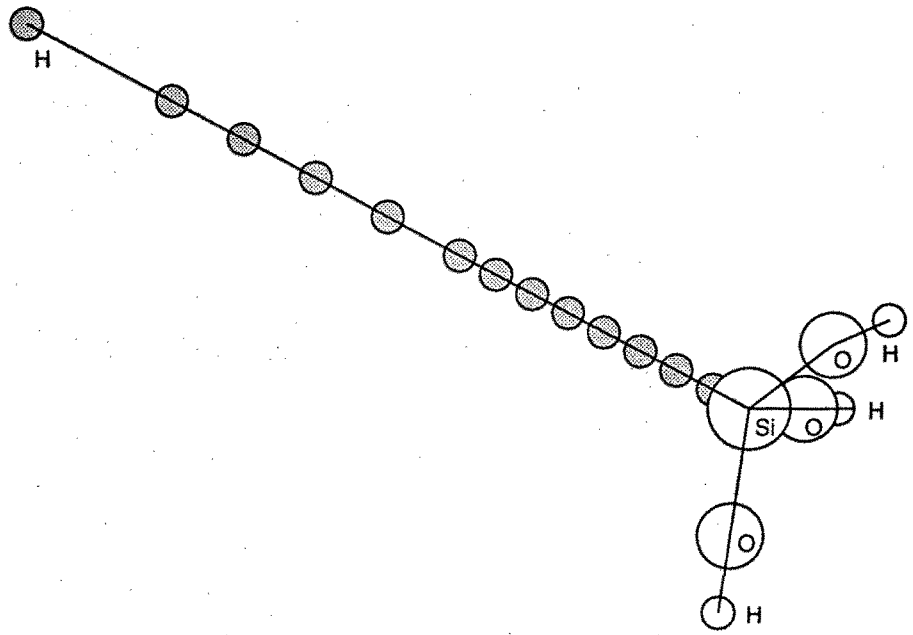

Figure 6.19. The Si–H cluster model for stability calculation.

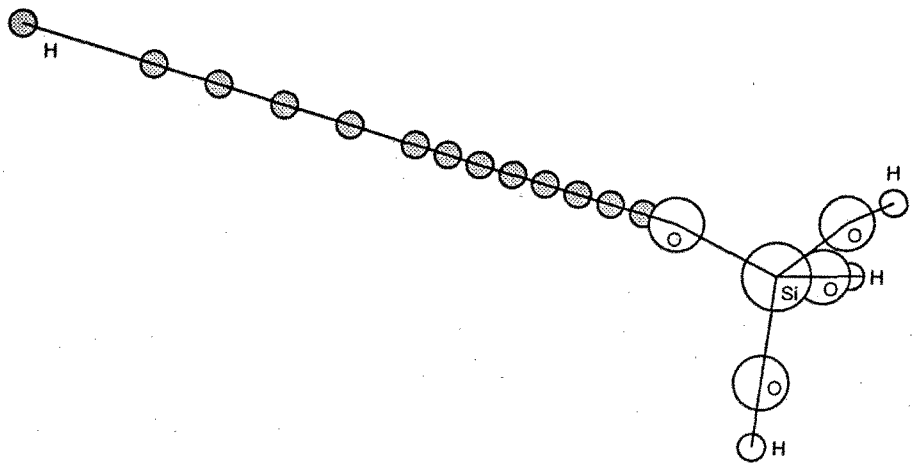

Figure 6.20. The Si–O–H cluster model for stability calculation.

H atom exists during calculation. This figure shows that the difference from the minimum (stable, optimized) point to the isolated point in SiO–H cluster is larger than that in Si–H cluster. This suggests that the defect Si–OH is more stable than the Si–H, and it agrees with the above experimental results. Figure 6.21 shows the dependence of the energy of ground state on the distance between Si and H. This figure shows that the difference from the minimum (stable, optimized) point to the isolated point in SiO–H cluster is larger than that in Si–H cluster. This suggests that the defect Si–OH is more stable than the Si–H, and it agrees with the above experimental results.

6.5.1.3 Si–O–O–H

The Si–O–O–H cluster model is shown in Fig. 6.22. The initial geometry of this cluster in the computational process is similar to that of the defect-free SiO_2; the Si–O bond length is 0.16 nm, the O–H bond length is 0.1 nm, the Si–O–Si bond angle is 144 °, the O–O bond length is 0.16 nm, and dangling bonds belonging to end oxygen atoms are terminated by hydrogen atoms similarity to model 1 and 2. The atoms are fixed except for the O–H atoms (which bonds to the Si–O) whose positions are optimized. The dependence of the energy of ground states on the O–H and the O–O distances was calculated by the semi-empirical MO method, and are shown in Fig. 6.23. The energy is little dependent on the small change of the O–H distance. Figure 6.24 shows the excited singlet state. This cluster is quasi-stable at near O–H = 0.1 nm and O–O = 0.15 nm. The transition energy from the excited singlet state to the ground state is about 3.6 eV, and the excitation energy from the

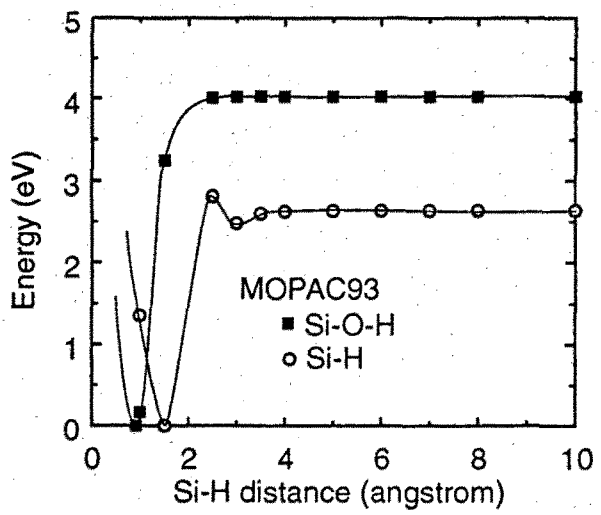

Figure 6.21. The dependence of the energy of ground state on the distance between Si and H. The clusters are H–Si–$(OH)_3$ and HO–Si–$(OH)_3$.

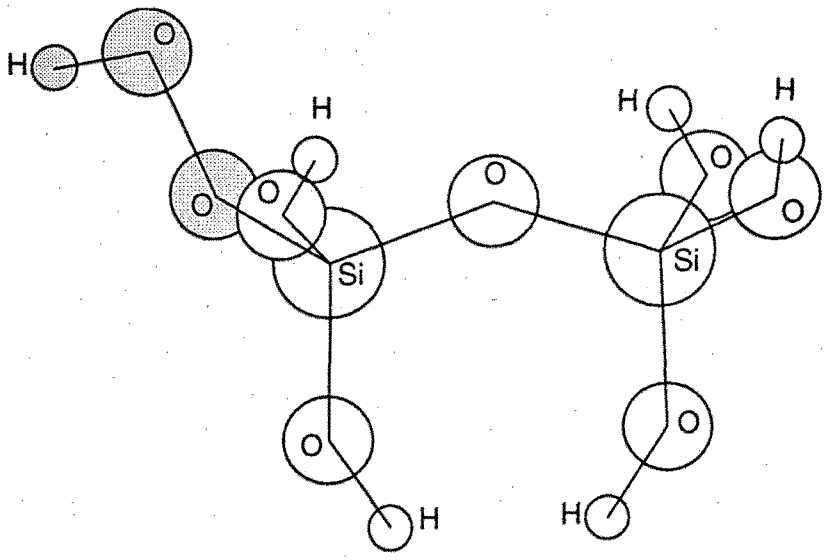

Figure 6.22. Si–O–O–H cluster model.

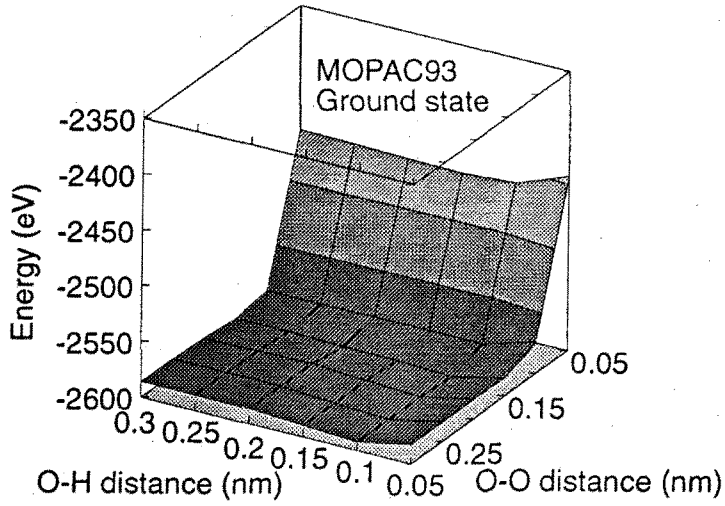

Figure 6.23. The total energy as functions of O–H and O–O distance, calculated by semi-empirical MO method in the Si–O–O–H cluster.

ground state to the excited singlet state is 6.2 eV. These transition energies roughly agree well with the 6.3 eV absorption band and the 3.5 eV photoluminescence peak measured in the photo-CVD SiO_2 thin film.

The energies about the another cluster in which OOH was inserted between two Si atoms (O_3Si–$\underline{O–O–H}$ · SiO_3) were calculated. The H and two O atoms are fully optimized, and the other atoms are fixed during calculation. This cluster has a dangling bond in one of two Si atoms, but this bond is not terminated. Thus, the ground state is doublet spin state in this cluster. As a result, the energies from ground state to 1st and 2nd excited states are 3.4 and 4.7 eV, and the energies from 1st and 2nd excited state to ground state is 0.7 and 3.2 eV. The energy from 2nd excited state to ground state (3.2 eV) is a little different from experimental value, but this cluster has dangling bond. This dangling bond may cause such difference between experimental and calculated value.

6.5.2 Energy Calculation by Ab-Initio Method

It is thought that the ab-initio computations provide better quantitative prediction than the semi-empirical method, because the semi-empirical method has many parameters that must be derived from experimental data. Therefore, the transition energy of only the plausible Si–O–O–H cluster model was analyzed by the ab-initio MO method to study the energy state precisely, because this cluster explains the experimental results best among the three cluster models. The cluster model was

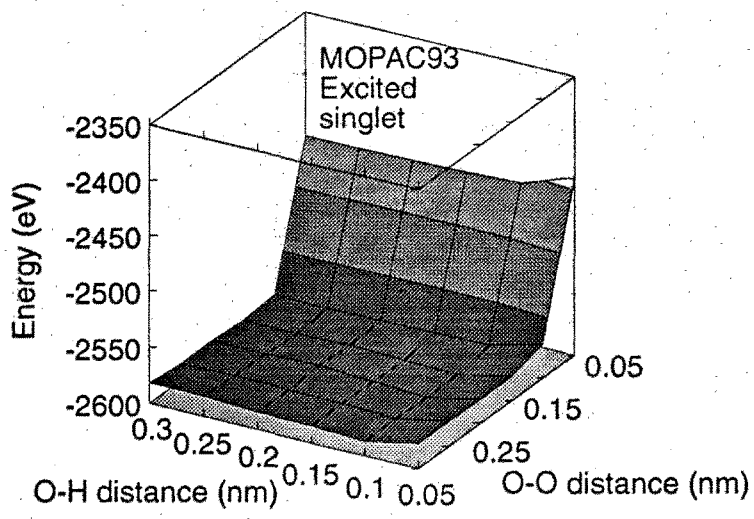

Figure 6.24. The excited singlet energy as functions of O–H and O–O distance, calculated by semi-empirical MO method in the Si–O–O–H cluster.

optimized in the same way as the semi-empirical method (The initial geometry is the same as model shown in Fig. 6.22; only the positions of O and H are optimized, and the other atoms are fixed during optimization). The transition energy from the ground state to the excited triplet is 6.40 eV and that from the ground state to the excited singlet state is 8.25 eV at its point. Then, structure of the excited states is optimized, and the excitation energy of its geometry is calculated. As a result, the excitation energy from the excited singlet state to the ground state is 3.89 eV, and that from the excited triplet state to the ground state is 2.52 eV. These values roughly agree with experimental 3.5 eV photoluminescence peak. These theoretical results suggest that the defect, which causes the 6.4 eV absorption and the 3.5 eV photoluminescence has atomic structure very similar to that shown in Fig. 6.22.

Thus, the transition energy for Si–O–O–H cluster model agrees with experimental one, but the excited state is different between the semi-empirical method and the ab-initio method. So, the transition energies of the Si–H and the Si–O–H cluster models were also calculated using the ab-initio method to make sure of that only the Si–O–O–H (model 3) agrees with experimental one. The calculation procedures are the same as semi-empirical method. Table 6.2 shows the summary of the transition and the excitation energies. The transition energies of Si–H and Si–O–H cluster models are different from experimental ones (optical absorption and photoluminescence).

In this section, the structures of the hydrogen-related defects were compared with our experimental data on SiO_2 thin films deposited by photo-CVD. However, it has

Table 6.2. The transition energies of Si–H, Si–O–H and Si–O–O–H, calculated by the ab-initio method.

	Si–H	Si–O–H	Si–O–O–H
Ground to triplet	8.43	8.43	6.40
Ground to singlet	10.03	10.03	8.25
Triplet to ground	8.43	–	2.52
Singlet to ground	10.03	–	3.89

(eV), the symbol – represents no minimum energy.

been reported that hydrogen-related defect such as (≡Si–O–H) exists in conventional thermally grown SiO_2 films [20–22]. It is considered that these results are applicable to all kinds of SiO_2 thin films, and not only to the photo-CVD films. Especially, the Si_2H_6 gas was used in photo-CVD, there are hydrogen (which may be a radical) induced in the film during deposition, and then the concentration of hydrogen may be larger than the thermally grown oxide with dry O_2. Additionally to this, the reduction of photoluminescence intensity by annealing is conspicuous in photo-CVD SiO_2 thin films. Because the amount of defects in the SiO_2 thin films deposited by photo-CVD is larger than that in thermally grown films, the annealing temperature is higher than growth temperature of the photo-CVD SiO_2 thin films.

6.6 Si–Si Defect

It is reported that ab-initio MO calculation about the oxygen-vacancy (Si–Si) cluster ($(HO)_3Si–Si(OH)_3$) including 2 silicon atoms provides prediction that this cluster has 7.6 and 5.0 eV absorption and 2.7 eV photoluminescence [6, 7]. These calculations were carried out by using Gaussian 80H (Gaussian 80: HITAC version) and based on single-electron-configuration-interaction (SE-CI) [2]. However, this photoluminescence peak is not found in our photo-CVD SiO_2 thin film. So, I have tried to discuss the Si–Si cluster including three silicon atoms. Figure 6.25 shows the Si–Si defect cluster model including three Si atoms. The position X is the oxygen-vacancy. Si–O–H and Si–O–Si angle is 144 °. Si–O = 0.16 nm, Si–H is 0.1 nm. The excitation energies are calculated under the condition that the positions of only two Si atoms neighboring oxygen-vacancy (X) are optimized and the other atoms are fixed. Figure 6.26 shows that ground, excited triplet and excited singlet states. This figure shows the possibility of having 1.8 and 5.5 eV absorption and 1.96 and 0.35 eV photoluminescence, but these values do not agree with experimental ones. Figure 6.27 the calculated IR absorption spectrum. This figure shows some absorption peak, but these peaks also do not agree with experimental ones. Figure

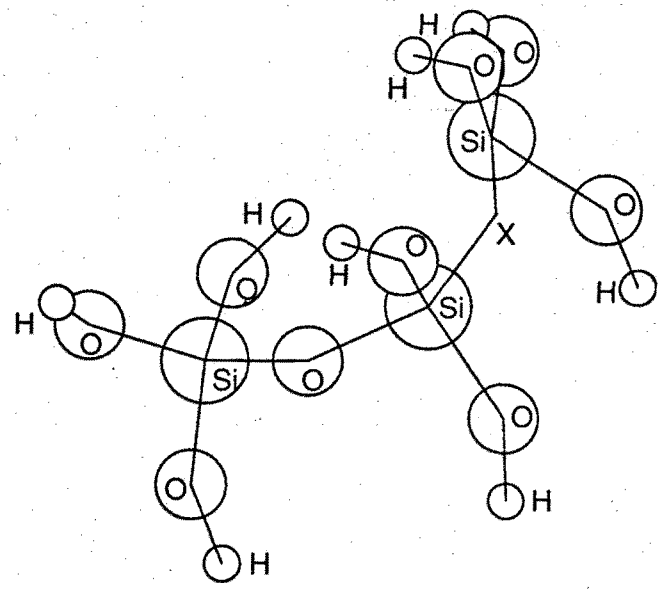

Figure 6.25. The Si–Si cluster model including three Si atoms.

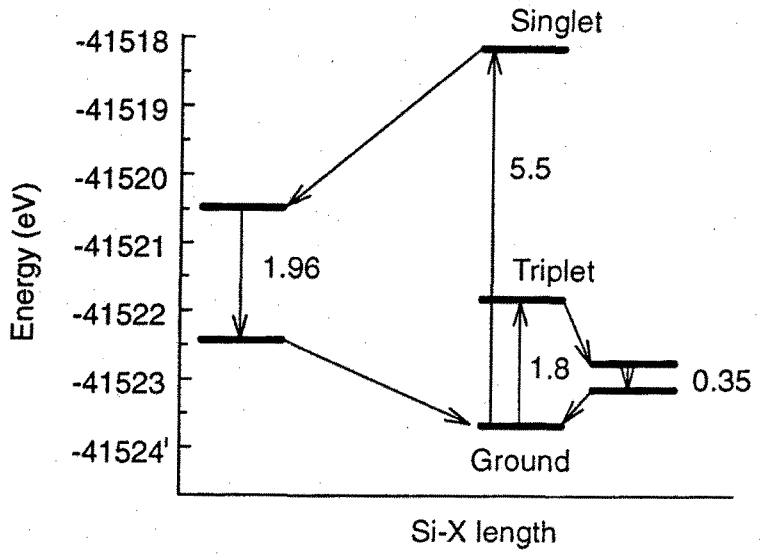

Figure 6.26. The energy transfer diagram of the Si–Si cluster model including three Si atoms.

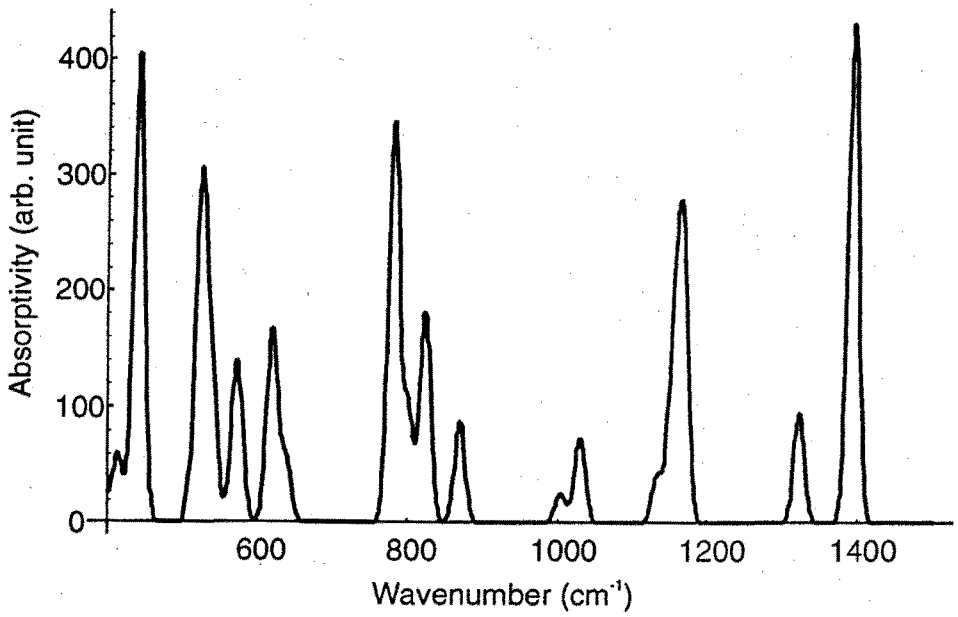

Figure 6.27. Calculated IR spectrum of the Si–Si cluster model including three Si atoms.

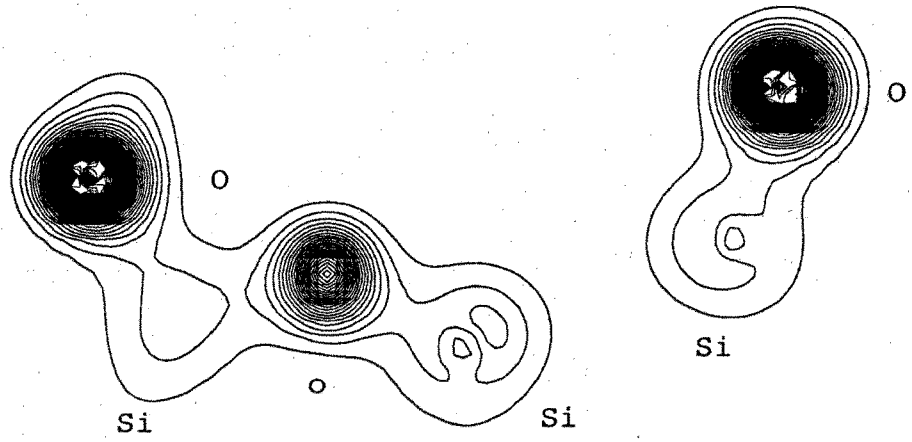

Figure 6.28. Calculated charge density of the Si–Si cluster model including three Si atoms.

6.28 shows the charge density calculated by MOPAC93. This view is the plane including O–Si–O–Si–X–Si–O. It is shown charge concentrates in O atoms. There is little charge between oxygen-vacancy (X), and dangling bond is not found.

Reference

[1] M. Kohketsu, K. Awazu, H. Kawazoe and M. Yamane: Jpn. J. Appl. Phys. **28** (1989) 622.

[2] R. Tohmon, Y. Shimogaichi, H. Mizuno and Y. Ohki: Phys. Rev. Lett. **62** (1989) 1388.

[3] M. Kohketsu, K. Awazu, H. Kawazoe and M. Yamane: Jpn. J. Appl. Phys. **28** (1989) 615.

[4] Y. Hibino and H. Hanafusa: J. Appl. Phys. **60** (1986) 1797.

[5] O'Keeffe and G. V. Gibbs: J. Chem. Phys. **81** (1984) 876.

[6] R. Tohmon, Y. Shimogaichi, H. Mizuno, Y. Ohki, K. Nagasawa and Y. Hama: Phys. Rev. Lett. **62** (1989) 1388.

[7] R. Tohmon, H. Mizuno, Y. Ohki, K. Sasagane, K. Nagasawa and Y. Hama: Phys. Rev. B. **39** (1989) 1337.

[8] T. Kanashima, R. Nagayoshi, M. Okuyama and Y. Hamakawa: J. Appl. Phys. **74** (1993) 5742.

[9] T. Kanashima, M. Okuyama and Y. Hamakawa: Jpn. J. Appl. Phys. **32** (1993) 3113.

[10] T. Kanashima, M. Okuyama and Y. Hamakawa: Appl. Surf. Sci. **79/80** (1994) 321.

[11] H. Nishikawa, R. Nakamura, R. Tohmon, Y. Ohki, Y. Sakurai, K. Nagasawa and Y. Hama: Phys. Rev. B **41** (1990) 7828.

[12] H. Imai, K. Arai, J. Isoya, H. Hosono, Y. Abe and H. Imagawa: Phys. Rev. B **48** (1993) 3116.

[13] made by J. J. P. Stewart, Fujitsu Limited, Tokyo, Japan (1993).

[14] Revision G.3, made by M. J. Frisch et al.: Gaussian, Inc., Pittsburgh PA, 1992.

[15] J. Robertson: *The Physics and Technology of Amorphous SiO_2*, ed. Roderick A. B. Devine (Plenum Press, New York and London, 1988) p. 91.

[16] David L. Griscom: *The Physics and Technology of Amorphous SiO_2*, ed. Roderick A. B. Devine (Plenum Press, New York and London, 1988) p. 125.

[17] *Rika Nenpyo* (Scientific Constant Tables) ed. Kokuritu Tenmondai (Maruzen, Tokyo, 1989) p. 439.

[18] J. B. Foresman and Æ. Frisch: *Exploring Chemistry with Electronic Structure Methods: A Guide to Using Gaussian* (Gaussian, Inc., Pittsburgh, 1993) p. 55.

[19] Y. Matsui and S. Tsuneyuki: Kotai Buturi **23** (1988) 888 [in Japanese].

[20] R. A. B. Devine, J-L. Leray and J. Margail: Appl. Phys. Lett. **59** (1991) 2275.

[21] K. Nagasawa, Y. Hoshi, Y. Ohki and K. Yahagi: Jpn. J. Appl. Phys. **25** (1986) 464.

[22] K. Nagasawa and Y. Hama: J. Appl. Phys. **68** (1990) 1212.

[23] Y. Murakami: J. Appl. Phys. **75** (1994) 5302.

[24] H. Satake, N. Yasuda and A. Toriumi: *Extended Abstracts of the 19995 Int. Conf. on Solid State Devices and Materials, Osaka, 1995* (Japan Society of Appl. Phys.) p. 264.

Chapter 7

Conclusion

A series of comprehensive investigations on the characterization of the defects in the SiO_2 thin films by optical properties and molecular orbital method has been carried out. The conclusions obtained in this thesis work are summarized as follows.

1. SiO_2 thin films have been deposited at low temperature (RT–300 °C) by using photo-CVD. The source gases are Si_2H_6 and O_2, and the excitation light source is a deuterium lamp. Refractive indexes of these films grown at more than 50 °C are 1.45 which is very close to one of thermally grown SiO_2 film.

2. 6.3 and 7.6 eV absorption peaks are found in the SiO_2 thin film deposited on MgF_2 substrate by photo-CVD. Film thickness dependence, the annealing effects and source gas-flow-rate-ratio during deposition of structural and electrical properties, are studied. These results suggest that the origin of 6.3 eV peak is localized near SiO_2/MgF_2 interface and relates an oxygen-excess defect, but the origin of 7.6 eV peak is distributed in the film and relates an oxygen-deficient defect.

3. Photoluminescence excited by monochromated deuterium lamp (7.7 eV) have been studied. As a result, the 2.7, 3.6–3.8 and 4.4 eV photoluminescence peaks are found in the SiO_2 thin film deposited on Si substrate at high temperature (300 °C), and only 2.7 and 3.6–3.8 eV peaks are found in one deposited at low temperature (30 °C).

4. Photoluminescence excited by ArF (6.4 eV) and F_2 (7.9 eV) excimer laser have been studied. As a result, the 2.4, 3.4–3.5 and 4.3–4.4 eV photoluminescence peaks are found. The films were deposited on Si substrate by photo-CVD. Annealing effects suggests that the 2.4 and 3.4–3.5 eV are caused by oxygen-excess defects, and 4.3–4.4 eV is caused by oxygen-deficient defect. When the deposition temperature is high (300 °C), the origins (defects) of 2.4 and 3.5 eV peaks are localized near Si/SiO_2 interface, but one of 4.4 eV is distributed in the film.

5. ArF and F_2 excimer laser irradiation effects have been studied. 6.3 eV absorption peak is decreased by both ArF and F_2 excimer lasers irradiation, but 7.6 eV absorption peak is decreased by only F_2 excimer laser. Moreover, the change of ESR spectra shows Si–Si bond is cut into dangling bond by F_2 excimer laser irradiation. The 3.4–3.5 and 4.3–4.4 eV photoluminescence peaks are decreased monotonously by ArF excimer laser irradiation, but 2.4 eV peak is increased with the irradiation shot number at the beginning of irradiation and then decreased. Annealing effects and ESR spectra changes suggest that oxygen-excess defect is cut into dangling bonds, and oxygen and this bond are combined into oxygen-excess defect by ArF excimer laser irradiation.

6. The physical geometry of oxygen-excess defect cluster (Si–O–O–Si) has been constructed, and the transition energies were calculated by semi-empirical MO method. The cluster in which only the positions of O atoms are optimized and other $Si(OH)_3$ atoms are fixed, gives agreement with experimental results. Its geometry is Si–Si coupling with O–O perpendicularly. Moreover, ab-initio MO calculation about this cluster provides a prediction that this cluster has 2.4 eV photoluminescence in the transition from excited singlet to ground state, and this result shows good agreement with measured photoluminescence peak energy and transition life-time.

7. The physical geometry of hydrogen-related defect clusters (Si–H, Si–O–H, Si–O–O–H) has been constructed, and the transition energies have been calculated by semi-empirical MO method. As a result, Si–O–O–H cluster is agreement with experimental result. Moreover, ab-initio MO calculation about this cluster provides a prediction that this cluster has 3.9 eV photoluminescence and 6.4 eV absorption in the transition from excited singlet to ground state. This gives good agreement with measured photoluminescence and optical absorption peaks.

Appendix A

Molecular Orbital Method

A.1 Introduction

Calculation method of Molecular orbital analysis is explained in detailed in this appendix. In this chapter, summarize. There are two MO method, one is ab-initio, the other is semi-empirical [1–6]. The theoretical bases are the same, but semi-empirical method uses much experimental parameters.

A.2 Schrödinger Equation

Quantum mechanics explains how entities like electrons have both particle-like and wave-like characteristics. The Schrödinger equation describes the wavefunction of a particle. The Schrödinger equation can be simplified using the mathematical technique as separation of variables. For the problems in which we are interested, this separation is valid, and we focus entirely on the familiar time-independent Schrödinger equation.

$$\mathcal{H}|\Phi>=\mathcal{E}|\Phi> \tag{A.1}$$

$$\mathcal{H}=-\sum_{i=1}^{N}\frac{1}{2}\nabla_i^2-\sum_{A=1}^{M}\frac{1}{2M_A}\nabla_A^2-\sum_{i=1}^{N}\sum_{A=1}^{M}\frac{Z_A}{R_{iA}}+\sum_{i=1}^{N}\sum_{j>i}^{N}\frac{1}{r_{ij}}+\sum_{A=1}^{M}\sum_{B>A}^{M}\frac{Z_AZ_B}{R_{AB}} \tag{A.2}$$

where M_A is the ratio of atom A mass to electron mass, Z_A is atomic number of A, N is electron number, M is atom number, R_{AB} is the distance between atoms A and B, r_{ij} is the distance between electrons i and j and R_{iA} is the distance between electron i and atom A.

Atomic Unit

The fundamental equations of quantum chemistry are usually expressed in units designed to simply their form by eliminating fundamental constants. The atomic

unit of length is the Bohr radius.

$$a_0 = \frac{h^2}{4\pi^2 me^2} = 0.529177249\text{Å} \tag{A.3}$$

Coordinates can be transformed to bohrs by dividing them by a_0. Energies are measured in *hartree*, defined as the Coulomb repulsion between two electrons separated by 1 bohr.

$$1\text{hartree} = \frac{e^2}{a_0} \tag{A.4}$$

The Born-Oppenheimer Approximation

The Born-Oppenheimer approximation is the first of several assumption used to simplify the solution of the Schrödinger equation. This approximation is reasonable since mass of the nucleus is thousands times greater than that of an electron. The nuclei move very slowly with respect to the electrons, and the electrons react essentially instantaneously to changes in nuclear position. Put another way, the nuclei looked fixed to the electrons, and electronic motion can be described as occurring in a field of fixed nuclei. So, we can construct an electronic Hamiltonian which neglects the kinetic energy term for the nuclei and Coulomb repulsion between tow nuclei as a constant.

$$\mathcal{H}_{\text{elec}} = -\sum_{i=1}^{N} \frac{1}{2}\nabla_i^2 - \sum_{i=1}^{N}\sum_{A=1}^{M} \frac{Z_A}{R_{iA}} + \sum_{i=1}^{N}\sum_{j>i}^{N} \frac{1}{r_{ij}} \tag{A.5}$$

This Hamiltonian is then used in the Schrödinger equation describing the motion of electrons in the field of fixed nuclei.

$$\mathcal{H}_{\text{elec}}\Phi_{\text{elec}} = \mathcal{E}_{\text{elec}}\Phi_{\text{elec}} \tag{A.6}$$

Solving this equation is

$$\Phi_{\text{elec}} = \Phi_{\text{elec}}(\{\vec{r}_i\};\{\vec{R}_A\}) \tag{A.7}$$

$$\mathcal{E}_{\text{elec}} = \mathcal{E}_{\text{elec}}(\{\vec{R}_A\}) \tag{A.8}$$

It depends on the nuclear coordinates. Then, Total energy under fixed nuclei is

$$\mathcal{E}_{\text{tot}} = \mathcal{E}_{\text{elec}} + \sum_{A=1}^{M}\sum_{B>A}^{M} \frac{Z_A Z_B}{R_{AB}} \tag{A.9}$$

A.3 Hartree-Fock Theory

Molecular Orbital

Molecular orbital theory decompose Ψ into a combination of molecular orbitals.

$$\{\psi_i \mid i = 1, 2, \ldots, K\} \tag{A.10}$$

Generally, a normalized, orthogonal set of molecular orbitals are chosen.

$$\int d\vec{r}\phi_i^*(\vec{r})\phi_j(\vec{r}) = \delta_{ij} \tag{A.11}$$

The simplest and possible way of making Φ as a combination of these molecular orbitals is by forming their Hartree product.

$$\Phi(\vec{r}) = \sum_{i=1}^{\infty} a_i\phi_i(\vec{r}) \tag{A.12}$$

Slater Determinant

However, Hartree product is not be antisymmetric, since interchanging two of the $\vec{r}_i$'s — equivalent to swapping the orbitals of two electrons — does not result in a sign change. The simplest antisymmetric function that is a combination of molecular orbitals is a determinant.

$$\begin{aligned}\Psi(x_1, x_2, \ldots, x_N) &= (N!)^{-1/2}\begin{vmatrix} \psi_1(x_1) & \psi_2(x_1) & \ldots & \psi_N(x_1) \\ \psi_1(x_2) & \psi_2(x_2) & \ldots & \psi_N(x_2) \\ \vdots & \vdots & \ddots & \vdots \\ \psi_1(x_N) & \psi_2(x_N) & \ldots & \psi_N(x_N) \end{vmatrix} \\ &\equiv |\psi_1\psi_2\cdots\psi_N> \end{aligned} \tag{A.13}$$

Basic Set

Next approximation involves expressing the molecular orbitals as liner combination of a pre-defined set of one-electron functions known as basis functions (or Atomic Orbital; AO).

$$\psi_i = \sum_{\mu=1}^{K} C_{\mu i}\phi_\mu \tag{A.14}$$

where $C_{\mu i}$ are known as the molecular orbital expansion coefficients.

The Variational Principle

The problem has now become how to solve for the set of molecular orbital expansion coefficients, $C_{\mu i}$. Hartree-Fock theory takes advantage of the variational principle, which says that for any antisymmetric normalized function of the electronic coordinates. Then, the expectation value for the energy will always be greater than the energy for the exact wavefunction.

$$\mathcal{E}_0 > \mathcal{E}_{\text{exact}} \tag{A.15}$$

In other words, the energy of the exact wavefunction serves as a lower bound the energies calculated by any other normalized antisymmetric function.

The Roothaan-Hall Equations

The variational principle leads to following equations describing the molecular orbital expansion coefficients, derived by Roothaan and by Hall.

$$\sum_{\nu} F_{\mu\nu} C_{\nu i} = \varepsilon_i \sum_{\nu} S_{\mu\nu} C_{\nu i}, i = 1, 2, \ldots, K \tag{A.16}$$

or can be rewritten in matrix form.

$$FC = SC\varepsilon \tag{A.17}$$

where each element is a matrix. S is called overlap matrix.

$$S_{\mu\nu} \equiv \int dr_1 \phi_\mu^*(1) \phi_\nu(1) \tag{A.18}$$

F is called the Fock matrix.

$$\begin{aligned} F_{\mu\nu} &= H_{\mu\nu}^{\text{core}} + \sum_{a}^{N/2} \sum_{\lambda\sigma} C_{\lambda a} C_{\sigma a}^* [2(\mu\nu|\sigma\lambda) - (\mu\lambda|\sigma\nu)] \\ &= H_{\mu\nu}^{\text{core}} + \sum_{\lambda\sigma} P_{\lambda\sigma} [2(\mu\nu|\sigma\lambda) - (\mu\lambda|\sigma\nu)] \end{aligned} \tag{A.19}$$

Where P is the density matrix. Equation A.17 is not linear and must be solved iteratively. The procedure which does so is called the Self-Consistent Field (SCF) method.

The general strategy used by the SCF method (after initial setup steps) is as follows:

- Evaluated the integrals.
- Form the Fock matrix.
- Solve for the density matrix.
- Test for convergence. If it fails, begin the next iteration. If it succeeds, go on to perform other parts of the calculation (such as population analysis).

A.4 Ab-Initio Method

Ab-initio methods compute solutions to the Schrödinger equation using mentioned theory on the basis of the first principle.

A.5 Semi-Empirical Method

There are some semi-empirical methods, for example Complete Neglect of Differential Overlap (CNDO), Intermediate Neglect of Differential Overlap (INDO), Modified Intermediate Neglect of Differential Overlap (MINDO), Modified Neglect of Diatomic Overlap (MNDO), Austin Model 1 (AM1), Parametric Method 3 (PM3). MNDO, MINDO/3, AM1, PM3 methods use a restricted basis set of one s orbital and three p orbitals (p_x, p_y, p_z). and neglect diatomic overlap integrals in the secular equation (The overlap of two atomic orbitals which are on different centers or atoms are set to zero). In addition to this, all two-electron integrals involving charge clouds arising from the overlap of two atomic orbitals on different centers are ignored.

$$(\mu\nu|\lambda\sigma) = \int dr_1 dr_2 \phi_\mu^*(1)\phi_\nu(1) r_{12}^{-1} \phi_\lambda^*(2)\phi_\sigma(2) \tag{A.20}$$

The MNDO and AM1 one-center two-electron integrals are derived from experimental data on isolated atoms. The values of PM3 one center two-electron integrals were optimized to reproduce experimental molecular properties. In addition, core-core term was approximated and calculated by using parameters. For example, AM1 and PM3 core-core terms are

$$\begin{aligned} E_N(A,B) &= E_N^{\mathrm{MNDO}}(A,B) \\ &+ \frac{Z_A Z_B}{R_{AB}} \left(\sum_k a_{kA} e^{-b_{kA}(R_{AB}-c_{kA})^2} + \sum_k a_{kB} e^{-b_{kB}(R_{AB}-c_{kB})^2} \right) \end{aligned} \tag{A.21}$$

The extra terms define spherical Gaussian functions, the a, b and c are adjustable parameters. PM3 has two Gaussians per atom, while AM1 has between two and four.

Reference

[1] K. Ono, T. Sakai, Y. Mochizuki: *Atarashi Ryoshi Kagaku* (A. Szabo, N. S. Ostlund: Modern Quantum Chemistry) (Tokyo Daigaku Syuppankai, Tokyo, 1987) [in Japanese].

[2] T. Hirano, K. Tanabe: *Bunshikidoho MOPAC Gaido Bukku* (Guide book for Molecular Orbital Method — MOPAC) (Kaibundo, Tokyo, 1991) [in Japanese].

[3] H. Kihara, N. Uchida and S. Ikuta: *Bunshikidoho* (Molecular Orbital Method) ed. E. Osawa (Kodansha, Tokyo, 1994) [in Japanese].

[4] E. Osawa, T. Hirano and K. Honda: *Keisankagaku Nyumon* (Introduction to computational chemistry) ed. E. Osawa (Kodansha, Tokyo, 1994) [in Japanese].

[5] J. B. Foresman and Æ. Frisch: *Exploring Chemistry with Electronic Structure Methods* (Gaussian Inc., Pittsburgh, 1993).

[6] J. J. P. Stewart: *MOPAC 93 MANUAL* (Fujitsu, Tokyo, 1993).

Vita

Kanashima Takeshi was born in Toyonaka, Osaka, Japan on Sep. 26, 1968. He graduated from Kitano senior high school, Osaka. He entered Osaka university, faculty of engineering science on April, 1987. He received Master of Engineering degree in Electrical Engineering on March, 1993 from Osaka university.

Publications

Academic Journals

- T. Kanashima, R. Nagayoshi, M. Okuyama, Y. Hamakawa: "Optical characterizations of photo-induced chemical vapor deposition produced SiO_2 films in vacuum ultraviolet, ultraviolet and visible region ": J. Appl. Phys., **74**, (1993), 5742
- T. Kanashima, M. Okuyama and Y. Hamakawa: "Photoluminescence and Its Excimer Laser Irradiation Effects in SiO_2 Film Prepared by Photo-Induced Chemical Vapor Deposition ": Jpn. J. Appl. Phys., **32** (1993) 3313
- T. Kanashima, M. Okuyama and Y. Hamakawa: "Photoluminescence of SiO_2 films grown by photo-induced chemical vapor deposition ": Appl. Surf. Sci., **79/80** (1994) 321
- T. Kanashima, M. Okuyama and Y. Hamakawa: "Theoretical Analysis of Oxygen-Excess Defects in SiO_2 Thin Film by Molecular Orbital Method ": impress in Jpn. J. Appl. Phys.
- H. Yamamoto, S. Iwasaki, K. Okumura, T. Kanashima, M. Okuyama and Y.Hamakawa: "Characterization of Charged Traps near Si–SiO_2 Interface in Photo-CVD SiO_2 Film ": impress in Jpn. J. Appl. Phys.

International Conference

- T. Kanashima, M. Okuyama and Y. Hamakawa: "Photoluminescence and Its Excimer Laser Radiation Effects in Photo-Assisted Chemical Vapor Deposition SiO_2 Film ": SYMPOSIUM ON DRY PROCESS, TOKYO, Japan, Oct. 29–30, 1992
- T. Kanashima, M. Okuyama and Y. Hamakawa: "Photoluminescence of SiO_2 films grown by photo-induced chemical vapor deposition ": International Conference on Photo-Excited Processes and Applications, Sendai, Japan, Oct. 13–15, 1993
- T. Kanashima, M. Okuyama and Y. Hamakawa: "Theoretical Analysis of Oxygen-Excess Defects in SiO_2 Thin Film by Molecular Orbital Method ": International Conference on Solid State Devices and Materials, Osaka, Japan Aug. 21–24, 1995
- H. Yamamoto, S. Iwasaki, K. Okumura, T. Kanashima, M. Okuyama and Y.Hamakawa: "Characterization of Charged Traps near Si–SiO_2 Interface in Photo-CVD SiO_2 Film ": International Conference on Solid State Devices and Materials, Osaka, Japan Aug. 21–24, 1995

List of Figures

List of Tables